Use of Multi-Fidelity and Surrogate Models to Reduce the Cost of Developing Physics-Based Systems

James L. Hebert

B.S. in Electrical Engineering, Magna cum Laude, May 1982, Texas Tech University
M.S. in Electrical Engineering, Dec 1983, Air Force Institute of Technology
M.S. in Systems Engineering, Dec 2008, U.S. Navy Post Graduate School

A Dissertation submitted to

The Faculty of
The School of Engineering and Applied Science
of The George Washington University
in partial satisfaction of the requirements
for the degree of Doctor of Philosophy

May 17, 2015

Dissertation directed by

Timothy Eveleigh
Adjunct Professor of Engineering Management and Systems Engineering

Shahryar Sarkani
Adjunct Professor of Engineering Management and Systems Engineering

ProQuest LLC.
789 East Eisenhower Parkway
P.O. Box 1346
Ann Arbor, MI 48106 - 1346

The School of Engineering and Applied Science of The George Washington University certifies that James Leland Hebert has passed the Final Examination for the degree of Doctor of Philosophy as of March 16, 2015. This is the final and approved form of the Dissertation.

Use of Increasing Fidelity and Surrogate Models in the Design and Development of Physics-Based Systems

James L. Hebert

Dissertation Research Committee:

Timothy Eveleigh, Professorial Lecturer in Engineering Management and Systems Engineering, Dissertation Co-Director

Shahryar Sarkani, Professorial Lecturer in Engineering Management and Systems Engineering, Dissertation Co-Director

E. Lile Murphree, Professor Emeritus of Engineering Management, Committee Member

Thomas Mazzuchi, Professor of Engineering Management and Systems Engineering & of Decision Sciences, Committee Member

Shahram Sarkani, Professor of Engineering Management and Systems Engineering, Committee Member

Dedication

I dedicate this dissertation to my wife, Pat, and my children, Clifton, Amanda, Charles, and Kathryn, and my father, Clifton J. Hebert, and my mother, Edna Lee Hebert, for their love and because they have been a constant inspiration for me.

Acknowledgements

Many people have contributed to the achievement of this dissertation. I would like to start by thanking my advisors, Dr. Tim Eveleigh and Dr. Thomas Holzer who consistently offered profound insight, tough refocusing when needed, needed humor, and persuasive motivation. I would like to thank Dr. Shahryar Sarkani for his support. I would also like to thank my dissertation committee, especially Dr. Tim Eveleigh, who invested their time and energy in making this dissertation the best it could be. I would like to thank Dr. John Ball, who provided support, advice on all aspects of this research and help with programming scripts. He is directly responsible for giving me the encouragement necessary to achieve this goal. I would like to thank Dr. Joanna Ingham for her invaluable reviews and suggestions to my journal article and this dissertation. I could not have made it without her support, help and encouragement. I would like to thank the U.S. Navy for providing the financial support and a fellowship to pursue this degree. I would like to give a big thanks to my wife, Pat Hebert, who as my spouse and best friend provided so much support and understanding. Finally, I would like to thank God who has provided me with endless blessings in the form of opportunities and strength throughout my entire life.

Abstract of Dissertation

Use of Increasing Fidelity and Surrogate Models to Reduce the Cost of Developing Physics-Based Systems

ABSTRACT:

Building complex physics-based systems in a timely cost-effective manner, that perform well, meet diverse user needs, and have no bad emergent behaviors is a challenge. To meet these requirements the solution is to model the physics-based system before building it. Modeling and Simulation capabilities for these type systems have advanced continuously during the past 20 years thanks to progress in the application of high fidelity computational codes that are able to model the real physical performance of system components. The problem is that it is often too time consuming and costly to model complex systems, end-to-end, using these high fidelity computational models alone. Missing are good approaches to segment the modeling of complex systems performance and behaviors, keep the model chain coherent and only model what is necessary. Current research efforts have shown that using multi-fidelity and/or surrogate models might offer alternative methods of performing the modeling and simulations needed to design and develop physics-based systems more efficiently. This study demonstrates that it is possible reduce the number of high fidelity runs allowing the use of classical systems engineering analysis and tools that would not be possible if only high fidelity codes were employed. This study advances the systems engineering of physics-based systems by reducing the number of time consuming high fidelity models and simulations that must be used to design and develop the systems. The study produced a novel approach to the design and

development of complex physics-based systems by using a mix of variable fidelity physics-based models and surrogate models. It shows that this combination of increasing fidelity models enables the computationally and cost efficient modeling and simulation of these complex systems and their components. The study presents an example of the methodology for the analysis and design of two physics-based systems: a Ground Penetrating Radar (GPR) and a Nuclear Electromagnetic Pulse Bounded Wave System.

Index Terms- Systems Engineering, Multi-fidelity Models, Surrogate Models, FDTD, Kriging

Table of Contents

List of Figures

List of Tables

List of Abbreviations

3D	Three Dimensions
1D-FDTD	One Dimension Finite Difference Time Domain
3D-FDTD	Three Dimension Finite Difference Time Domain
ABC	Absorbing Boundary Conditions
AoA	Analysis of Alternatives
BWS	Bounded Wave Simulator
CEM	Computational Electromagnetic
CFD	Computational Fluid Dynamics
CPU	Central Processing Unit
DACE	Design and Analysis of Computer Experiments
DHS	Department of Homeland Security
DoD	Department of Defense
DOE	Design of Experiments
DOE	Department of Energy
DSM	Design Structure Matrix
E Field	Electric Field
EM	Electromagnetic
EMP	Electromagnetic Pulse
FDTD	Finite Difference Time Domain
GB	Giga-byte
GPR	Ground Penetrating Radar
GPU	Graphics Processing Unit

H Field	Magnetic Field
HF	High Fidelity
INCOSE	International Council on Systems Engineering
KCL	Kirchoff's Current Law
KVL	Kirchoff's Voltage Law
LHS	Latin Hypercube Sampling
LMD	Lumped Matter Discipline
M & S	Modeling and Simulation
MBSE	Model Based Systems Engineering
MDO	Multidisciplinary Design Optimization
MSE	Mean Squared Error
NAS	National Academy of Science
NEMP	Nuclear Electromagnetic Pulse
NOAA	National Oceanic and Atmospheric Administration
NOTES	Naval Ordnance Transient EMP Simulator
NSWCDD	Naval Surface Warfare Center Dahlgren Division
OAD	Orthogonal Array Design
PEC	Perfect Electrically Conducting
PERT	Program/Project Evaluation Review Technique
PSPICE™	Personal Computer Simulation Program with Integrated Circuit Emphasis (circuit simulation software)
PML	Perfect Matching Layer
RAM	Random Access Memory

RLC	Resistance Inductance Capacitance
S-FDTD	Stochastic Finite Difference Time Domain
SE	Systems Engineering
SF_6	Sulfur Hexafluoride Gas
SM	Surrogate Modeling
SPAS	Surface Penetrating Active Sensors
UD	Uniform Design

List of Symbols

$\nabla x E$	curl of the electric field
∇ x H	curl of the magnetic field
ε	permittivity
ε_r	relative permittivity
ϵ_o	permittivity of free space = $8.854185X10^{-12}$ Farads per meter
n	Fresnel reflection coefficient
σ	conductivity
μ	permeability
μ_r	relative permeability
μ_o	permeability of free space = $4 X 10^{-7}$ Henry per meter.
Δt	time of propagation of the wavefront diagonally across the maximum cell dimension
dx, dy, dz	change in distance x, y, z
$\frac{\partial B}{\partial t}$	rate of change of the magnetic flux
$\frac{\partial D}{\partial t}$	rate of change of the electric field
$\frac{\partial q}{\partial t}$	rate of change of the charge
$\frac{\partial i}{\partial t}$	rate of change of the current
$\frac{\partial v}{\partial t}$	rate of change of the voltage
c	the speed of light in vacuum: 299,792,458 m/s
c	capacitance
E	electric field

H	magnetic field
I, i	current
i, j, k	cell indices
J	current density
kV/m	kilo-Volts per meter
L	inductance
m	meters
$m(x)$	approximation (meta-) model m
ns	nano-second
R	resistance
$\Re^n$	n source values
$\Re^m$	m response values
s	surrogate response value(s)
S_1	root of the solution of the series RLC circuit
S_2	root of the solution of the series RLC circuit
t	time
V, v	voltage
x or x_i	input parameter value(s) of x
X_f	the feasible region of the n-dimensional parameter vector x
y or y_i	response parameter value(s) of y

Chapter 1 - Introduction

Systems engineering of complex systems is challenged by the cost and complexity of modeling the performance of component physical systems that contribute to the understanding of higher, system level performance. It is not realistic to model a system with a single detailed high fidelity model; a series of models of multiple fidelities is required. This is particularly true of complex electromagnetic systems and other physics-based systems. "Mathematical models in which the equations that constitute the model are those used in physics to describe or define the physical phenomenon being modeled are referred to as physics-based models." [National Research Council 2002] These complex physics-based systems are physical systems that are controlled and driven by physical laws (i.e complex electromagnetic systems and Maxwell's Laws/Equations). There is an increase in the use of high fidelity models based on proven accurate Computational Fluid Dynamics (CFD) and Computational Electromagnetic (CEM) codes to optimize system parameters, explore complex system designs and evaluate a system's output responses to changes. Due to the expense in time and resources to run these high fidelity models, many approaches or frameworks using multi-fidelity models or surrogate models, that reduce computational time and expense, are being researched. Such a framework is proposed and used to investigate the effects of inputs parameters to the performance of a ground penetrating radar (GPR) and to solve a systems engineering problem that required the modification of a nuclear electromagnetic pulse (NEMP) bounded wave system (BWS). This paper presents details about their investigation and the problems that were solved, the systems engineering processes that were followed, and the modeling approaches that were used. For both processes, this dissertation presents a novel framework that uses time

efficient models with differing fidelities where the interfaces provide a source of performance parametrics and a balance between the performance of components with that of the overall system and surrogate models to reduce computation times.

The primary focus of this study is to reduce the cost, time, and resources needed to perform development and design related modeling and simulations of physics-based systems and thereby allow the use of standard systems engineering (SE) tools. The International Council on Systems Engineering (INCOSE) defines systems engineering as "an interdisciplinary approach and means to enable the realization of successful systems. It focuses on defining customer needs and required functionality early in the development cycle, documenting requirements, then proceeding with design synthesis and system validation while considering the complete problem." [INCOSE 2011] Bahill and Dean present the process as comprised of the following seven tasks:

- ***S****tate the problem.* Stating the problem is the most important systems engineering task. It entails identifying customers, understanding customer needs, establishing the need for change, discovering requirements and defining system functions.
- ***I****nvestigate alternatives.* Alternatives are investigated and evaluated based on performance, cost and risk.
- ***M****odel the system.* Running models clarifies requirements, reveals bottlenecks and fragmented activities, reduces cost and exposes duplication of efforts.
- ***I****ntegrate*. Integration means designing interfaces and bringing system elements together so they work as a whole. This requires extensive communication and coordination.
- ***L****aunch the system.* Launching the system means running the system and producing outputs -- making the system do what it was intended to do.
- ***A****ssess performance.* Performance is assessed using evaluation criteria, technical performance measures and measures -- measurement is the key. If you cannot measure it, you cannot control it. If you cannot control it, you cannot improve it.

- ***Re-evaluation.*** Re-evaluation should be a continual and iterative process with many parallel loops. [Bahill and Dean 2009]

This study concentrates on the third of the seven tasks (model the system) that comprise the simplified systems engineering life cycle process illustrated in Figure 1.

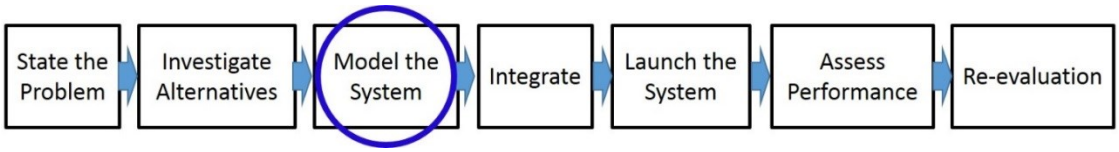

Figure 1. The Systems Engineering Life-Cycle Process [Bahill and Dean 2009]

Many believe that models can be representations of the real world and simulations allow the model to provide predictions or investigations of a system's real world behavior over time. Because of this notion, modeling and simulation (M&S) are prevalent in the majority of systems engineering endeavors. A definition of "system" was developed by the INCOSE: "A system is a construct or collection of different elements that together produce results not obtainable by the elements alone." [INCOSE 2007] Their definition extends M&S to a long list of elements, some physics-based, e.g. governed by the laws of physics, and others whose elements include people, software, policies, documents, etc. The military and defense domain, in particular within the United States, has been the main M&S champion, in the form of funding as well as application of M&S, in modern military organizations is part of the acquisition/procurement strategy. Specifically, M&S is used to conduct events and experiments that influence requirements and training for military systems. As such, M&S is considered an integral part of systems engineering of military systems. Other application domains, however, are currently catching up. M&S in the fields of medicine, transportation, and other industries is poised to rapidly outstrip the

Department of Defense's (DoD) use of M&S in the years ahead, if it has not already happened. [Collins et al. 2011] A number of these domains are illustrated in Figure 2.

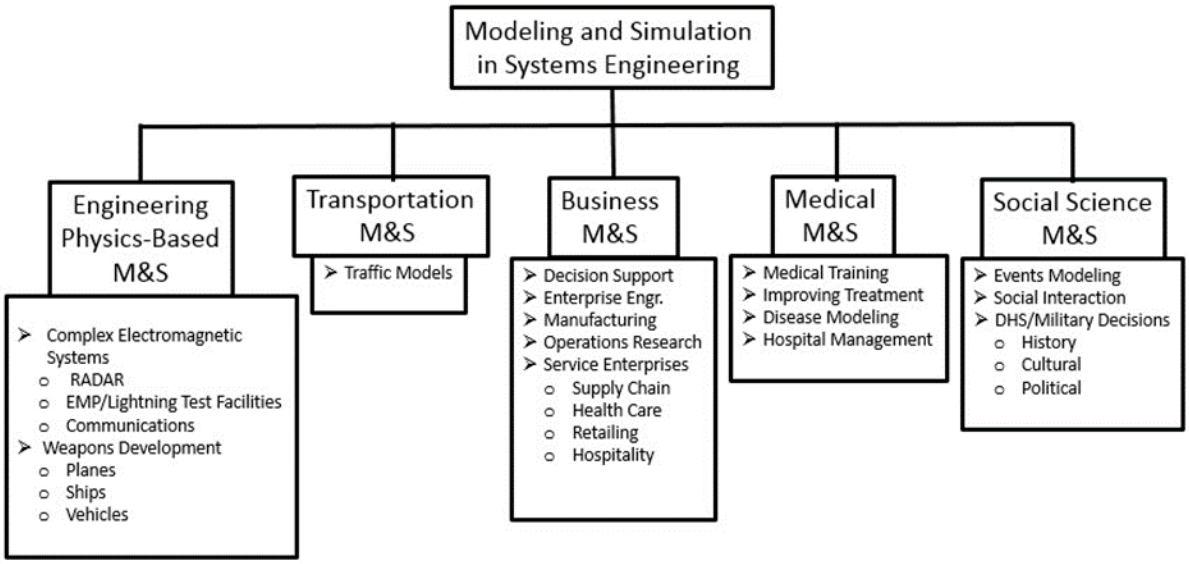

Figure 2. Example of Modeling and Simulation in Systems Engineering [Banks 2009]

1.0 Physics-Based Models

Physics-based models are controlled and driven by physical laws (e.g. Maxwell's Laws and Equations for EM models, and Navier–Stokes equations for fluid dynamics models). Systems engineering of complex physics-based systems is challenged by the cost and complexity of modeling individual component system performance and higher system level performance. Full scale high-fidelity (HF) simulations based upon well-established computational physics-based codes now play a major role in the design, development, and test planning of complex physical systems. "Such system analysis codes play a central role in the design process since they aid designers and scientists in validating new designs and studying the effect of altering key parameters on product and/or system performance." [Lim 2010] As these models became more precise, they also became more expensive in terms of computational time. Studies have shown that complex system simulations using

expensive HF engineering codes may be unfeasible or take hours to days to run, even on the most capable super computers. [Andres 2014; Forrester et al., 2008; Simpson et al., 2008] New and efficient approaches are needed to reduce the run times for these high fidelity models; particularly when the design requires reverse engineering, evolutionary development, or system optimization. A framework that reduces the time and cost of these simulation runs should appeal to systems engineers because it enables them to use well proven statistical and other SE analysis tools for the design and development of complex physics-based systems.

Turner states that optimal engineering designs are difficult problems to solve. He explains that "Often, the optimization problem is difficult to formulate, and if it can be formulated, the number of design variables is often substantial, the design variables may be continuous, discontinuous or discrete, the relationships between design variables and performance indices is generally nonlinear, and the optimization problem involves multiple competing objectives. As if complex, nonlinear, hyper dimensional and multi-objective optimization problems were not difficult enough, "real" designs must also be manufactured in a world where exact tolerances are generally not achievable, and therefore robust-optimal design solutions are a true measure of optimality. However, the problem is not hopeless, as it is ever more feasible to solve the "approximate" problem via surrogate modeling methods." [Turner 2014]

Gorissen, et al. stated that "Computer based simulation has become an integral part of the engineering design process. Rather than building real world prototypes and performing experiments, application scientists can build a computational model and simulate the physical processes at a fraction of the original cost. Despite continual advances

in computing power, the complexity of analysis codes, such as finite element analysis and CFD, seem to keep pace with computing advances. [Gorissen et al. 2007]

To put numbers on this problem, Wang found "...it is reported that it takes Ford Motor Company about 36-160 hours to run one crash simulation. [Wang 2006] and Gu et al. found "…for a two-variable optimization problem, assuming on average 50 iterations are needed by optimization and assuming each iteration needs one crash simulation, the total computation time would be 75 days to 11 months, which is unacceptable in practice." [Gu 2001] Goriseen goes on to explain that "For most realistic problems the high computational cost of simulator codes and the high dimensionality of the design space simply prohibit this direct approach, thus making these codes unusable in engineering design and multidisciplinary design optimization (MDO). Consequently, scientists have turned towards up front approximation methods to reduce simulation times." [Gorissen et al. 2007]

1.1 Statement of the Problem

In modern physics-based systems' engineering offices, the computational power required to support informed decisions can be can be prodigious. Even with the latest and most powerful computer systems, systems engineers may wish to base their design and development decisions on more data than can be provided using classical high fidelity computational codes. They may want to use additional systems engineering analysis and optimization tools that require the running of a range of possible inputs to enhance the systems output or to investigate and potentially reduce variability or uncertainty in a particular design or approach. What is needed is a methodology that provides increased insight into the performance of or problems with physics-based systems beyond the

necessarily limited analysis runs afforded through the use of time consuming and expensive high fidelity models alone.

1.2 Hypotheses

The primary hypothesis of this study is that there are modeling and simulation approaches that make possible the use of systems engineering decision making tools by reducing the time and cost of these activities during the design and development of complex physics-based complex systems. Specifically, we hypothesize that multi-fidelity modeling and the use of surrogate models can be used in a methodology that enables the efficient allocation of resources, time and cost, for the optimization and performance evaluation/validation of these systems without sacrificing rigor. We further hypothesize that reductions in time consuming high fidelity modeling and simulations allows expanded use of systems engineering related sensitivity and other analyses to evaluate the changes in a system's output response to changes in nominal controlled and uncontrolled input parameters.

1.3 Purpose of the Research

The purpose and long range objectives of this effort are to develop a structured framework for the use of decision based models of increasing fidelity and efficient surrogate models to assist planners and decision makers in the design and development of physics-based systems. The framework should encompass both a problem-solving philosophy and a collection of methods. The philosophy is to use the goals of objectives and goals of the program manager as an explicit consideration in the choice of model and outputs needed for the problem or system being analyzed. This involves model decision analysis in an engineering environment. In the collection of models available, high fidelity

models are generally the most accurate but resource constraints and other program considerations may require the most efficient model at the lowest level of fidelity that answers the question. The model appropriate for requirements analysis may not be the same as that needed to analyze alternative designs. They both may be different from the model for design and development. From an industrial perspective the requisites is not a method that yields "the optimal solution", but methods that could be applied to a wide range of problems and employed together with the tools presently used in industry and give near optimal solutions in a reasonable time frame. [Olvander 2009] The new framework should be applicable for all of these uses.

1.4 Significance

Modeling and simulation is particularly important in the development of complex physics-based systems because in today's rapidly changing technological environment there is not enough time or money to build the number of physical simulators necessary to evaluate the performance of complex systems in the many environmental and operational conditions in which they must operate. The cost of correcting problems in complex physics-based systems greatly increases with the maturity of the system. Modeling and simulation facilitates the early investigation of variables and responses and allows the use of traditional systems engineering statistical methods and other tools to reduce uncertainty and aid in program management decisions during the design and development stage of a systems acquisition. It can provide early predictions of system performance allowing engineering-level tradeoff analysis of potential technologies and systems. Deficiencies can be investigated individually and solutions developed early in the system's development. High fidelity physics-based computation models are capable of performing these studies

but they are too expensive in time and computational load. There may be several alternative designs during the design and development phase. These can be evaluated using faster running low fidelity models to reduce the number to: only those feasible in the design space, those which are affordable, or those that best meet the stakeholders' requirements. Multi-fidelity models can be applied as the alternative designs are narrowed. Insight into the problems being studied can be gained by the use of meta or surrogate models. Surrogate models and lower fidelity models look for answers in the gaps between the limited analyses allowed when using only high fidelity models alone. They can provide better correlation between the data gained from different physical models and/or experimentation. Surrogate models can provide the systems engineer with enhanced understanding and decision making by providing additional information from modeling and simulation and other sources in a useful and productive way. Finally, component and more time consuming and computationally expensive models of higher fidelity can be employed to evaluate, test and qualify chosen configurations or designs. At each level of fidelity the systems engineer has the choice of decreasing computational time and expense by the use of surrogate models. A methodology that assists the systems engineer in implementing this approach would be of great value.

1.5 Scope and Limitations

This effort focuses on that part of systems engineering as the professional discipline that designs and develops complex physics-based systems. The systems engineer has technical responsibility for the system. These principles guided the application of modeling and simulation of the system during the design and development phase. This study investigates the way in which models of increasing fidelity and efficient surrogate models can assist these planners and decision makers while at the same time observing the need to

reduce the cost of time consuming high fidelity models and simulation. It seeks to develop a structured framework for the application of multi-fidelity at the lowest level necessary to answer the decision maker's needs and concentrates on applying surrogate models to further reduce the cost of modeling and simulations in the design and development of physics-based systems. It does not cover the models and simulations used during any acquisition phase outside of the design and development of a physics-based system. It also does not cover or present examples of systems engineering tools such as regression analysis etc. because these are covered in many readily available texts on systems engineering.

1.6 Organization of this Study

There are a number of cost saving approaches and techniques that systems engineers might employ to get fairly accurate estimates of a system's performance instead of using only HF computational code analysis. Some of those state-of-the-art approaches include the use of multi-fidelity models and surrogate models. These are introduced in the next section. A framework for applying these models in the design and development of complex physics-based systems is presented in Chapter 3, the methodology section. This framework combines systems engineering design of experiments with simulation and modeling to ensure that two cost reducing techniques are always followed. The first is the use of the lowest fidelity model required to answer the problem, and the second is to use surrogate models where needed to reduce the number of simulations that require high fidelity models. The framework is demonstrated in Chapter 4, where we describe the modeling and simulation of a GPR, and then further illustrated in the capstone design and modification of a NEMP/BWS using this approach. We end with a conclusion section that details the findings of the study.

Chapter 2 – Literature Review

New physics-based systems are designed to numerous stakeholder requirements including performance, reliability, safety and other criteria. Computer simulations of physical processes are used to analyze these systems in terms of their inputs and outputs that relate to these requirements. This often requires the use of high fidelity computational engineering or physics codes such as computational fluid dynamics, computational physics, or computational electromagnetics. Stakeholders, decision makers and engineers who use these results must answer the question: How much confidence do I have in these results? The primary means to quantify this confidence is verification and validation. Verification requires an assessment of the accuracy of the results. Validation is an assessment of how well the computational results compares to measured real-world experiment data. To achieve high confidence often requires large quantities of inputs and determining the changes in outputs. This can represent more data than can be provided by using accurate but extremely time consuming high fidelity physical models. This study concerns the use of models and simulations to support the design and development of physics-based systems. The design process paradigm uses decision-making models to describe design alternatives and optimization methods that search the design space for the best design among all possible design options. [Olvander 2009] For physics-based systems, the allure of the very accurate physical high fidelity models is natural. The problem is that these models are often extremely time consuming and can preclude the use of systems engineering decision making tools and techniques. This literature review addresses the major areas that effect the choices of lower fidelity models that can take the place of them: modeling and simulation, high fidelity models, the use of multi-fidelity model and

surrogate models, the Finite Difference Time Domain high fidelity electromagnetic computational code and systems engineering.

2.0 Background

Because it may not be realistic to only use detailed HF models exclusively in the design and development of a complex physics-based system and because of the need to reduce the computational time, cost and complexity of this modeling, a literature search was conducted to survey approaches used to model system performance and identify techniques that might present a more efficient approach. Many approaches or frameworks found use multi-fidelity models. Others use surrogate models. Some examples of these are provided in the following sections. Both approaches may reduce computational time and expense. When addressed in the literature, most of these approaches are geared to address specific physics-based systems like an aircraft wing or an electromagnetic filter. In this literature review we seek a more generalized approach.

2.1 Modeling the System

In recent years, systems engineers have seen a dramatic increase in the use of HF computational M&S in the design and development of physics-based systems. Models based on proven accurate high fidelity CFD and CEM and other computational codes are routinely used to optimize and validate complex system designs and evaluate system output responses to changes. For example, Ong et al. state "[…] in many complex engineering design problems where HF analysis models are used, each function evaluation may require Computational Structural Mechanics (CSM), Computational Fluid Dynamics (CFD), or Computation Electromagnetics (CEM) simulations costing minutes to hours of supercomputer time." [Ong et al. 2005] Many recent approaches or frameworks, such as

those presented in Table I, use multi-fidelity models or surrogate models to reduce computational time and expense. Table I presents a list of works that applied multi-fidelity and surrogate models as a design tool in place of HF models in the design of aircraft components and EM system components such as filters and antennas. Normally, these surrogate or meta-models replace some computational functions within the HF code. Surrogate models can reduce the time and expense of searching for promising designs by standing in for high fidelity expensive design evaluations or simulations. They can allow the optimization of various design input metrics (such as weight, aerodynamic drag, cost, etc.) in less times and lower cost than using the very accurate high fidelity models.

Full scale HF simulations based upon models that use well-established computational codes play a major role in the design, development and test planning for physics-based systems. “Such analysis codes play a central role in the design process since they aid designers and scientists in validating new designs and studying the effect of altering key parameters on product and/or system performance.” [Lim 2010] Complex physics-based systems are physical systems that are controlled and driven by physical laws (i.e complex electromagnetic systems and Maxwell’s Laws/Equations). High fidelity computational codes are mathematical models that provide reasonable performance predictions of these physics-based systems. As models become more precise, they become expensive in terms of computational time and resources with modeling expense sometimes exceeding traditional build and try techniques. This is particularly true when these computationally expensive programs are used for: (1) solving an inverse engineering problem, (2) performing an evolutionary design, or (3) optimizing a system. Systems

engineers need accurate data and often must make a clear decision whether a HF simulation is required or if data from a lower fidelity or surrogate model might be good enough.

Table I presents a list of recent papers that are representative of the types of meta-models (surrogate) models and the components for which they were used as a design tool. The works reviewed in Table I used multi-fidelity models for problems that include low-fidelity surrogate models in the design of aircraft components and EM system components, such as filters and antennas. Based on this part of the review, it was clear that multi-fidelity models and simulation are on-going research and improvement topics.

Table I. Design Efforts using Multi-fidelity Codes with Surrogate Models

Reference Date	Journal Article Name	Area	Multi-Fidelity Approach	Systems Modeled
Koziel, et al. 2012	Computational-Budget-Driven Automated Microwave Design Optimization Using Variable-Fidelity Electromagnetic Simulations	EM Optimization	Coarser models for low fidelity and finer models depending on computational budget	Fourth order ring resonator bandpass filter dual band bandpass filter microstrip wideband antenna
Kuya, et al. 2011	Multifidelity Surrogate Modeling of Experimental and Computational Aerodynamic Data Sets	Aero	Multi-fidelity Co-Kriging regression surrogate model with Latin Hypercube	Inverted wing with counter-rotating vortex generators in ground effect
Koziel, et al. 2011	Space-Mapping Modeling of microwave devices using multi-fidelity electromagnetic simulations	EM	Space Mapping Surrogate with coarse mesh data Space Mapping high fidelity model with base locations	Micro-strip Chebyshev bandpass filter, Double-folded stub filter, two-section low-pass elliptic filter
Couckuyt, et al. 2010	Surrogate-Based Infill Optimization Applied to Electromagnetic Problems	EM	Expected improvement approach	Microwave filter textile antenna
Crevecoeur, et al. 2010	A two-level Generic Algorithm for Electromagnetic Optimization	EM	Fast coarse model	Algebraic test function die press model, octagonal double-layer electromagnetic shield
Koziel, et al. 2009	Multi-fidelity Optimization of Microwave structures Using Response Surface Approximation and Space Mapping	EM Optimization	Surface approximation	Microwave structures
You, et al. 2009	Kriging Model Combined with Latin Hypercube Sampling for Surrogate Modeling of Analog Integrate Circuit Performance	EM	Kriging with Latin Hypercube surrogate	Integrate circuit (operational amplifier)
German, et al. 2009	A Multi-fidelity Modeling Approach for Cosite Interference analysis	EM	Multiple models of different fidelity	Cosite electromagnetic interference analysis
Chandila 2002	Strategy for Global Optimization Post-optimality Using Local Kriging Approximations (Master Thesis)	Operations Research Structural	Kriging local and global optimization	Engine piston torpedo mission analysis structural truss
Queipo, et al. 2005	Surrogate-Based Analysis and Optimization	Multiple	Survey of multiple methods	Space Craft injector nozzle
Booker, et al. 1998	Optimization using surrogate objectives on a helicopter test example	Aero Design & Optimization	A comparison of several approaches	Helicopter rotor blade design
Siah, et al. 2004	Fast Parameter Optimization Using Kriging Meta-modeling	EM	Hybrid Kriging metamodeling DIRECT global optimization algorithm	Slotted Array FM (frequency modulation) antenna and cable vehicle chassis and cable

2.2 Multi-fidelity Physics-Based Models

In many areas multi-fidelity models have been used to overcome the limitations imposed by high computational cost associated with the use of high-fidelity multidisciplinary optimization techniques in the design of new systems. This is particularly

true for physics-based systems that must be characterized by high-fidelity codes such as computational electromagnetics. This is important when one or more parameters become a cost function or a constraint because numerous high fidelity model runs are necessary due to uncertainty or the need to optimize the system.

Fidelity, as defined by the Simulation Interoperability Workshop Integration Study Group, is "The degree to which a model or simulation reproduces the state and behavior of a real world object or the perception of a real world object, feature, condition, or chosen standard in a measurable or perceivable manner." [Hughes et al. 2003] Fidelity is also considered to be an absolute measure of M&S representational closeness to reality as compared to validity which is considered to be a judgment. [Hughes et al. 2003]

"Essentially, all models are wrong, but some models are useful" [Box et al. 1987]

With this insightful quote in mind, one might deduce that a perfect simulation is probably impossible to achieve. Therefore measuring fidelity is an essential step to determine the usefulness of a model or simulation. A multitude of methods to measure fidelity exist; some are quantitative while others are qualitative. [Duncan 2006]

Braak and Ern found that, in various cases, the most accurate and validated physics-based models for numerical simulations of reactive flows could not be chosen because of a profusion of computational costs. They suggest that simpler, lower fidelity models of different complexity, scales and accuracy be used to reduce these costs. [Braak and Ern 2004] More recent academic studies, some highlighted in Table I, discuss using multi-fidelity models to solve specific design problems. Unlike these academic studies, the

example provided in Chapter 4 of this study presents a direct industrial application of these models, a Nuclear Electromagnetic Pulse Bounded Wave System. A common recurring theme in most of the papers reviewed is that is the systems engineer should choose the most efficient lowest fidelity model and simulation that answers the design problem or question, satisfies the stakeholder's needs and provides the results that the stakeholder can trust.

Multi-fidelity models consist primarily of two types of physics-based approaches:

1. Use different physics-based models and compare or validate the results by a comparison of the output responses of the system to the same set of inputs and conditions.
2. Use a high fidelity model with considerably lower resolution.

The first approach is demonstrated in the NEMP/BWS example presented in Chapter 4. This example uses a resistance inductance capacitance (RLC) circuit as a low fidelity model, a Personal Computer Simulation Program with Integrated Circuit Emphasis (PSPICE™) medium fidelity model and a FDTD high fidelity model to modify and design the system. The second multi-fidelity approach was described by Koziel as a two-step approach for designing small microwave filters. [Koziel 2011] Koziel explains this approach as "Our technique is based on utilizing an 'intermediate', coarse-discretization EM model." [Koziel 2011] For the second step, a surrogate is used to turn a coarse-grid physical model output of basis points into a fine-grid surrogate model approximation. eField™ demonstrates this second approach and gives an example of the computation time for two FDTD models of "fdtd1" and "fdtd2", one with a coarser grid size as shown in Table II. [eField 2015] The one with a coarser 1.6 mm grid size required 358,200 cells to

define the problem space and one with a finer 0.8 mm grid cells size required 4.78 times as many cells, 1,745,000 cells. The lower fidelity coarse grid problem took 80 minutes for 20,000 times steps and the fine grid took 145 minutes for the same number of time steps. Again, the systems engineer should choose the most efficient lowest fidelity model and simulation regardless of the model or the grid size that answers the design problem or question, satisfies the stakeholder's needs and provides the results that the stakeholder can trust.

2.3 Meta-models (Surrogate Models)

"Surrogate models, also called meta models or response surface models, are used as particular substitutes for the complex numerical models, while being computationally cheaper to evaluate". [Blanning 1975; Kourakos and Mantoglou 2013] Luo and Lu present an excellent example of how surrogates can be used to find methods to increase the efficiency of the time consuming tasks of groundwater remediation. [Luo and Lu 2014] They found that a surrogate driven simulation and optimization technique is an effective tool to solve this problem. [Ahlfeld et al. 1988; Guan and Aral 1999; Liu et al. 2000; Schaerlaekens et al. 2006; Md Azamathulla et al. 2008] "However, the enormous computational cost of running such simulations multiple times, limits the applicability of the simulation optimization techniques in a complex groundwater remediation optimization process." [Qin et al. 2007; Razavi et al. 2012] One method that reduces this computational burden is replacing the numerical models with efficient surrogate models. [Sreekanth and Datta 2010; Jin et al. 2001] In a review of current surrogate methods Simpson et al. explains that using surrogate models is commonplace. They state: "The use of statistical techniques to build approximations of expensive computer analysis codes

pervades much of today's engineering design. These statistical approximations, or meta-models, (also referred to as surrogate models) are used to replace the actual expensive computer analyses, facilitating multi-disciplinary, multi-objective optimization and concept exploration." [Simpson et al. 2008] These models replace some computational functions within the HF code.

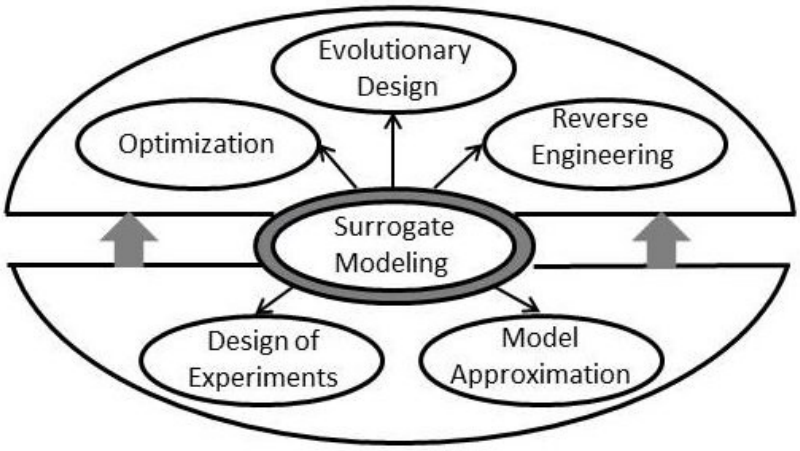

Figure 3. The Role of Surrogate Modeling

Figure 3 shows the role of surrogate modeling in support of design of physics-based systems. Surrogate modeling is a process by which complex or computationally expensive models (in time and cost) are represented by a simpler model as an interpolation of a set of data. It involves: generating a limited number of basis points using the HF code, choosing a surrogate model to represent the data and fitting the model to those basis points. Surrogate models are often used to decrease computation time and effort by replacing expensive solvers in the HF code with computationally cheap efficient solvers of less fidelity or approximation models. Bilicz provides an example: "To overcome the challenges arisen by the computation cost of the numerical EM simulators (computational electromagnetic codes), surrogate modeling (SM) is getting more and more wide spread in

electromagnetics." [Bilicz 2011] Surrogate models allow the systems engineer to use traditional design and development methods that could not be used if only HF models were used. Without using surrogate models, the high cost and expense of employing HF codes for design and development may not allow the use of SE techniques to provide decision makers with a confidence level as to the system's performance. Eason agrees: "Surrogate models allow the use of traditional optimization algorithms for otherwise intractable problems." [Eason, J. et al. 2012] Bohling recommends that: "When the deterministic expensive EM code is used for reverse engineering, evolutionary design or for parameter optimization development then the use of surrogates, like the Kriging method that can reduce cost, time and effort should be considered." [Bohling 2013] Kriging is an "optimal interpolation based on regression against observed z value of surrounding data points, weighted according to spatial covariance values." [Bohlin 2013]

2.4 Applying Meta-models

Crevecoeur et al. described general meta-models. Given a physics-based computational EM model with input parameters $x \in X_f \supset \Re^n$ and response $y \in \Re^m$ such as

$$y = f(x) \tag{1}$$

approximation model m can be built. X_f is the feasible region of the *n*-dimensional parameter vector *x*. The meta-model is much more efficient to run than its corresponding time-consuming physics-based model and yields the possibility of gaining additional

$$s = m(x) \tag{2}$$

insight into the functional relationship between input parameters and responses. This meta-model can be used to perform reverse engineering, evolutionary design, or design

optimization within multi-fidelity frameworks. The responses, *s* and *y*, need to be similar so that the meta-model is correctly used within these frameworks. It is important to note that these meta-models are interpolations of the data from physics-based models but are not physics-based. They relate the inputs with the outputs no matter what produces the output. [Crevecoeur et al. 2008] The choice of the type of meta-model used depends on the problem. The basic steps describe how to use surrogate or meta-models is show in Figure 4.

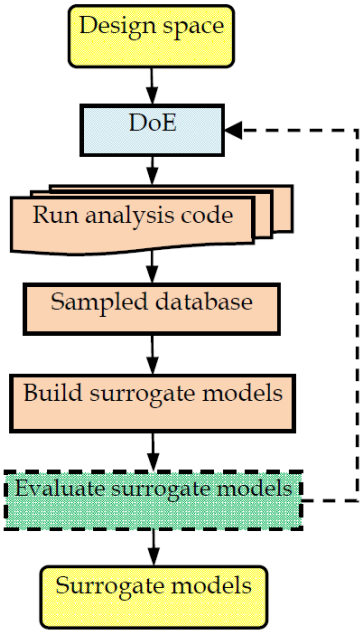

Figure 4. Frameworks of Building Surrogate Models [Han and Zhang 2012]

The basic steps for using surrogate models follows:

1. Select a set of input values of the basis or sample points ($x_1, x_2, x_3, x_4, \ldots, x_n$) for the input variable of interest. The accuracy of the surrogate model depends strongly on the number and the locations of the basis points in the design space. The choice is aided by using Design of Experiments (DOE) that generate a series of experimental procedures (Figure 5). Some options for the selection of these basis

or sample points are simple random sampling, stratified sampling and Latin hypercube sampling.

2. Use these basis or sample points to obtain a corresponding set of high fidelity output values pairs for the system (y_1, y_2, y_3, y_4, …., y_n). These can come from measurement of the actual systems output or by running the high fidelity model at these sample or basis points.

3. Choose and construct a metamodel or surrogate model to represent the model. MacDonald, Simpson and others reviewed different surrogates and gave recommendations on different surrogates for different problems. [MacDonald 2009; Simpson et al. 2008] Jin's team compared different surrogate models based on multiple performance criteria such as accuracy, robustness, efficiency, transparency and conceptual simplicity. They recommended using a radial basis function for high-order nonlinear problems and Kriging for low-order nonlinear problems in high dimension spaces and polynomial response surfaces for low-order nonlinear problems. [Jin et al. 2002] Other studies also compared meta-model types. [Lim 2010; Wang 2006] "When deterministic or expensive EM codes are used for reverse engineering, evolutionary design, or parameter optimization, the use of surrogates, like the Kriging method, should be considered to reduce cost, time and effort. Kriging is an optimal interpolation based on regression against an observed z value of a surrounding data point (called a basis point) weighted according to spatial covariance values." [Bohlin 2013]

4. Evaluate the accuracy of the surrogate model. Try the selected surrogate model with the basis points and compare the interpolated response or output data of the

surrogate model to the output of the high fidelity model at a number of points other than the original basis points.

These steps are illustrated in Figure 5.

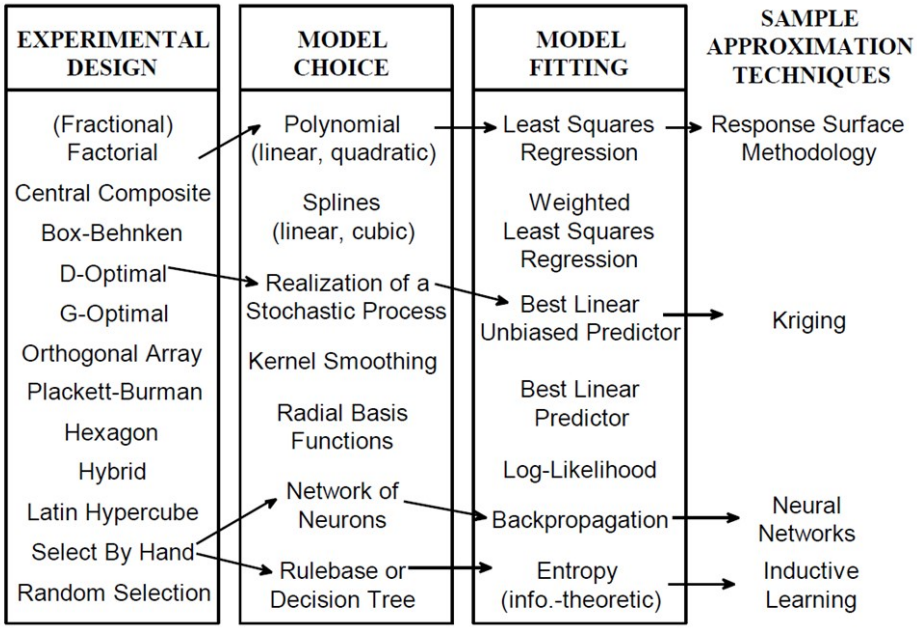

Figure 5. Techniques for Metamodeling [Simpson, 2013]

If the surrogate produces an output that mimics the underlying high fidelity model's output as closely as needed over the entire design space, it provides a useful, cheap model that can be used instead of the time consuming high fidelity model to gain insight into the total behavior of the system over the entire design space.

Using the systems engineering life cycle process, the NEMP/BWS example reported in Chapter 4 of this study extends the application of these surrogate models to the design of an entire system using a series of increasing fidelity physical models, starting with the lowest fidelity physical model necessary to answer the problem or question. This example uses three physics-based electrical and EM models and two surrogate models. The design of experiments for these two surrogate models is highlighted in Figure 5. The

specific surrogate modeling elements selected include the use of random selection of design points from the HF models, a polynomial curve-fitting function and a weighted least squares regression error-reducing technique. This set of points, function and regression techniques was used in a computationally efficient Kriging meta-model contained in the program Design and Analysis of Computer Experiments (DACE). "DACE is a MATLAB^{TM} Kriging Toolbox for working with Kriging approximations to computer models." [Lophaven 2012] Kriging was selected because: physics-based systems often produce outputs that have a Gaussian distribution and these only require a small number of basis points. Kriging allows a substantial saving in computational time over the cost of running the HF model alone.

2.5 Design of Experiments

David Montgomery states that one of the applications of experiment design is the identification of design parameters that work well over a wide range of conditions in order to determine the design parameters that most impact product performance [Montgomery 2009]. As shown in Figure 5, Design of Experiments (DOE) methods in the study are generally used to choose the locations of the sample or basis points when building a surrogate model. DOE is a procedure with the general goal of maximizing real-world applications of genetic algorithms the amount of information gained from a limited number of sample points. [Giunta et al. 2001] Currently, there are different DOE methods which can be classified into two categories: "classic" DOE methods and "modern" DOE methods. The classic DOE methods, such as full-factorial design, central composite design (CCD), Box-Behnken and D-Optimal Design, were developed for the arrangement of laboratory experiments, with the consideration of reducing the effect of random error. In contrast, the

modern DOE methods such as Latin Hypercube Sampling (LHS), Orthogonal Array Design (OAD) and Uniform Design (UD) [Fang et al. 2000] were developed for deterministic computer experiments without the random error as arises in laboratory experiments. Further information on classic and modern DOE methods was presented by Giunta et al. [Giunta et al. 2001] In this study, DOE is used to evaluate and target those inputs and multi-fidelity or surrogate models that achieve outputs that closely agree with those resulting from high fidelity models or actual system measurements.

2.6 Kriging

Kriging is a methodical approach used to interpolate the values of an output parameter when only a few values (i.e., basis points) are known. In complex systems, these basis points are usually found by running the HF computational code at a few points to generate known values. In reality, these values can come from any source that relates control input parameters to some output parameters. Measured values produce these points directly. Calculated values using higher fidelity analog electrical models produce exact and deterministic output data. Measured values can have variations due to systematic errors in measurement, or due to the data acquisition method. Kriging is designed to handle these errors by assuming they have a Gaussian distribution. The Kriging algorithm requires a kernel, a mathematical function, that best curve fits the known data. Some commonly used kernel functions include: circular, exponential, linear and Gaussian. The Kriging program uses this function to produce surfaces that pass through each of the known data points in the area around the known data points. Once the mathematical equation that best fits the variance is chosen, it can be used to estimate the surface at other values. Xiong presents an excellent example of the sampling basis points used in a Kriging model in two dimensions

in Figure 6 and the corresponding predicted output point based upon those 16 input basis points in Figure 7. [Xiong 2008]

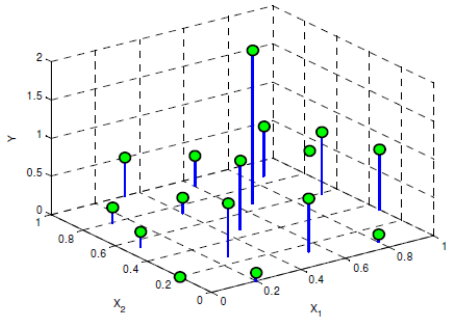

Figure 6. The sampling (basis) points (16) used in a Kriging model in two dimension [Xiong 2008]

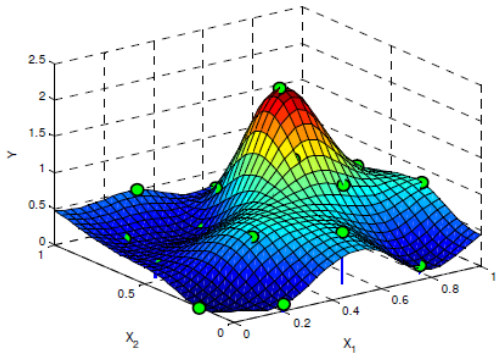

Figure 7. Kriging predicted values at the output based on sixteen basis points [Xiong 2008]

Kriging generates its output through an interpolation of a limited number of basis points from the higher fidelity physical model. The cost savings come from the fact that running an interpolation program like Kriging requires a small fraction of the computational time and cost of the corresponding higher fidelity code.

2.7 Finite Difference Time Domain (FDTD) Models

FDTD is an accurate high fidelity electromagnetic code. FDTD solves Maxwell's equation in the time domain. FDTD calculates the electromagnetic field value in a finite problem space at discrete steps in time. FDTD, a high fidelity computational electromagnetic code, was the high fidelity model and simulations for both examples presented in Chapter 4 of this study. Because time domain calculated waveforms can be transformed into the frequency domain, by using a Fourier transform, FDTD provides a broadband output with a single execution of the program. This would be contrasted with frequency domain techniques that must solve the problem one frequency at a time. A

distinct advantage of using FDTD is that it has excellent scaling capabilities as the problem size grows. FDTD techniques relate the surface currents and charges in a problem space that are modeled by Maxwell's curl equations which are:

$$\nabla x\, E = -\frac{\partial B}{\partial t} \tag{3}$$

$$\nabla \text{ x H} = \text{J} + \frac{\partial D}{\partial t} \tag{4}$$

These equations are used to develop a solution approach known as the finite difference formulation. A detailed development of the equations for the three dimensional version of the FDTD code is presented in a thesis by Williford and in Appendix B of this study. [Williford 1985] FDTD models the propagation and interaction of an electromagnetic wave in a region of space that may contain any object. This method is different from the integral equation method in that it analyzes the interaction of the incident wave with a portion of the structure at a given instant in time rather than solving the entire problem at once. Yee first suggested the FDTD formulation for solving Maxwell's two curl equations (1) and (2), stating that the derivatives in these equations could be expressed as differences of the field values between neighboring positions, both temporally and spatially. [Yee 1966] These difference equations yield the values of the field at a given location in time and space if the values at all positions in the problem space are known at an earlier time.

Yee developed the FDTD algorithm in 1966 as a method to compute the waveforms of pulses scattered from infinitely long, rectangular cross section, conducting cylinders. [Yee 1966] Rymes used FDTD to analyze data from direct lightning strikes to a NOAA C-130 aircraft. [Rymes 1981] This code was later modified and used by Hebert and Sanchez-Castro to analyze the data from inflight lightning strike measurements by a CV-580 aircraft [Hebert and Sanchez-Castro 1987] and by Williford to explore the validity of different

boundary conditions using FDTD to model an F-16 aircraft. [Williford 1985] Williford, Jost and Hebert found using FDTD absorbing boundary conditions with FDTD produced better results than the perfectly electrically conducting (PEC) reflective boundary conditions originally used by Yee but at the cost of longer run times. [Williford, et al. 1986] It was during these efforts that the passion to find a less time consuming method to perform this type modeling and simulation was born. In 1984, at the request of his branch manager, then Lt. Hebert performed the analysis of CV-580 lightning interaction with aircraft data. Only a few iterations of the airframe's FDTD model, written in FORTRAN 77, were run over a period of weeks, but the bill from the centralized main frame computer center was over $180,000. This same analysis today could be performed at a small fraction of this cost on a standard PC using MATLAB^{TM}; but it would still take weeks to perform this extremely time consuming high fidelity analysis.

These efforts showed that FDTD was useful for the modeling and analysis of electromagnetic interaction with systems. This type code is easily adapted to a variety of materials in the problem space leading directly to its choice to analyze GPR data. FDTD is also regularly used in the analysis of the interaction of electromagnetic waves with test objects making it a clear choice for investigating the design of the bounded wave portion of the nuclear electromagnetic pulse/bounded wave simulator in the example of Chapter 4. In addition, nonlinearities and time-varying quantities can be represented in the problem space grid, if the needed equations can be written at the appropriate location. Finally, FDTD codes written in MATLAB^{TM} are easily adapted to parallel processing and multi-processor systems including graphics processing unit (GPU) processors. GPU-accelerated

computing is the use of a GPU together with a central processing unit (CPU) to accelerate scientific, analytics, engineering, consumer and enterprise applications. [NVIDIA 2015]

The solution of an electromagnetic interaction problem by the FDTD technique is straight forward. For our system model, the problem space is divided into a lattice of uniform sized cells. As shown in Figure 8, the gridding procedure involves placing the components of the electric (E) and magnetic (H) fields around a unit cell and evaluating the field components at alternate half-time steps. The electric fields are located on the edges of the box and the magnetic fields are positioned on the faces as shown in the Yee Cell. This orientation of the fields is known as the Yee cell. [Yee 1966] They are the basis for FDTD. Time is divided into small steps where each step represents the time required for the field to travel from one cell to the next. Because of the space between the magnetic fields and the electric fields, the values of the fields with respect to time are offset. The electric and magnetic fields are updated using a leapfrog scheme where first the all of the electric fields in the space and then all of the magnetic fields, are computed for each step in time.

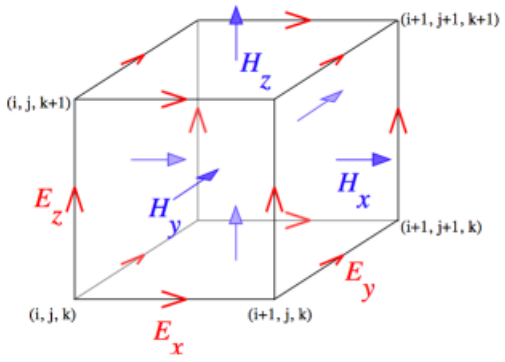

Figure 8. 3D Yee Cell [Yee 1966]

By alternating between the Electric (E field) and Magnetic (H field) fields, a central difference expression can be developed for both the space and time derivatives that

maintains a higher degree of accuracy than either a forward or backward difference formulation. The FDTD process flow is shown in Figure 9.

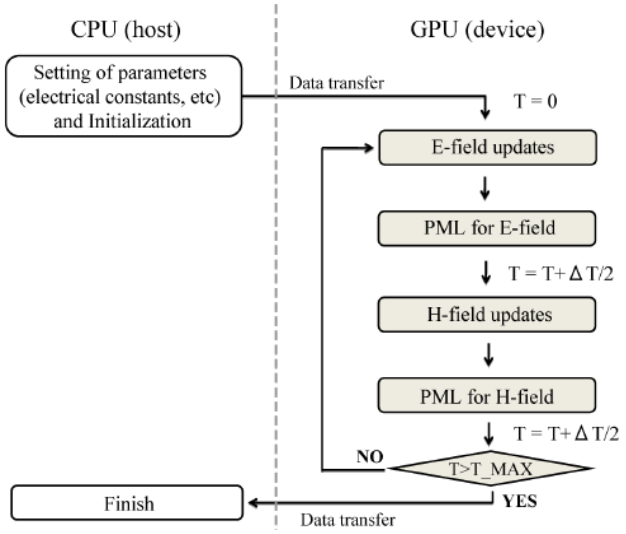

Figure 9. The FDTD Process Flow [Nagaoka and Watanabe 2010]

The problem solution proceeds by time-stepping throughout the problem space, repeatedly solving the finite difference form of Maxwell's two curl equations. In this fashion, the incident wave is tracked through the problem space as it intercepts and interacts with the targets, at layer interfaces and with other objects in the problem space. In other words, any item with material electrical and magnetic properties can be gridded up into the space and the interaction with source electrical field can be calculated. The cell size that makes up the problem space is the most important constraint in any FDTD model. It determines both the step size in time and the upper frequency limit for the calculation. In practice the cell's size is set so that 10 cell sizes equal the wavelength of the upper frequency of interest.

The major drawback for FDTD is the computation time required. Table II presents a summary of computation times for FDTD type problems reported by several researchers.

Table II. Runtimes for FDTD Examples

Researcher	What was modeled	Boundary Condition Type	CPU	Computer Memory	Number of cells	Number of Time steps	Time to complete simulation (min)	20,000 time steps (min)	40,000 time steps (min)
eField™ 2015	Pacemaker w/PIFA in human body	Absorbing	1 processor on AMD Dual Core Opteron 285 at 2.6 GHz	16 GB	358,200	20,000	80	80	160
eField™ 2015	Pacemaker w/PIFA in human body	Absorbing	2 processors on AMD Dual Core Opteron 285 at 2.6 GHz	16 GB	1,745,000	40,000	290	Unknown	290
Kawanda, et al. 2012	Acoustic waves using 4th order compact finite differences	Rigid totally reflection	Intel Core i7 processor 930 at 3.9 GHz	Unspecified	2,097,152	500	3.43	137.36	274.72
Kawanda, et al. 2012	Acoustic waves using 4th order compact finite differences	Rigid totally reflecting	Intel Core i7 processor 930 at 3.9 GHz	Unspecified	4,096,000	500	6.99	267.66	535.31
Kawanda, et al., 2012	Acoustic waves using 4th order compact finite differences	Rigid totally reflecting	Intel Core i7 processor 930 at 3.9 GHz	Unspecified	7,077,888	500	9.42	376.64	753.27
Kawanda, et al., 2012	Acoustic waves using 4th order compact finite differences	Rigid totally reflecting	Intel Core i7 processor 930 at 3.9 GHz	Unspecified	12,812,904	500	11.62	464.89	929.79
Kawanda, et al., 2012	Acoustic waves using 4th order compact finite differences	Rigid totally reflecting	Intel Core i7 processor 930 at 3.9 GHz	Unspecified	16,777,216	500	13.55	542.07	1084.15
Nagoaka, et al. 2010	Human body	8 layer perfect matching	Intel Xenon X5450 (3.0 GHz)	16 GB	14,760,420	Unspecified	104.92	unknown	unknown
Pinton, et al. 2012	Propagation through the human skull	unknown	UNIX Cluster 16 CPUs	128 GB	1.86×10^5	Unspecified	7200	unknown	unknown

All of the examples show that for one run using a set of input variables, it takes from 160 to 7200 minutes. This would be unacceptable if the system engineer needs to optimize the design or to decrease uncertainty in the systems performance. Pinton et al. provides insight into the very large computational cost of modeling the human brain. [Pinton 2012] They explain that the simulation for the setup shown in Figure 10 has approximately 1.86×10^9 grid points for each field variable. The custom parallelized FDTD simulation code, written in C, FORTRAN 77™ and Open MPI runs on a Linux cluster running a Cent OS 5 operating system with 16 CPUs and 128 GB of RAM. The run-time on this system is 120 hours." [Pinton et al. 2012] He also provides a view of the savings that can be realized by using a simpler interpolation model: "By comparison, the Delaunay interpolation scheme [Dulaunay 1934] requires on the order of one minute of computation time and it can run on a standard computer, with no special memory requirements". [Pinton et al. 2012] In Table II, eField™ provides another example of the modeling: n implanted planar inverted-F antenna for a cardiac pacemaker. [eField™ 2015]

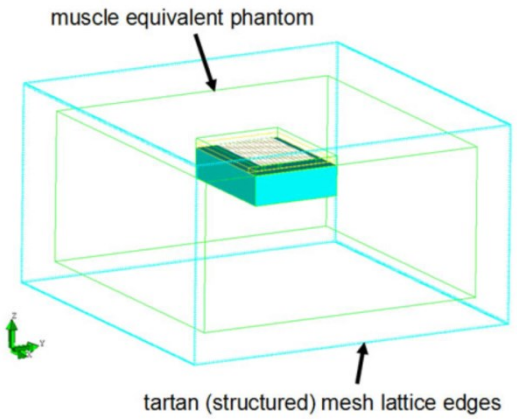

Figure 10. Tartan FDTD Meshing of a Pacemaker with PIFA Placed Inside Muscle Equivalent Phantom [eField™ 2015]

eField™ gives an example of the computation time for two FDTD model "fdtd1" and "fdtd2" with 1.6 mm and 0.8 mm grid cells sizes. Using the more accurate smaller size mesh it took 290 minutes (4.82 hours) for one run. To perform an optimization set of runs, 10,000 iterations would take 2013 days making the use of systems engineering tools practically impossible. Contrast this with using a surrogate model: to produce ten basis points for a surrogate model using the high fidelity FDTD would only take two days and to produce the 10,000 surrogate produced responses would take only a few minutes. To validate ten of the surrogate produced responses using the HF FDTD code at different chosen points would take two additional days. Like most physics-based computational models, FDTD is computationally intensive and most problems require a fast computer (such as today's i7 quad core processors) with a substantial amount of computer memory (16 GB RAM). Each FDTD cell identifies six unique fields and stores six material values (See Appendix B). This requires 30 bytes of memory for each cell: 24 for fields and six for material properties. The memory required is the number of cells times 30 plus about 10% for overhead functions. For execution time, it strongly depends on the performance of the computer processor. The total number of operations for each time step is roughly 80 (operations per cell) times the number of cells times the number of time steps. In one of the examples shown in Table II above, a problem space with 1,745,000 cells took 290 minutes to perform 40,000 time steps. This was on a computer with one processor on an AMD Dual Core Opteron 285 2.6 GHz with 16 GB memory. In contrast, surrogate models can provide highly accurate decision making information is a small fraction of the computation time when compared to using the high fidelity FDTD method to perform the same task. Modeling using FDTD techniques, although time consuming, has the advantage

in that it allows the observation of changes in response to changing input variables without the expensive cost of physical experiments and tests. But this high fidelity code, although very accurate, still suffers the problem of being very time consuming preempting its classical use for some systems engineering optimization methods. A more cost effective methodology is needed that includes the use of efficient multi-fidelity and surrogate models.

2.8 Systems Engineering

One of the most challenging tasks for a systems engineer is the efficient allocation of resources in time and costs for the optimization and performance evaluation/validation of complex physics-based systems such as those used in defense and transportation industries during their design and development. Recently time and cost limitations have resulted in the increased use of accurate high fidelity modeling and simulation. A typical physics-based system has a number of controlled and uncontrolled parameters that can have a significant impact on these type systems. By making small changes or variations in the nominal value of input parameters. Systems engineers can use sensitivity analysis to investigate how a system's output behaves due to variations in inputs parameters and to rank their importance in the output or performance. Oberguggenberger et al. discuss the sensitivity of output values in engineering models with respect to variations in the input parameters. They state that "Such an analysis is an important ingredient in the assessment of the safety and reliability of structures. A major challenge in engineering applications lies in the fact that high computational costs have to be faced. Methods have to be developed that admit assertions about the sensitivity of the output with as few computations as possible." [Oberguggenberger et al. 2008] A typical physics-based system has a large

number of controlled and uncontrolled parameters that can have a significant impact on the performance of the system. The systems engineer uses sensitivity analysis that applies small changes to the system's input value and determines the resulting change in the output response, to understand a system's behavior due to variations in the inputs and to determine how important variations in that input are. Final operational tests for physics-based systems and the use of high fidelity models and simulations are expensive and time consuming and may not allow the design and generation of sufficient data points to allow statistically valid conclusions at the required level of confidence. By applying an improved methodology that includes systems engineering, multi-fidelity and surrogate models, a more effective allocation of resources may be realized. Olvander discusses the usage of simulation-based optimization to support the design of complex engineering systems. He explains that: "To beat the competition to the market it is also necessary with a rapid system development process. For these reasons, the design of heterogeneous systems with great demands on functionality and safe behavior deserves a great deal of attention. Especially in the early conceptual phase of the design process, the designer needs efficient tools that make it possible to compare different design solutions and to analyze the whole system and not just a part. Tools are also needed, that can relate design decisions at detail level to high-level requirements in order to ensure traceability in the design. Figure 11 depicts a system design process where modeling, simulation and optimization are introduced to support and speed up the design process. In the proposed system design process, the iterative part of the design process is formalized and partly automated with the help of an optimization algorithm." [Olvander 2009]

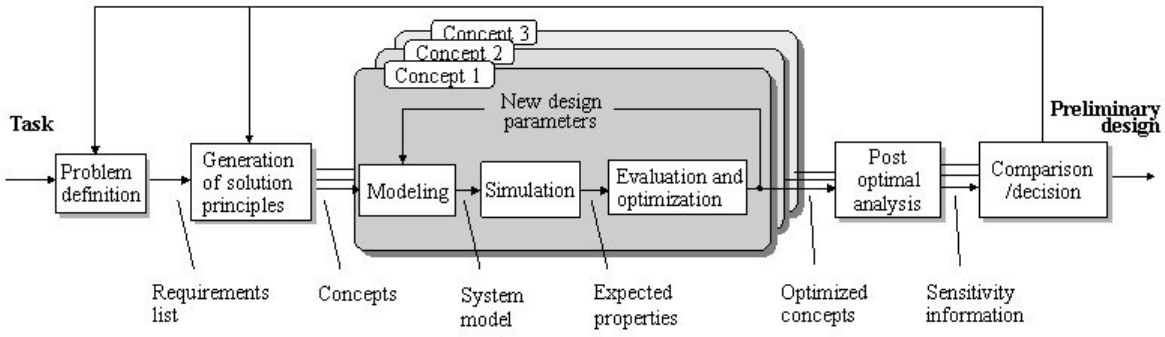

Figure 11. The System Design Process [Olvander 2009]

When exploring potential concepts for meeting the stakeholders' requirements, any already existing systems should be evaluated first. Identify any performance deficiencies that might require modification for the predecessor system to meet present or future needs. Pre-existing systems have the advantage of being easier to evaluate in terms of performance, development risks and costs. If a new system is required, systems engineers use modeling and simulation to analyze the system performance of candidate solutions then generate a set of optimal alternatives. Optimization requires the evaluation of system responses to inputs of the various designs.

The INCOSE defines systems engineering as "an interdisciplinary approach and means to enable the realization of successful systems. It focuses on defining customer needs and required functionality early in the development cycle, documenting requirements, then proceeding with design synthesis and system validation while considering the complete problem." [INCOSE 2011] Modeling of interfaces at multiple levels of abstraction aids in understanding system complexity [Bahill and Dean 2009] Systems engineering as a technical discipline needs both qualitative and quantitative tools/methods to understand customer requirements, explore design options, design robust

and optimized systems and validate designs in the intended environments. [Jehangir 2015] Jehangir explains that systems engineering "…. tools and methods can be broadly categorized by their use. The categories and some examples under these categories are shown below:

***Requirements Management*:** Model Based Systems Engineering (MBSE), Systemic Textual Analysis, Viewpoint Analysis, Quality Function Development (QFD), Functional Modeling, Need Means Analysis, Function Means Analysis, Holistic Requirements Model, Stakeholder Map

Design: Heuristics, Taguchi Method, Design Structure Matrix (DSM), N2 Analysis, Matrix Diagram, Value Stream Mapping (VSM) Project

Management: Earned Value Management System (EVMS), Gantt Chart, Program/Project Evaluation Review Technique (PERT), Suppliers, Inputs, Process, Outputs and Customers (SIPOC)

Problem Solving: System Optimization, System Dynamics, Ishikawa Diagram, 5 Whys, Quality Clinic Process Chart (QCPC), Relentless Root Cause Analysis (RRCA), Mistake Proofing; Functional Failure Mode and Effects Analysis

Collaboration: Next Generation Technology (NGT), Multi-Factor Analysis (MFA), Affinity Diagrams, Context Diagram, Benchmarking

Decision Making: Risk Cubes, Cost-Risk-Benefit Analysis, Pugh Matrix" [Jahangir 2015]

Categories that are missing from his list are those concerned with the systems engineering tool used for the design and development of physics based systems. The following categories are missing from his list of systems engineering tools. They are tools that are used for the design and development of physics based systems.

Modeling and Simulation: Reverse engineering, optimization, sensitivity analysis, uncertainty analysis.

Statistics: parametric studies, statistical models.

Statistical systems engineering methods are used to understand and optimize parameters and reduce uncertainty. Ranges of allowed variables found in the simple fidelity models are transferred to models of high fidelity. While statistics plays a significant role in decision making with each fidelity level of models and simulation, it is particularly important at the primary level and intermediate level. "This is particularly true when:

(1) It is impossible or too expensive to replicate the threat environment or the operational environment in which the system must operate such as nuclear EMP or Space.

(2) Extremely complicated physical systems whose mathematical models result in high order of difference equations.

(3) Field test and evaluations are limited due to a limited number of test systems, the cost of testing or other constrained program resources.

Statistics facilitates the evaluation and analysis of system performance by decreasing the uncertainty and risk with each increasing fidelity level of models and simulation." [Carson 2004]

These and other systems engineering techniques can be applied in the design and development of complex physics-based systems to improve the design cycle time and reduce risk during final system development and integration. There are many sources that discuss the classical systems engineering "V-model" shown in Figure 12. This model is a traditional way to visualize the systems engineering process.

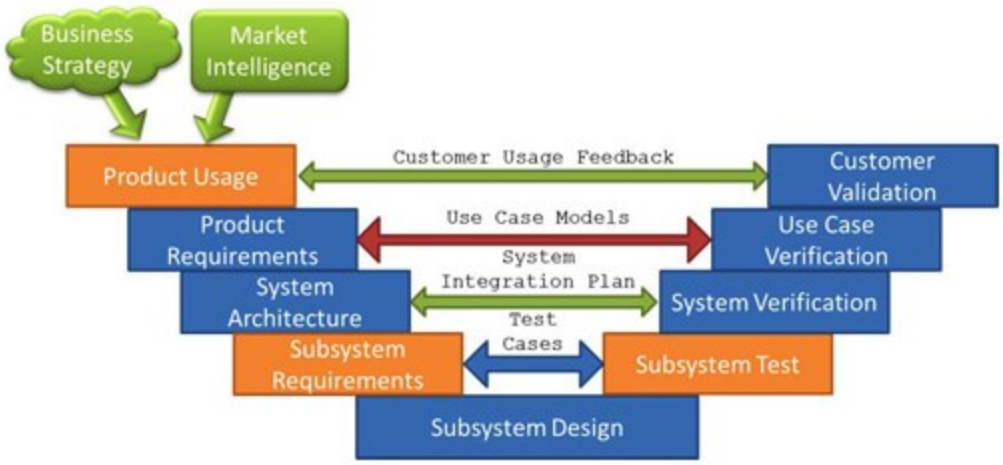

Figure 12. Continuous Feedback in the Development Cycle [Torgerson 2013]

Using less time consuming models, while reducing the number of high fidelity models and high fidelity runs required can directly support the Systems System Decision Process by allowing the use of classical systems engineering tools. The Systems Decision Process was developed by the Parnell and Driscoll at the Department of Systems Engineering, U.S. Military Academy show here in Figure 13.

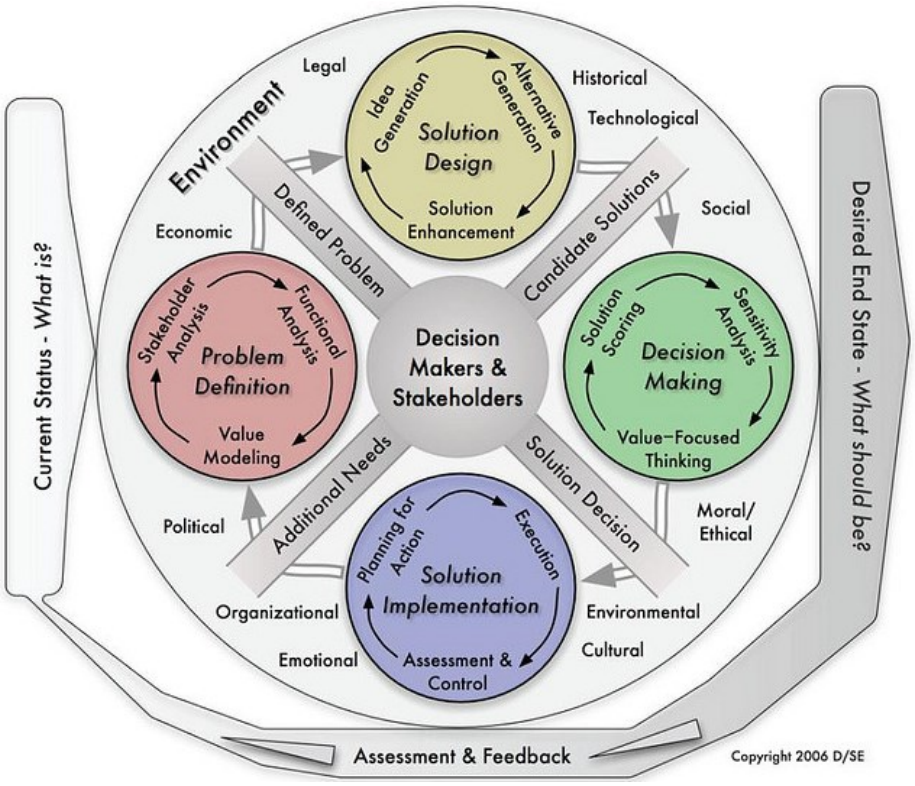

Figure 13. System Decision Process [Parnell 2008]

Their decision process has four phases that take the system from the present state to the desired end state. These phases are 1) Problem Definition, 2) Design and Analysis, 3) Decision Making and 4) Implementation. As shown in Figure 13, the process begins with the current state. If a system already exists it becomes the baseline for modifications or candidate new systems. Decision makers and stakeholders determine critical metrics for evaluating potential solutions. Defining the final system desired and its attributes, decisions are made by evaluating the output of models that simulate the system performance of alternative solutions. The Parnell process depends strongly on the feedback from stakeholders and decisions during all four phases of the systems development. [Parnell 2008]

Systems engineering tools, like the ones listed above, are used during the system architecture and subsystem design to drive the system architecture and subsystem definition is a way that best suits the needs of the stakeholders or customers. In the System Decision Process, these tools are particularly important during the system design analysis based upon the modeling and simulation of the physics-based system. Using high fidelity models to design a complex physics-based system could take years to perform the simulations required for the systems engineer to develop baseline system alternatives. If only high fidelity models are used this type of system during these activities, there likely will not be enough quality system performance data to analyze and optimize the system's design. For this reason it is vital that a methodology be developed that will decrease the use of time consuming high fidelity models and replace them with multi-fidelity, meta, or surrogate models; provide the required response data in the quantities required to allow analysis with systems engineering tools and techniques for optimization of system performance in terms of customer's needs; and allow the design and development of the physics-based systems in cheaper and much short time periods.

Chapter 3 - A Framework for Reducing Cost of Physics-Based Systems

In this chapter, we present a framework where modeling and simulation using multi-fidelity and surrogate models provide significant time savings and allow the use of systems engineering tools to optimize the performance of the physics-based systems. Because of their accuracy it is easy to know when to use high fidelity models: anytime you have the time and resources to use them. Multi-fidelity models and surrogate models are widely used to estimate a system's performance, particularly in the early design stage, due to their ability to reduce the time and cost of modeling and simulation for design exploration. In applying modeling and simulation there are many situations where modeling and low fidelity models and simulations are appropriate. Some common guiding principles found in the literature review include:

- It is important to apply modeling in a way that maximizes its impact; otherwise someone will say it is too expensive.
- Introduce modeling early on when it can really make a difference. [Nopper 2012]
- Use the lowest fidelity model that answers the question.
- Use low fidelity models to identify controllable and uncontrollable inputs.
- Most problems are ill-defined at onset. Use low fidelity models to:
    - Identify constraints on the decision variables.
    - Define measures of system performance and an objective function.
    - Determine a range of potential solutions.
- Use low fidelity models to interrelate the inputs and the measures of performance.
- Use low fidelity models and simulation to define what is important and what is not and how important various parameters are.

- The low fidelity models provide insight and good test cases for later higher fidelity models.
- Low fidelity models allow investigations of the sensitivities of the models to variations in controlled and uncontrolled inputs.
- Low fidelity models allow the use of statistical systems engineering methods to understand and optimize parameters and reduce uncertainty.
- Ranges of allowed variables found in the lower fidelity models are transferred to models of high fidelity.

As the system's development enters the analysis of alternatives phase, higher fidelity models and simulations may be required to compare each candidate system's performance, to identify road blocks and to provide decision makers with data upon which a selection might be made. At each level, statistics are often used to assist in these decisions. The final system(s) are modeled and their performance is simulated using very high fidelity physical models such as three dimensional finite difference codes and other commercial codes. This chapter suggests a framework for the design and development of physics-based systems.

3.1 Modeling Framework

For the design and development of physics-based complex systems, a modeling framework that prescribes using the lowest fidelity model that answers the question and suggests surrogate models in place of HF computational codes is presented in Figure 14. This framework allows the choice of using a surrogate with each different increasing fidelity physical model. The potential savings from employing this framework includes: (1) the reduced cost of using less complex lower fidelity physical models; and (2) the

reduced cost of employing a surrogate model in place of codes at all levels of fidelity. For a particular system's design, the modeler may end up using two or more different physical models of increasing fidelity. The answers obtained from these lower fidelity models may decrease the number of times the computationally expensive higher fidelity code must be run and the choice of surrogate models at each level can reduce computational time and expense even further.

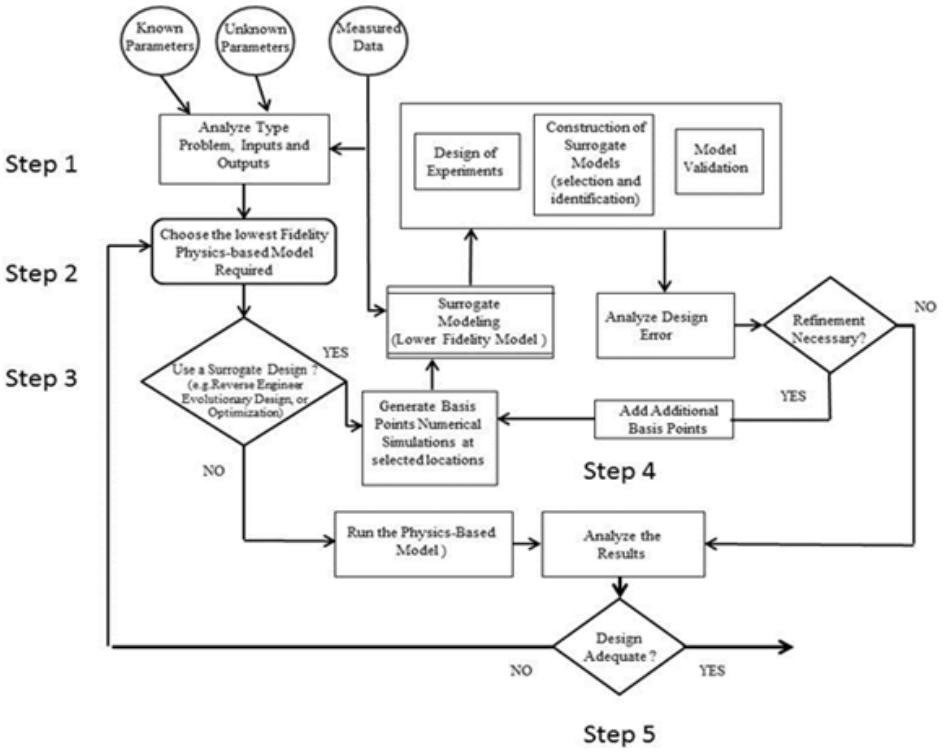

Figure 14. Multi-Fidelity and Surrogate Model Framework

3.2 Detailed Steps

Step 1. Parameter Identification. In a design problem, "we are interested in calculating the values of certain parameters, $\hat{p}$, from the set of parameters, p, given known inputs i and desired output value, o, and a fixed structure, M. This type of problem is normally solved by using an optimization technique which finds the parameter values which

generate the desired outputs. It is also called a specification problem." [Cameron 2001] During this step, the modeler identifies and compiles the known and unknown inputs, outputs and measured parameters. The known parameters may include information from:

(1) earlier developed systems,

(2) system performance and other requirements,

(3) engineering experience of subject matter experts and

(4) other sources.

Parameters that require reverse engineering are usually unknown. Measured test data from similar systems or previously built systems is often used to modify or improve an existing system. Measured data is often used to reverse engineer the lumped parameters of the lowest fidelity physical model. "The reverse engineering problem is formulated in fashion of an optimization problem where the unknown material (variable) properties are included as design variables." [Zhu 2008]

Step 2. Use Subject Matter Experts. The systems engineer uses subject matter experts to assist in the choice of physics-based models. Model selection can be as much an art as it is a science. With a clear understanding of the questions and how models can answer them, the experts provide insights based on heuristics into what a model can and cannot do. "The model is developed with the view that the system is exercised under varying conditions with varying inputs. As the outputs unfold, their results are recorded and tabulated so as to review appropriate responses when similar conditions and inputs are present in the model". [Sokolowski 2012] If not sure which model is best, several models can be tried at a fraction of the cost of running the HF computational models. To reduce runtime computation cost, the lowest fidelity model that answers the question is used.

Step 3. Choice to use a Surrogate Model. The actual steps for selecting and using surrogate models is presented in Section 2.4. In designs that require reverse engineering, an evolutionary design, or system optimization, cost reduction may be realized by using a surrogate model in place of the corresponding selected physics-based model. If a surrogate model is selected, the physics-based code is run a few times to generate a limited number of sample basis points that are selected by a design of experiments. The surrogate model is constructed and the model is run then validated using error checking techniques such as mean squared error. "When the deterministic expensive EM code is used for reverse engineering, evolutionary design or for parameter optimization development then the use of surrogates, like the Kriging method that can reduce cost, time and effort should be considered." [Bohling 2013] An efficient surrogate model requires less computational resources and time than the corresponding physics-based model. For the example in this study, a Kriging surrogate model is used to reverse engineer and optimize input parameters based on an output measured data waveform from a NEMP/BWS. The procedures for selecting and using Kriging and other surrogate models are presented in several of the papers cited in Chapter 2.3 and some are highlighted in Table I. If no surrogate model is needed, then the surrogate model steps are by-passed and the physics-based model is used.

Step 4. Analyze. In this step, the results from simulations using multi-fidelity physics-based models and/or surrogate models are compared and analyzed. Repeating what was presented in Step 4 of Section 2.4.: Evaluate the accuracy of the surrogate model. Try the selected surrogate model with the basis points and compare the interpolated response or output data of the surrogate model to the output of the high fidelity model at a number of points other than the original basis points. Determine the mean squared error between the

surrogate model's predicted output points (other than the basis points) and the same points using the high fidelity code. If too large input additional points into the surrogate model or proceed to step 5 in order to choose a different physics-based model of higher fidelity.

Step 5. Decide. In this step, the modeler must decide if the model's output or results have adequately answered the problem or question, namely "was the lowest fidelity model that meets the stakeholder's needs correctly chosen and will the stakeholder be satisfied and trust the resulting model and simulation?" If the answer is positive, then proceed with the acquisition of the system. If the answer is negative, then go back and choose a higher-fidelity physics-based model and repeat Steps 2 through 5. Each time the design loop (Steps 2 – 5) is run, there is a choice if a surrogate model should be developed and employed. If the surrogate produces an output that mimics the underlying high fidelity model's output as closely as needed over the entire design space, it provides a useful, cheap model that can be used instead of the time consuming high fidelity model to gain insight into the total behavior of the system over the entire design space. For the NEMP/BWS example presented in Chapter 4, three physics-based models of increasing fidelity were employed. A Kriging surrogate model was used with a MATLAB™ electric circuit model and again with the very HF FDTD model, but not with the PSPICE™ model.

Chapter 4 - Results of Applying the Framework

Two examples of the methodology developed during this study are presented. One demonstrates only the multi-fidelity portion of the framework and the second shows the entire framework. The modeling framework was used to design and/or modify two real world examples. The first is a relatively simple GPR system and the second is a study capstone example: a NEMP/BWS, a complex electromagnetic system. Modeling and simulation results of a system analysis using high fidelity FDTD techniques are presented. The analysis for the GPR example was performed early in the research phase and investigated only the use of multi-fidelity models for investigating the electromagnetic reflections of target objects buried in the ground. When this research was performed the framework developed in this study did not include the choice of using surrogate models so they are not included in this example. The requirements and the measured data from that activity were used herein to apply, design, demonstrate and validate the models resulting from the application of the cost reducing multiple fidelity physics-based electrical and EM models. The NEMP/BWS example includes a design and development problem that employs the entire framework including both multi-fidelity and surrogate models to reduce the number of time consuming high fidelity model runs required.

4.1 GPR Example

The increasing fidelity methodology presented in this study lends itself well to the design and development of physics-based systems like Ground Penetrating Radars. Investigations performed early in the research phase of this study include multi-fidelity models of a GPR's performance. These experiments make purposeful changes to the GPR's propagation model inputs such as conductivity and permittivity. The resulting changes in

the output response are identified and reported. These changes are optimized to enhance the GPR's ability to detect and identify buried objects. This subsection provides an example of how the propagation of GPR systems can be modeled using multi-fidelity models.

Performance issues with GPRs need to be isolated in order to optimize the radar's ability to detect and identify buried objects. Using a systems engineering approach, FDTD models were used to characterize the variables associated with the GPR to improve GPR detection processes so that they were minimally affected by external sources of variability. These experiments make changes to the GPR's inputs while measuring the output response to identify issues and optimize performance. FDTD computer simulations produce idealistic environments that allow examination of the individual effects on the response. This example provides a systems engineering overview of the operations and processes of GPR systems and how MATLAB^{TM} based FDTD computer simulations can be used to model and improve them.

4.1.1 Ground Penetrating Radar Models

Ground penetrating radar systems are used in many areas as a nondestructive investigation tool including soil management, archeology, mine clearing and infrastructure evaluations. The over-arching requirement of a GPR is to detect objects buried in the ground. Different fidelity level models and simulation can be used to perform the system analysis required to isolate and understand the factors that affect a GPR's ability to detect and identify these buried objects. These GPR computer models and simulations allow the systems engineer to design a GPR to do what they should do without carefully controlled field experiments that are costly in terms of time and other resources. The effects of

changing simple variables such as surface and soil constituent properties on the GPR radar's output are not separable. Often the effects are unidentifiable in measurements made under field conditions. A synthetic data set produced by FDTD computer simulations allows the separation of input variables to better understand their effects on the output response of the radar. These simulations produce idealistic environments and test configurations to allow close examination of the individual effects of these variables on the response. This example presents a version of FDTD code that has been implemented in MATLAB™ to model and simulate a GPR's performance. This version of the code is intended for use by researchers to observe, analyze and understand how different system input variables affect the GPR and its performance.

Modeling the GPR as a system using multi-fidelity models allows a set of specially designed experiments where deliberate changes are made to the input variables so that changes in the output response can be observed and performance limiting issues can be easily identified. Three MATLAB™ models and simulations are presented in this section of the dissertation:

(1) A model for calculating the Fresnel reflection and transmission coefficients for perpendicular and parallel polarity incident waves as a function of grazing angle,

(2) A one-dimensional (1D) Finite Difference Time Domain (1D-FDTD) model for comparison with the Fresnel model and

(3) A three-dimensional (3D) Finite Difference Time Domain (3D-FDTD) FDTD model to allow simulation of the response to the GPR of changing various inputs.

The amount of energy that is reflected at the boundary of two media (e.g., soil and buried target) with different permittivity is given by the Fresnel coefficient. The changes

in output response were observed while controlling various input variables. The initial results of controlling the conductivity and permittivity of the soil and targets are presented. Conductivity is a measure of a material's ability to conduct an electric current. Permittivity relates to a material's ability to transmit (or "permit") an electric field.

David Montgomery states that one of the applications of experiment design is the identification of design parameters that work well over a wide range of conditions in order to determine the design parameters that most impact product performance. [Montgomery 2009] Variables to be considered in simulation of the GPR as a system are:

(1) radiated waveform,

(2) depth of penetration versus frequency,

(3) transmitter antenna type,

(4) height and grazing angle,

(5) surface, soil and target properties,

(6) target characteristics,

(7) clutter,

(8) moisture content,

(9) interference,

(10) receiver antenna type,

(11) signal collection resolution and rate,

(12) signal processing techniques and

(13) optimizing response of all input variables to maximize detection and reduce false alarm rate.

Our initial research focused on two input variables that were found to greatly affect the GPR's output response: conductivity and permittivity. A detailed examination of the response of the system to changing these two input variables allowed for optimization to obtain the most accurate possible output response. The systems engineering goal of this modeling and simulation effort is to define what a GPR system should be based on the systems response to input variables rather than applying a classical approach of determining of what a GPR can be by building and measuring the system's performance.

4.1.2 GPR System Analysis

This section discusses the motivation for using the SE tools of modeling and simulation in the development of the systems engineering GPR computer model and the selection of FDTD techniques to perform the system simulations and analyses. Surface penetrating active sensors (SPAS) such as GPR and ultrasound have hundreds of real world applications for their ability to "see into" and characterize solid and semi-solid substrates. As such, they are highly desirable functional components for a growing number of advanced systems. The computer models and mathematics for surface penetrating active sensors can be quite involved with only a few sensor models developed for specific instruments, for specific applications and/or for specific environments of use. To date, no general sensor system characterization models exist that can deterministically characterize sensor technology or examine the parametrics and tune in a response to an intended environment of use and a desired target resolving capability. The ability to deterministically match system sensing needs to SPAS capabilities would be of great interest to the systems engineer. At present, it is very difficult for all but the most highly trained experts to know what SPAS capabilities might work under what given set of

conditions. This example using multi-fidelity models presents an extensible approach towards the allocation of sensing performance requirements to SPAS solution technologies determined by analysis of the system's responses to changes in various input parameters. [Hebert et al. 2012]

The goal of this systems engineering analysis is to identify GPR system deficiencies and what can be done to improve the system's performance. Five important steps in the systems engineering process include:

(1) critical needs are identified,

(2) current capabilities are assessed,

(3) new or existing capabilities are explored,

(4) prototyping or modeling and simulation are implemented and

(5) final system deployed.

The multi-fidelity models for this research facilitate the system analysis required by steps 2, 3 and 4 in the engineering process. This approach could provide the systems engineer with a requirements-driven solution synthesis by better characterizing and populating the architectural trade space with valid SPAS alternatives that represent a range of possible SPAS solutions.

To analyze the GPR as a system we must first understand the components and functions of the GPR. This radar is used for the detection of objects buried below the surface. A simplified model of the GPR consists of a transmitting and receiving antenna, a source connected to the transmitting antenna and signal processing equipment connected to the receiving antenna. The type of antennas, choice of the transmitted signal and method of signal processing are all system variables that affect the output response and

performance of the GPR. As such each is a candidate for optimization as part of the GPR's system architecture and design.

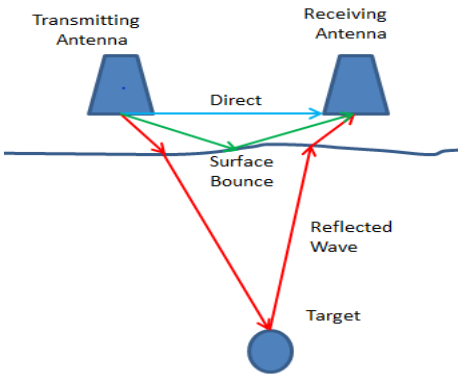

Figure 15. Schematic drawing of typical GPR [Hebert et al. 2012]

Figure 15 shows a GPR system and operating environment with the signals that are generated by the system. Filtering out the interference caused by the direct and the ground bounce signals in order to see the reflection of the return from the target may be necessary. The operating environmental variables that must be modeled in a GPR simulation include the two antennas, the electrical characteristics: permittivity, ε, conductivity, σ, and permeability, μ, of the air above the surface, the subsurface and the target. Other variables include the height above the surface of the antenna, the separation distance between the antenna and the depth of the target. Most of these variables are related or dependent on the other variables such that modeling them one at a time would cause unaccounted for errors in the output response. The best that can be done is to control the variables one at a time, while including all the variables in the GPR model and simulation. The research presented here includes a 3D-FDTD system analysis of the GPR that accounts for many of these variables simultaneously within the problem space.

Table III. Relative permittivity, ε_r. and EM velocity for selected geological materials [Baker 2007]

Material	ε_r: Davis and Annan (1969)	ε_r: Daniels et al. (1995)	Velocity (m/ns)	Velocity (ft/ns)
Air	1	1	0.3	0.96
Distilled water	80		0.03	0.11
Fresh water	80	81	0.03	0.11
Sea water	80		0.03	0.49-0.57
Fresh water ice	3-4	4	0.15-0.17	0.35-0.49
Sea water ice		4-8	0.11-0.15	0.28-0.35
Snow		8-12	0.09-0.11	0.35-0.50
Permafrost		4-8	0.11-0.16	0.40-0.57
Sand, dry	3-5	4-6	0.12-0.17	0.18-0.31
Sand, wet	20-30	10-30	0.05-0.09	0.57-0.70
Sandstone, dry		2-3	0.17-0.21	0.31-0.44
Sandstone, wet		5-10	0.09-0.13	0.35-0.49
Limestones	4-8		0.11-0.15	0.37
Limestone, dry		7	0.11	0.35
Limestone, wet		8	0.11	0.25-0.44
Shales	5-15		0.08-0.13	0.33-0.40
Shale, wet		6-9	0.10-0.12	0.18-0.44
Silts	3-30		0.05-0.13	0.18-0.44
Clays	5-40		0.05-0.13	0.16-0.44
Clay, dry		2-6	0.12-0.21	0.40-0.70
Clay, wet		15-40	0.05-0.08	0.16-0.25
Soil, sandy dry		4-6	0.12-0.15	0.40-0.49
Soil, sandy wet		15-30	0.05-0.08	0.16-0.25
Soil, loamy dry		4-6	0.05-0.08	0.40-0.49
Soil, loamy wet		15-30	0.07-0.09	0.22-0.31
Soil, clayey dry		4-6	0.12-0.15	0.40-0.49
Soil, clayey wet		10-15	0.08-0.09	0.25-0.31
Coal, dry		3.5	0.16	0.53
Coal, wet		8	0.11	0.35
Granites	4-6		0.12-0.15	0.40-0.49
Granites, dry		5	0.13	0.44
Granites, wet		7	0.11	0.37
Salt, dry	5-6	4-7	0.11-0.15	0.37-0.49

One variable that has a large impact on a GPR's performance is the permittivity. Table III shows the relative permittivity and electromagnetic wave velocity for common subsurface materials. The amount of energy that is reflected at the boundary of two media with different permittivity is given by the Fresnel coefficient. For air to soil with permittivity, ε_r, and permeability, μ_r, the index of refraction (Fresnel reflection coefficient) is described by:

$$n = \sqrt{\frac{\epsilon\mu}{\epsilon o \mu o}} = \sqrt{\epsilon_r \, \mu_r} \tag{5}$$

This relationship is used to illustrate the changes in the electromagnetic waves at the interface of two materials with different permittivity and permeability in the results section below. One observes that electromagnetic waves pass through the earth and the receiving antenna records the timing and magnitude of the arriving energy. A GPR image is actually an image directly related to the dielectric properties of the subsurface. The dielectric constant controls the velocity and the path of electromagnetic waves, including those reflected off objects below the surface.

There are many versions of the 3D-FDTD code. Some are readily available for download on the internet. Commercial versions of the code and versions that are reported in scholarly journals come in packages that are not open source, and are not available for researchers. For this reason, a GPR model and simulation program implementing FDTD techniques was developed in MATLAB™.

Many different algorithms exist for target detection and identification, noise and interference suppression, removal of direct and air wave effects and correction of attenuation losses. The input data for the research and comparison of these algorithms is provided by the FDTD techniques implemented in the MATLAB™ code.

Many different algorithms exist for target detection and identification, noise and interference suppression, removal of direct and air wave effects and correction of attenuation losses. The input data for the research and comparison of these algorithms is provided by the FDTD techniques implemented in the MATLAB^{TM} code.

Previous researchers have successfully used 3D-FDFD techniques to investigate some aspects of a GPR's performance. [Yee 1966, Belli 2010] While helpful, these studies produced only limited results. Under some physical soil conditions, the recognized landmine signature, a typical target, possesses high quality contrast while under other conditions no signature is detected. Fritzsche demonstrated via modeling that GPR signals at 900 MHz would be strongly attenuated in moist soil. [Fritzsche 1995] Trang found through simulations and experiments with a GPR emitting signals operating at 600-800 MHz, that nonmetallic mines were easier to detect in moist soil.

The FDTD computer model implemented as part of this study facilitates the analysis of complex dielectric constant of soil and attenuation of GPR signals. In addition, the system model is capable of plotting the complex dielectric constant of soil coupled with the attenuation of GPR signals versus soil physical properties.

To predict the performance of electromagnetic sensor sub-systems, it is common practice to use models that estimate the soil's characteristics including dielectric properties. Trang found that no current model exists to completely describe all the electrical properties of a soil type. [Trang 1996] Measurements to baseline GPR operational performance made at many sites worldwide are helpful but still leave a great deal unknown due to uncertainties caused by factors such as soil composition, layering, clutter, rock and other undesired artifacts recorded in the measurement. Alternatively, the FDTD computer models and

simulations allow the variables associated with GPR systems to be researched and characterized.

FDTD techniques model many variables that are controllable while some variables are not. Using FDTD synthetic data allows one to control what might otherwise be undefined or uncontrollable variables. The systems engineering goal for the simulations is to find bounds for the input values of the uncontrollable variables which make the systems performance predictable and manageable. Thus a GPR system design can be optimized to effectively handle a wider variety of operational conditions.

Figure 16 shows a B-mode image of pavement thickness. A B-mode image is produced by sweeping a narrow beam while transmitting pulses and detecting echoes along a series of closely spaced scan lines. The algorithm for B-mode image simulation and processing includes calculation of the amplitude and two-way time delay of a signal reflected from each layer of a multi-layered media; simulation of echo signals, clutters, speckle and impulse noise; construction of a synthetic range profile; and image formation.

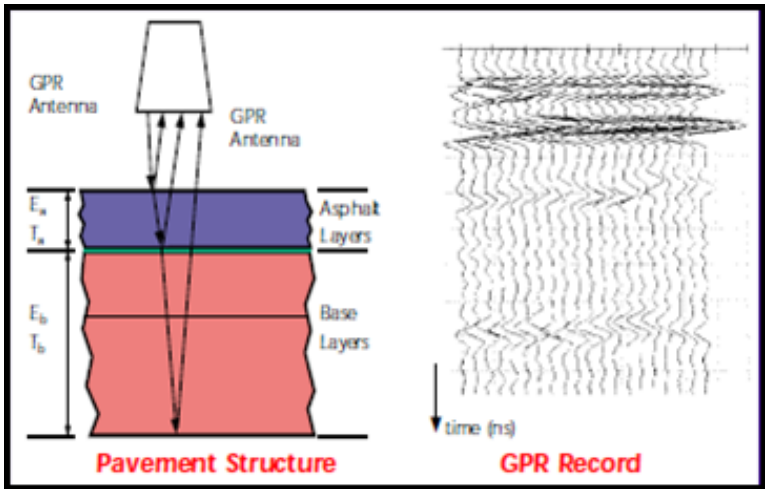

Figure 16. Example of a B mode plot [DOT 2015]

Belli et al. provided an excellent example of a subsurface tunnel modeled in FDTD, as illustrated in Figures 17 and 18. [Belli et al. 2010]

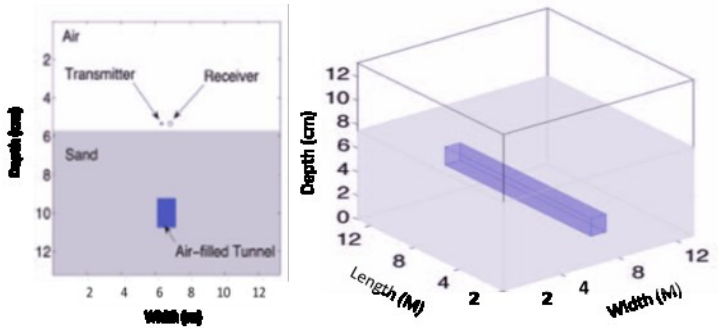

Figure 17. 3D tunnel geometry and detail of y − z plane indicating sensor location when θ = 0° [Belli et al. 2010]

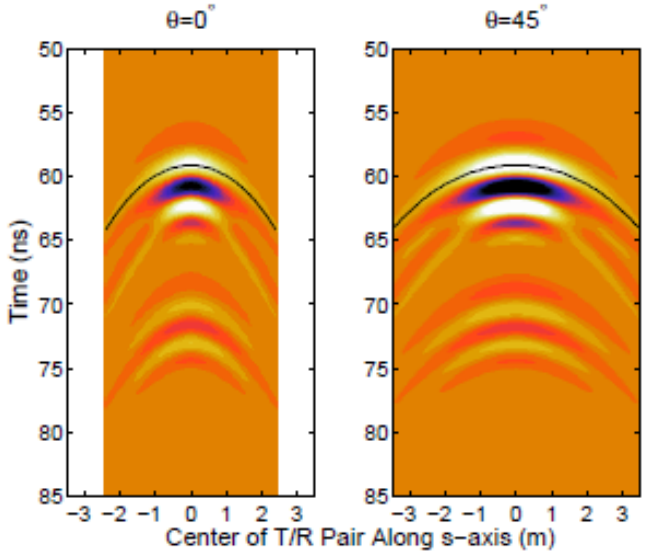

Figure 18. 3D-FDTD simulated B-scan contours
(air-filled tunnel buried in sand with backgrounds removed) [Belli et al. 2010]

These simulations show how measured GPR data can be faithfully modeled in FDTD and how FDTD simulations can be used to model a GPR system's performance. It shows that the FDTD model produces Typical B-scan contours and the extracted

hyperbolas for the tunnel example that can be seen in Figure 18 with the background reflection at the air/sand interface removed. Four angles are selected for 3D B-scan simulation: 0°, ≈23.96°, 45° and ≈ 53.13°. The hyperbolas extracted from the B-scan simulations were compared to a library of hyperbolas generated by 2D FDTD to determine the angle of the GPR waves travel path. By comparing the angles from the simulations with measured data, these angles were found to produce the B-scans that most closely match the measured ones. The results are summarized in Table IV. The determined angles are well matched to the actual angles. Again, and as expected, the case of $\theta = 45^{\circ}$ results in the largest error in determined θ.

Table IV. Tunnel Example Correlation Results [Belli et al. 2010]

3D simulation angle, Θ	Best 2D correlation	Maximum error (distance from tunnel in *s*-direction)	Mean error
0°	0°	180.0 ps at 2.25 m	73.9 ps
arctan (4/9) ≈ 23.96°	24°	93.8 ps at 2.63 m	38.0 ps
45°	24°	152.1 ps at 3.39 m	47.8 ps
Arctan (4/3) ≈ 53.13°	54°	535.9 ps at 4.0 m	206.2 ps

4.1.3 Simulation Results

This section contains the results of MATLAB™ Fresnel reflection coefficient models and TDFD models and simulations that clearly demonstrate, at different levels of fidelity, how the researcher can vary the media and targets buried in the media to systematically evaluate the GPR's performance. Using the framework, without surrogate models, simple models like the ones presented in these simulation results are used to evaluate individual

variables and that the higher fidelity FDTD model provides highly accurate results of the GPR's performance.

Dependence on Frequency: System analysis begins by selecting one input and determining its effect of the system's performance. If one extends the analysis of system inputs to the effects of frequency on the depth and resolution like that presented by GST, the results shown in Table V show the relationship between resolution, "blind" zone and reflection depth with reference to the antenna used. [GST 2012] The simulated measurements are made in a media whose relative dielectric permittivity, $\varepsilon_r = 4.0$ and the specific attenuation is 1 to 2 dB/m. Reflection depth is the detection depth of a flat boundary with reflectance equal to 1.

Table V. Frequency Dependence [GST 2012]

	Antenna						
Parameter	**2 GHz**	**900 MHz**	**500 MHz**	**300 MHz**	**150 MHz**	**75 MHz**	**38 MHz**
Resolution, m	0.06-0.1	0.2	0.5	1.0	1.0	2.0	4.0
"Blind" zone, m	0.08	0.1-0.2	0.25-0.5	0.5-1.0	1.0	2.0	4.0
Depth, cm	1.5-2	3-5	7-10	10-15	7-10	10-15	15-30

Controlling Conductivity: The 1D-FDTD model, a one-dimensional version of FDTD, allows one to investigate the effect of controlling one variable at a time. Figure 19 shows the results of a FDTD simulation where the specific conductance, σ, of the media is controlled and set to 5.0 Siemens/meter, the relative electrical permittivity, ε_r, set to 1.0, the frequency set to 2 GHz and with a grid dimension of $dx = 0.75$ cm or 20 divisions per wavelength. The figure shows the attenuation of the fields in this media as function of time.

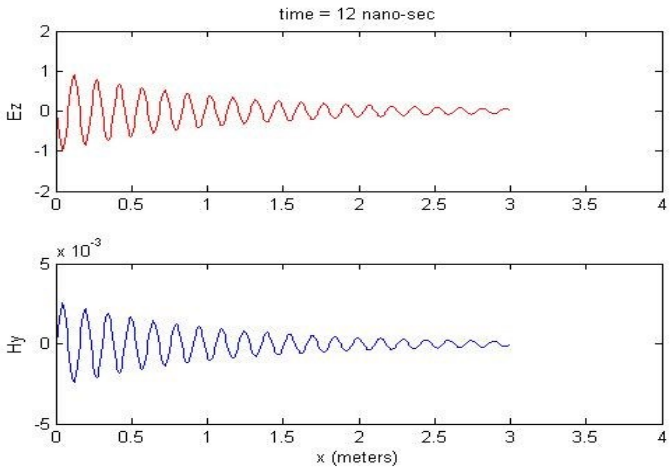

Figure 19. Example of Controlling Sigma

Controlling Permittivity: Another example of system analysis by controlling one variable at a time is the constituent property of permittivity. Permittivity is a property that describes the ability of the media to store electric charge. It can also affect the frequency, wavelength, or amount of energy that is transmitted or reflected.

A graphic showing the boundaries and reflections from layers of different permittivity is shown in Figure 20. The reflection and transmission of the electromagnetic waves at each earth media layer interface depends upon the difference of the permittivity of each layer. The signal received by the GPR receive antenna sub-system is a mixture of the reflection and delays propagating through the multi-layer paths. A representative profile for the different layers is presented.

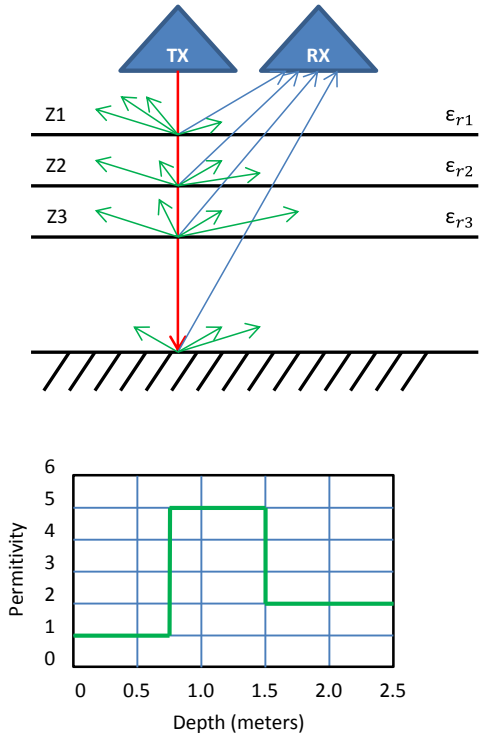

Figure 20. Controlling Permittivity [Hebert et al. 2012]

The reflection and transmission coefficients for two layers with relative permittivity's of $\varepsilon_{r1} = 2.0$ and $\varepsilon_{r2} = 4.0$ is shown in Figure 21. The reflection and transmission amplitude coefficients are shown for both perpendicular and parallel polarizations of EM waves incident from normal to 90 degrees. For $\varepsilon_{r1} = \varepsilon_{r2}$, there is total transmission and no reflection.

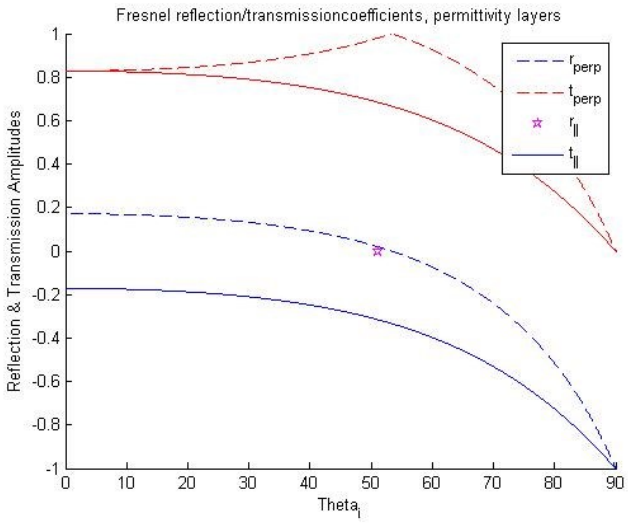

Figure 21. Fresnel reflection and transmission coefficients [Hebert et al. 2012]

Figure 22 shows the ability of the single dimensional 1D-FDTD simulation to model the effects of different values of permittivity on the propagation of electromagnetic waves. The specific conductance of the media is set to $\sigma = 0$ Siemens/m and the value of permittivity is controlled at $\varepsilon_r = 1.0$ and $\varepsilon_r = 10$. The media is nonmagnetic with permeability equal to free space, μ_0. The simulation shows how ε_r affects both the frequency and the speed of propagation. Both graphs show 12 nano-seconds of propagation. The higher the ε_r, the slower the wave propagates. This delay gives insight into how deep a reflecting target might be if the ε_r is known or a method to determine the ε_r if the depth of the reflecting object is known.

Using the multi-fidelity framework presented in Section three, this exercise allows one to understand GPR physical processes better by controlling variables that are modeled; first by a series of simple models followed by the more complex high fidelity FDTD model. It demonstrates the ability of the model to perform a bistatic polarimetric simulation of the GPR. Using a simple FDTD model and simulation with perfectly matching boundary conditions, a FDTD simulation of rods at half a meter depth was performed. The

homogeneous media show the expected result that polarized electromagnetic waves induce larger currents in the direction in which the wave and rod are oriented. Exposed to a polarized EM wave in the x direction, the x-directed rod has larger induced currents in the x-direction, while the y-directed rod has a strong tendency to induce currents in the y-direction if the EM wave is polarized in the y direction. This explains why GPR migration algorithms, developed on a matched-filter response basis, are used to both detect and determine the shape of a buried pipe like object.

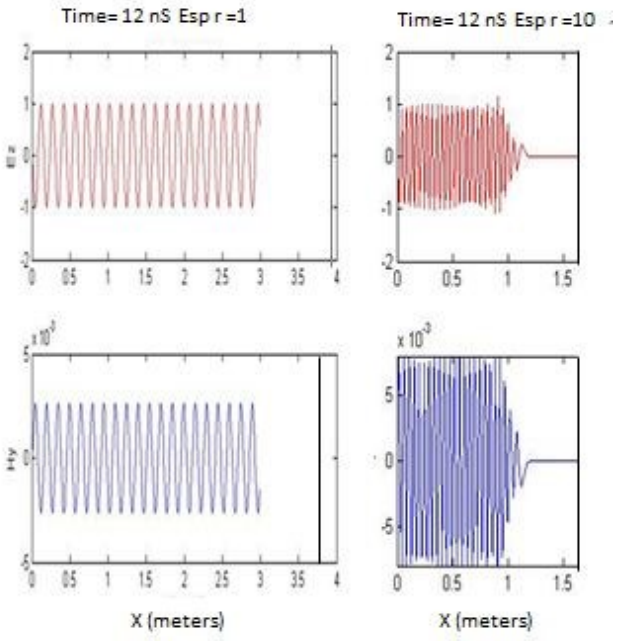

Figure 22. Effect of permittivity on propagation [Hebert et al. 2012]

Using the high fidelity FDTD model, Gürel et al presents an excellent example of prism modeling. [Gürel et al. 2001] In Figure 23, the FDTD model simulates two conducting prisms of 21 x 21 x 16 cells that are buried five cells under the ground and separated by twenty cells. The A-scan waveforms are calculated and presented next to B-scan results. In Figure 22, the higher fidelity FDTD model shows the scattering results for a cavity and a dielectric object, with a permittivity of $\varepsilon_r = 1.0$ and $\varepsilon_r = 8$, respectively, are

presented. The two targets are buried twenty cells apart and five cells under the ground that is modeled with a relative permittivity of $\varepsilon_r = 4.0$. Figure 22 illustrates the typical A-scan and B-scans expected and demonstrates the ability of the FDTD model to simulate the GPR system's performance with respect to one than one variable at a time. In Figure 24(a) the targets are dielectric objects and a cavity in the ground. Note that the amount of reflection from the two objects closely follows the Fresnel reflection and transmission coefficients illustrated in Figure 19 for layers with the values of $\varepsilon_r = 4.0$ for the soil and $\varepsilon_r = 8$ for the dielectric object and $\varepsilon_r = 4.0$ for the soil and $\varepsilon_r = 1$ for the void. The results in the return from the cavity being larger than the return from the dielectric object. The results of this FDTD simulation are consistent with those using lower fidelity Fresnel reflection and transmission coefficients models to calculate the reflection from the objects.

In the second simulation, the dielectric object is replaced by a conducting prism. The reflection from the perfectly conducting prism is nearly 100% and much larger than the reflection of the cavity.

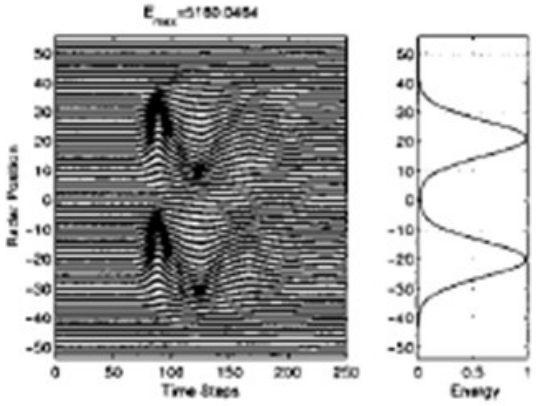

Figure 23. Two perfectly conducting prisms buried 5 cells under the ground and separated by 20 cells [Gürel et al. 2001]

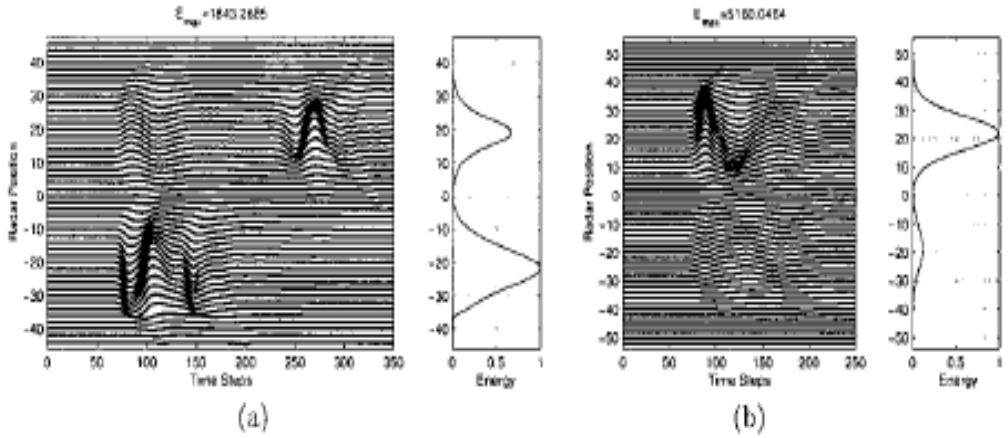

Figure 24. Two objects buried 5 cells under the ground and separated by 20 cells. (a) a cavity and a dielectric object and (b) a cavity and a perfectly conducting prism [Gürel et al. 2001]

The MATLAB^{TM} Fresnel reflection coefficient models and TDFD models and simulations clearly show how the researcher can vary the media and targets buried in the media to systematically evaluate the GPR's performance. Simple models are used to evaluate individual variables and the HF FDTD model provides highly accurate results of the performance. These experimental results yield the conclusion that multi-fidelity models can be used to accurately simulate the GPR measurements and to faithfully analyze GPR data.

4.2 Nuclear Electromagnetic Pulse Bounded Wave Simulator (NEMP/BWS) Example

4.2.1 Requirements

Congressman Trent Franks, in testimony to the Cybersecurity, Infrastructure Protection and Security Technologies Subcommittee on September 9, 2012, expressed concern that: "the US society and economy are so critically dependent upon the availability of electricity that a significant collapse of the grid, precipitated by a major natural or man-made electromagnetic pulse (EMP) event, could result in catastrophic civilian casualties

(and that) this conclusion is echoed by separate reports recently compiled by the DoD, DHS, DOE, NAS, along with various other government agencies and independent researchers." [Frank 2012] To answer these and similar concerns, the Naval Ordnance Transient EMP Simulator (NOTES), illustrated in Figure 24, needed to be modified to allow threshold EMP testing from 1 to 100 kilovolts per meter (kV/m) with roughly constant (standardized) threat waveform characteristics. The NOTES was originally designed as a full threat simulator with an output of 100kV/m. Testing levels in the target area needed to be adjusted to lower voltages from 1 kV/m to full threat strength to determine upset levels, reset levels and destruction levels for testing critical infrastructure electronic systems like power switches and telephone switches. The NEMP/BWS was designed to cost effectively produce a wide range of threat levels while maintaining the proper standardized EMP threat waveform characteristics needed to assess the effects of an EMP pulse on electronic systems.

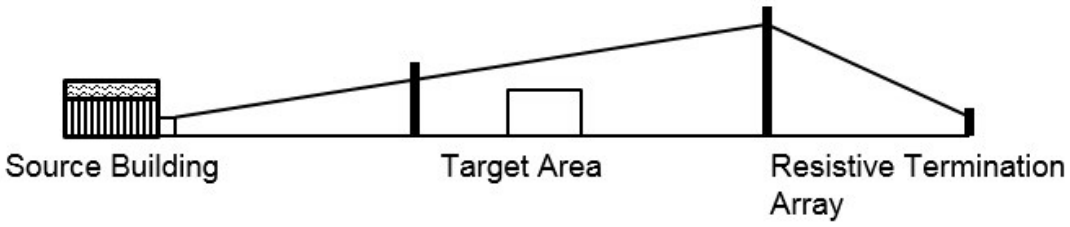

Figure 25. The NOTES NEMP/BWS

4.2.2 Stakeholder Analysis

Figure 26. Stakeholders in the Modification of NOTES

Figure 26 breaks the stakeholders into groups including the Project Systems Engineering Team that designed and modified NOTES. The Project Systems Engineering Team balanced the needs of all the stakeholders. The Congressional EMP Commission needed test data on the Nuclear EMP susceptibility and vulnerability of critical infrastructure systems for inclusion in their report to Congress on the ability of the United States to withstand a widespread EMP attack. The Naval Surface Warfare Center Dahlgren Division (NSWCDD) Environmental Office and Safety Office wanted assurance that the modifications would not adversely affect the environment around NOTES including workers, the public, natural resources and wildlife. The Safety Office required a new Standard Operating Procedures and Safety Assessment before the modified facility could operate. The NOTES Facility Operations needed its personnel trained to address any changes to the operating procedures and NOTES Maintenance Crews had to know how to maintain the modified facility. The Ordnance Range Operators had to issue passes and give clearance for crews to work at the NOTES facility as it is located on an active explosive

ordinance range. The NSWCDD wanted the new NOTES designed and the modifications made at the lowest technically achievable cost.

4.2.3 Analysis of Alternatives

For the analysis of alternatives (AoA) on how to modify the NOTES facility, the overriding considerations were the stakeholder needs, cost and performance. A diagram of the NOTES physical architecture that shows its major sub-systems and their parts is shown in Figure 26. The alternatives analysis effort provided the information needed by local decision makers to consider the costs and benefits of the proposed strategies to address the needed modifications to the NOTES System; the single alternative that was advanced into implementation was to modify only those parts of NOTES necessary to meet the requirements of all the stakeholders. These subsystems within the Pulser Control System are unshaded in Figure 26. The shaded systems in this figure required no modification: the Bounded Wave Section, the Dielectric Oil Handling System and the Sulfur Hexafluoride (SF_6) Gas System. Making the most use of the existing unmodified subsystems allowed configurations and measured data from the unmodified facility to be used as a guide in the analysis of the new one. The selection of subsystems to be changed also allowed many of the regulatory documents and approvals to remain intact such as the environmental assessment and operating procedures for all the unchanged systems. This system level AoA chosen alternative presented the least risk at the lowest price possible. It, also, sets the stage for the component level AoA that was conducted by applying the modeling framework presented in this dissertation.

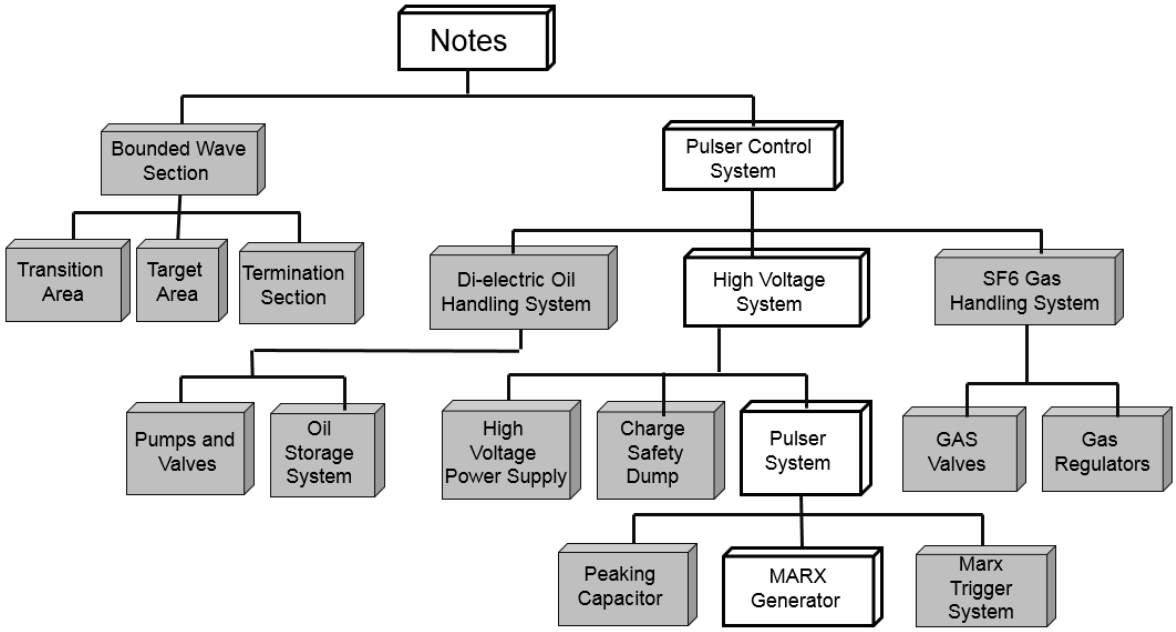

Figure 27. NOTES Physical Architecture
(No modification was required to the shaded boxes)

4.2.4 Demonstration of the Framework

The modeling framework was demonstrated using information and measured data from the unmodified and modified NOTES. The NOTES was modified in 2008, using a PSPICE™ model similar to the one presented in this paper. This measured data provides an excellent real physical industrial, rather than academic, example for demonstrating the framework presented in this paper. For this research and demonstration, an updated PSPICE™ model and several new multi-fidelity and surrogate models and simulations were used to generate the figures and data presented in this study.

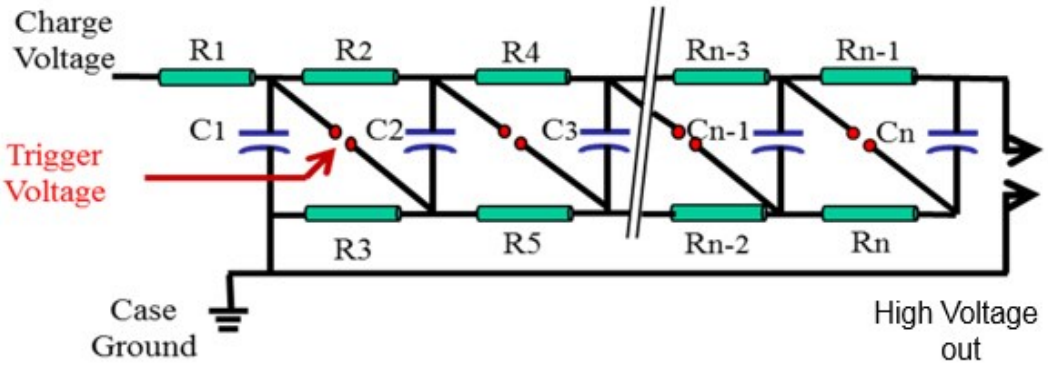

Figure 28. N-Stage Marx Generator

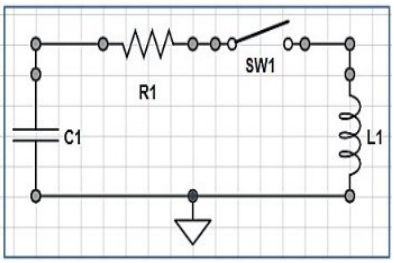

Figure 29. Simple RLC Circuit

4.2.4.1 Low Fidelity RLC Circuit Model and Simulation

Low fidelity electrical models are simplifications of Maxwell's equations in the form of lumped circuit parameters like resistance (*R*), capacitance (*C*), voltage (*V*) and current (*I*) that are modeled by simple relationships such as Ohm's or Kirchhoff's laws. [Bobrow 1995] The NOTES system includes: the MARX generator power source (Figure 29), a peaking capacitor to sharpen the rise time, a bounded wave section to provide uniform electrical fields in the target area (Figure 25) and a termination impedance section to prevent reflections. The measured data from the legacy 24 stage Marx Generator, shown in Figure 30, was used to determine the lumped circuit equivalent parameters of that component. The legacy generators were used because with them, the ability to perform EMP testing at the full and half threat levels of 100 KV/m and 50 KV/m had previously

been demonstrated and was well documented by tests on military systems such as the Navy's Standard Missile. A few years ago this Marx generator had been totally reconditioned and had proven very reliable and repeatable during operational tests. Measurements of the simulator's output were already recorded. Using this source, NOTES is capable of producing the standard threat waveform and no development was necessary to meet the full threat EMP test requirement. The waveform produced by the 24 stage Marx source was used as the standard for designing and developing the eight stage and single stage sources that were required to produce the threat waveform across the rest of the required range of 1kV/m to 50 kV/m. A key requirement for this effort was that the output of any other sources developed had to match the 24 stage output waveforms characteristics in the target area, but at the desired reduced output levels.

Figure 30. The NOTES Legacy 24 stage Marx Generator

Figure 30 shows the 24 stage Marx as installed at NOTES. The large white ring at the end wall is the peaking capacitor installed in the oil tank at the output of the Marx. The peaking capacitor is 137.16 centimeters in diameter including the 7.62 centimeter white field grading ring around the outside. It is located at 5.08 centimeters inches from output

wall. This peaking capacitor's output is determined largely by its adjustable (screw-in type) electrode at its output to where it connects to the transmission line. This size and spacing results in a peaking capacitor of approximately 240 Pico-Farads when the capacitor is submerged in DIALA-X^{TM} transformer oil. The trays that make up the legacy Marx are shown uninstalled in Figure 31. The legacy Marx consists of 14 trays, 12 trays that each contain two Marx stages for a total of 24 stages. There is one Trigger/Charging Tray interface to the charging system and an output tray is connected to the peaking capacitor. A closer look at the uninstalled tray shows that it contains the two capacitors, two spark gaps and the trigger and charging resistors associated with two full stages of a Marx. A low fidelity model of the Marx's operation is illustrated in Figure 28.

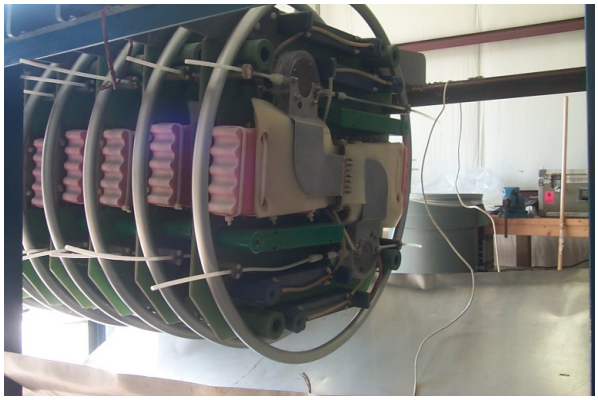

Figure 31. Capacitor Trays from the Legacy Marx

Applying the modeling framework (Step 2) a low fidelity lumped parameter simple over-damped series RLC model (Figure 29) was selected to reverse engineer the measured data from the unmodified NOTES output waveform to determine the lumped circuit electrical parameters of a simple NOTES model. This low fidelity physics-based model of the existing NEMP simulator is an over-damped RLC circuit:

$$i_c(t) = C\frac{dv_c(t)}{dt} = CS_1V_i\left(\frac{e^{S_1t}}{1-\frac{S_1}{S_2}}\right) + CS_2V_i\left(\frac{e^{S_2t}}{1-\frac{S_2}{S_1}}\right) \text{ Where } S_1 = \frac{-R}{2L} + \sqrt{\left(\frac{R}{2L}\right)^2 - \frac{1}{LC}} \text{ and}$$

$$S_2 = \frac{-R}{2L} - \sqrt{\left(\frac{R}{2L}\right)^2 - \frac{1}{LC}} \quad (6)$$

Continuing the framework into Step 3, this low-fidelity physics-based analog RLC model (where S_1 and S_2 are the roots of the solution of the series RLC circuit) was used to produce a sparse sample set of basis points for a Kriging surrogate model. Using the systems engineering life cycle process, this example extends the application of these surrogate models to the design of an entire system using a series of increasing fidelity physical models, starting with the lowest fidelity physical model necessary to answer the problem or question. The NEMP/BWS example uses three physics-based multi-fidelity electrical and EM models and two surrogate models. The design of experiments for these two surrogate models is highlighted in Figure 32.

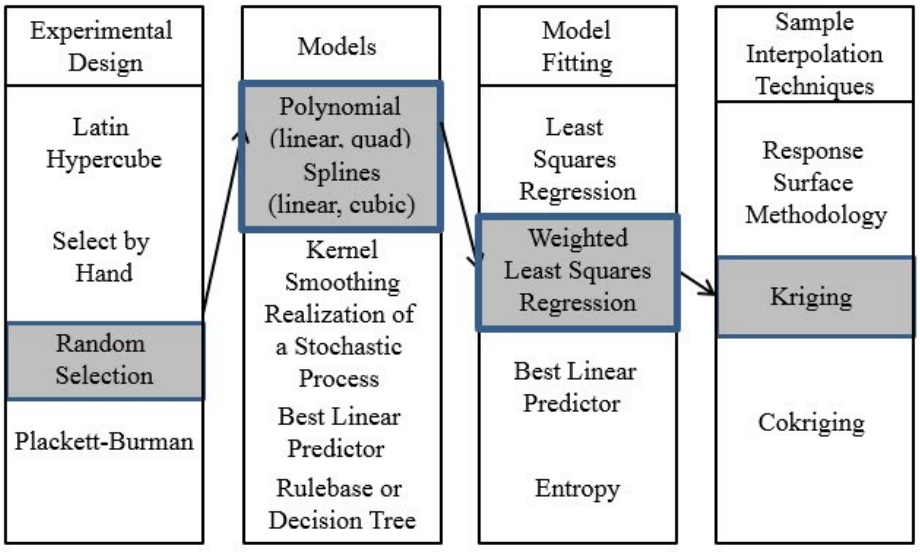

Figure 32.Design of Experiment for Surrogate Models used in the design of the NEMP/BWS.

The Kriging model results (Figure 33) were used to analyze the lumped circuit parameters of the NOTES system. The results of the Kriging model were compared with the total analog solution (Figure 34). The analog solution, programmed in MATLAB™, took two minutes to compute and plot on a Windows 64 bit computer with an Intel quad core eight thread CPU; the Kriging model, using the MATLAB™ DACE toolbox, took six seconds on the same computer.

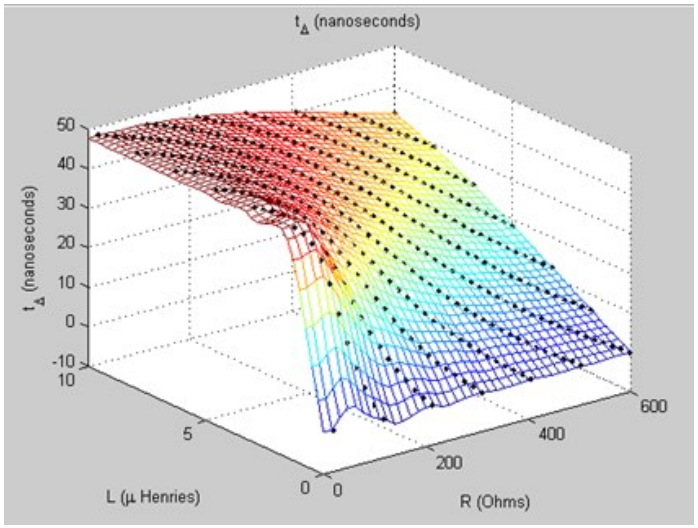

Figure 33. Kriging Approximation (dots are HF model produced basis points)

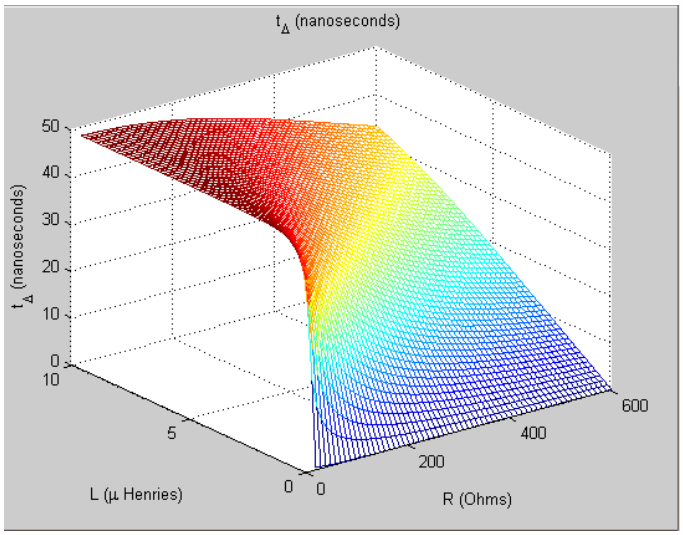

Figure 34. Analog Solution

Applying step three of the framework a second time, a Kriging surrogate model was used to reverse engineer the values of the resistor, *R,* and the inductor, *L*, using an analog object equation for the rise time that was developed using Equation 3. An expression for determining the time for the current to go from 10% to 90% of its maximum value was evaluated for each resistor inductor pair (R and L). Using the DACE Kriging Toolbox, a correlated linear kernel function was used to estimate the rise time (10% to 90% of maximum current) based on 60 basis points (*R* and *L* combinations) obtained by running the low fidelity RLC model 60 times. [Lophaven 2002] The number of basis points was selected based on checking the model's results by cross validation and examining the size of the mean square deviation. A graphic example of this is presented below. The Kriging estimate then allowed interpolation of the solution to a dense grid and selection of appropriate *R* and *L* values that can provide the required rise time. The Kriging solution was compared to the analog solution. (Figures 35 and 36)

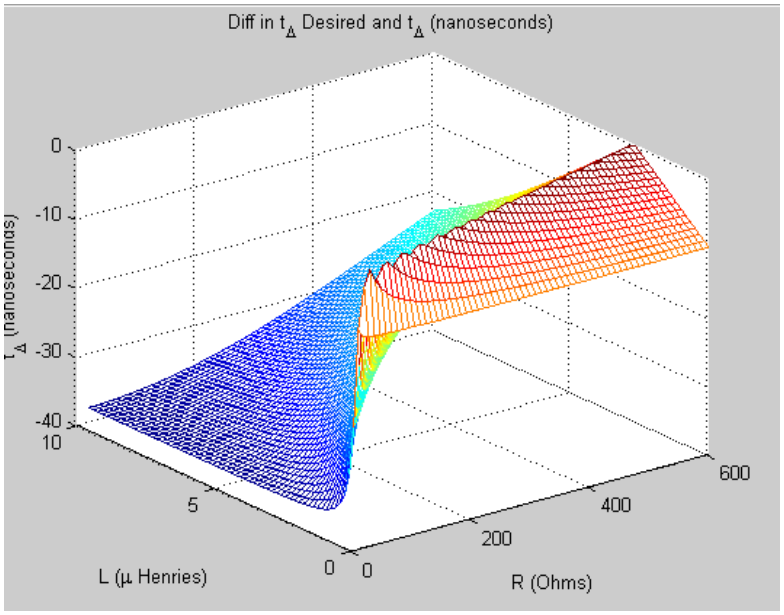

Figure 35. Analog Model Graph of rise time differences

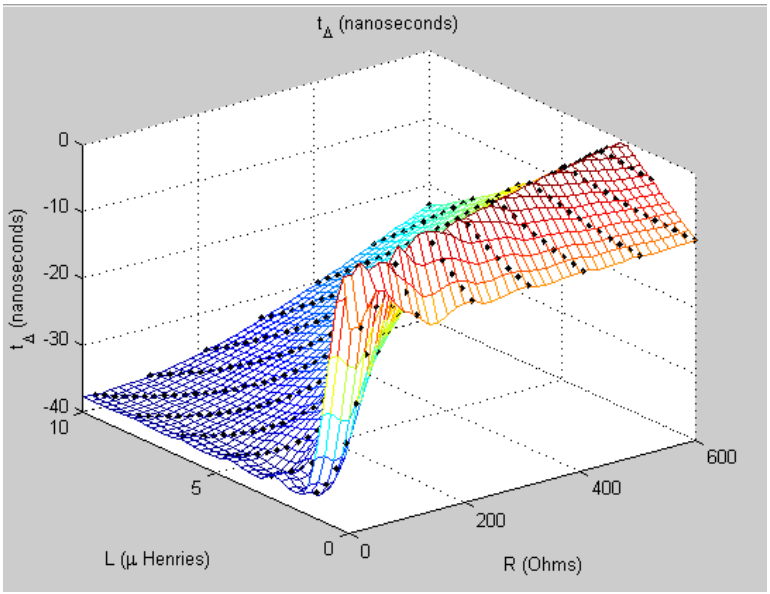

Figure 36. Kriging Approximation of rise time differences. (Dots at basis points)

The Kriging model is a lower-fidelity model than the RLC analog model. It provides the solutions for *R* and *L* with much less computational time and resources when compared to higher-fidelity RLC model at a fraction of the cost. For this simple example, the time and cost difference is relatively small when compared with a high fidelity model because the object function (RLC analog model) is not computationally intensive. If the complex model took 60 times as long it would result in even larger savings. For example, a 10,000 run regression analysis on a high fidelity model that takes one hour for one run compared to a surrogate model that takes one minute results in a savings of over 100 days of computation time. The plot of the values of *R* and *L* for a rise time of 10 nano-seconds (ns) is presented for the analog model in Figure 35 and for the corresponding Kriging approximation in Figure 36. In these figures, the interpolated results of the Kriging surrogate model closely match those of the full analog solution with an overall mean square error of less than 0.1ns for 60 Kriging basis sample points.

4.2.4.2 Medium Fidelity PSPICE™ Model

At Step 4, we determine that although the first RLC physical model was needed to determine the lumped circuit's resistor and inductor parameters, it was not adequate to answer the total design problem which requires the determination of the settings for the breakdown of the peaking capacitor switch in the NOTES source as a function of the output electrical field. The peaking capacitor switch closes due to over-voltage at a time determined by the type of dielectric and by the adjustable distance across the switch. Therefore, at Step 5 we go back to Step 2 where we chose a medium fidelity PSPICE™ model (Figure 37) to determine the values for these other parameters needed to produce the simulated electric field threat waveform in terms of rise time and wave shape and to vary the Marx Generator so its output ranged from 1 to 80 kV.

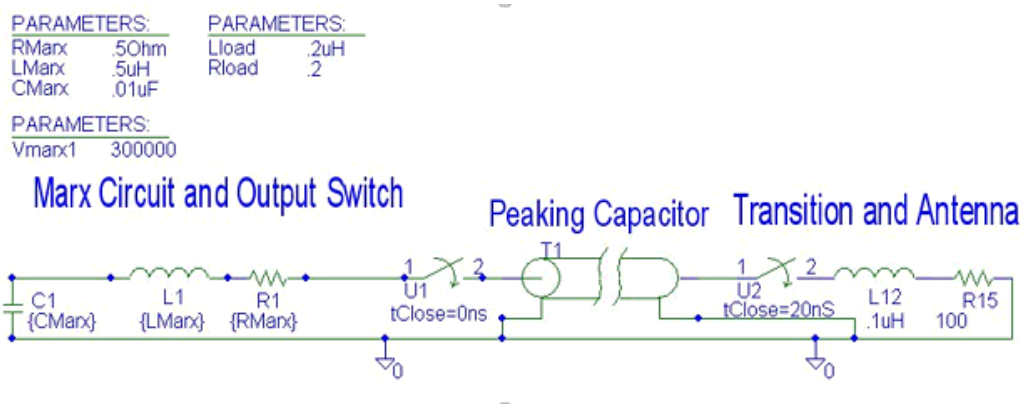

Figure 37. PSPICE™ Model of the NOTES.

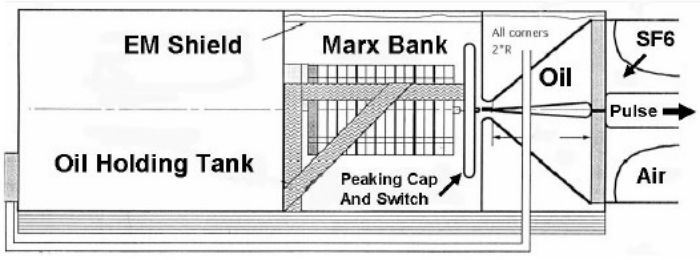

Figure 38. The NOTES Simulator Marx Generator.

The PSPICE™ model has higher fidelity than the RLC Model because it contains more system parameters such as: timing switches for charging, a peaking capacitor to provide the fast rise time required and a model of the target zone configuration as a short transmission line. Using the PSPICE™ model for parametric analysis showed that if the equivalent capacitance for each pulser is modified to be 10 nano-Farads (nF) and the basic geometry of the Marx generator, peaking capacitor and transition zone (Figure 38) remained roughly the same, then values from the simpler models could be used to vary the input voltage and the second switch closing time to produce the required threat waveform with the correct rise time and waveform shape. Simple curves that relate the breakdown voltage of transformer oil (Diala-X) and SF_6 (an electro-negative gas) to the product of the pressure and distance were used to determine when the peaking capacitor would self-breakdown. [Ushakov 2004] For the two lowest voltages, the gap could not be set precisely enough in oil, so a pressurized spark gap filled with SF_6, was placed between the peaking capacitors output electrodes. Analysis of the PSPICE™ results indicated that the required output switch closing time was 20 ns and that three Marx sources were necessary. Table VI presents a summary of the nominal operating conditions for the NOTES simulator.

Table VI. Nominal Notes Simulator Operating Conditions

Electric Field Target Area (kV/m)	Marx Voltage output (kV)	Marx Charge Voltage (kV)	Gap Distance Oil BD curves (inches)	Gap Distance SF_6 (inches)	Turns 10 (turn/inch)	Pressure (PSI)	Dielectric
100	1130	47	9	N/A	90		Diala-X
90	1017	42.3	8.5	N/A	85		Diala-X
50	565	23.5	4.9	N/A	49		Diala-X
25	282.5	11.75	1.89	N/A	19		Diala-X
7	79.1	3.29	0.29	N/A	3		Diala-X
3.5	39.55	1.645	N/A	5/100	N/A	10	SF_6
1.5	16.96	0.705	N/A	5/100	N/A	5	SF_6

The electric field in the target area, that was calculated by the higher fidelity PSPICE™ model (Figure 39), compares closely in shape, rise time and magnitude to the electric field measured in that area (Figure 40). The difference in the time of the peak of the measured waveform is an attribute of the measurement system and the peak of the simulated waveform – an attribute of the simulation output switch closing time. The rise time is the same.

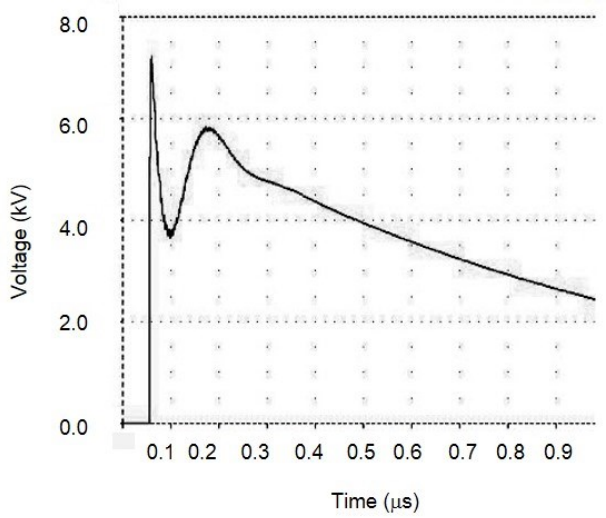

Figure 39. NOTES Output Waveform calculated using PSPICE™

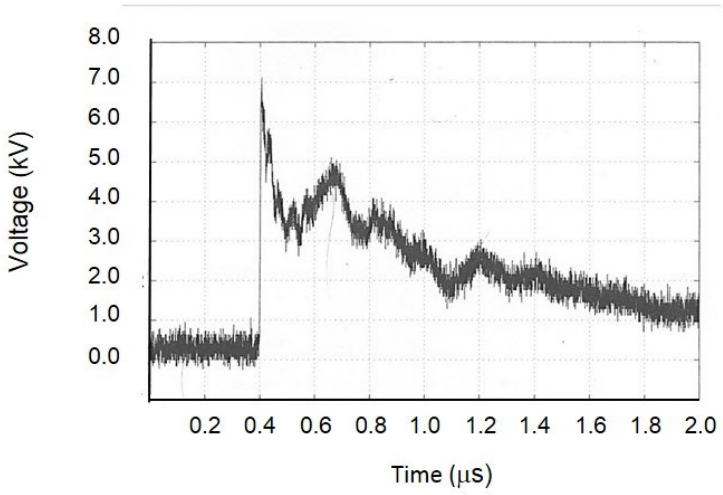

Figure 40. NOTES Output Waveform (measured)

4.2.4.3 High Fidelity FDTD Model

Again at Step 4, we determine that because the RLC and PSPICE™ models represent NOTES as lumped circuit electrical components, they do not accurately model the electric fields in the target area in the bounded wave portion of NOTES: this requires an accurate high fidelity EM model. Going back to Step 2, we chose the high fidelity FDTD model because the bounded wave portion is well modeled by the differential implementation of Maxwell's equations. FDTD codes, that implement the total form of Maxwell's equations, are computationally intensive, requiring considerable hours and computational resources to analyze complex EM problems. A problem with a grid size of 30 x 30 x 30 cells can take about four hours on a Windows 64 bit computer with an Intel quad core eight thread CPU.

The FDTD method has been demonstrated to accurately model the performance of a bounded wave EMP simulator as well as allow uncertainty analysis of the BWS. [Lu et al. 2008; Wei et al. 2011] "The FDTD method belongs in the general class of grid-based differential time domain numerical modeling methods." [Smith and Furse 2012] Time-dependent Maxwell's or Telegrapher's equations are discretized using central-difference approximations for the space and time partial derivatives. [Furse 2010] Only the bounded wave portion of the simulator was modeled, whereas in the other two methods presented, the RLC and PSPICE™ models, the entire NOTES system was modeled.

The measured electric field data points from previous NOTES efforts were used to define basis points for the objective functions in a two-step surrogate model. Koziel used this two-step approach for small microwave filters. In contrast to that approach, the entire BWS of NOTES was modeled. Koziel explains this approach as "Our technique is based

on utilizing an 'intermediate', coarse-discretization EM model." [Koziel 2011] For the second step, a surrogate is used to turn a coarse-grid physical model output of basis points into a fine-grid surrogate model approximation.

For the NOTES bounded wave section, the FDTD grid discretization used larger coarse-discretization cells, eight times larger than usual, sized to nearly the stability limits set by the Courant condition. The Courant condition is given by:

$$\Delta t \leq \frac{\sqrt{\Delta x^2+\Delta y^2+\Delta z^2}}{c} \quad \text{where } c \text{ is the speed of light in vacuum, 299,792,458 m/s} \quad (7)$$

Here Δt is the time of propagation of the wavefront diagonally across the maximum cell dimension. During each time step of the simulation, six field quantities are calculated for each cell. Using the larger discretization cell size decreases the number of total cells. By decreasing the number of cells by a factor of eight in each direction, the decrease in theoretical computation time is 98.4%. The result is a surrogate model of the FDTD model that uses a "coarser" set of basis points. "Because the coarse model is supposedly physics-based, the corresponding surrogate is expected to offer a good match over the entire region of interest. For the same reason, Surface Mapping surrogates (of physical models) typically need just a few basis points to achieve reasonably good accuracy." [Koziel 2011] This makes using surrogates for physics-based models attractive because significant computational time and cost savings can be realized without totally sacrificing accuracy. The time required for the one run with the FDTD code for the Bounded Wave System is presented in Table VII.

Table VII. NOTE BWS Computation Times

Researcher	What was modeled	Boundary Condition Type	CPU	Computer Memory	Number of Cells	Number of Time Steps	Time to complete simulation (min)	20,000 time steps (min)	40,000 time steps (min)
Hebert 2015	BWS section of NOTES	Perfect Matching Layer	1 processor on Quad Core CPU at 3.2 GHz	16 GB	372,000	20,000	75	75	150

The total grid space consisted of 372,000 cells including eight cells layers at the boundaries to implement the Perfect Matching Layer boundary condition. To complete one run with on a Windows 64 bit computer with an Intel quad core eight thread CPU using 20,000 time steps required 75 minutes and 150 minutes for 40,000 time steps.

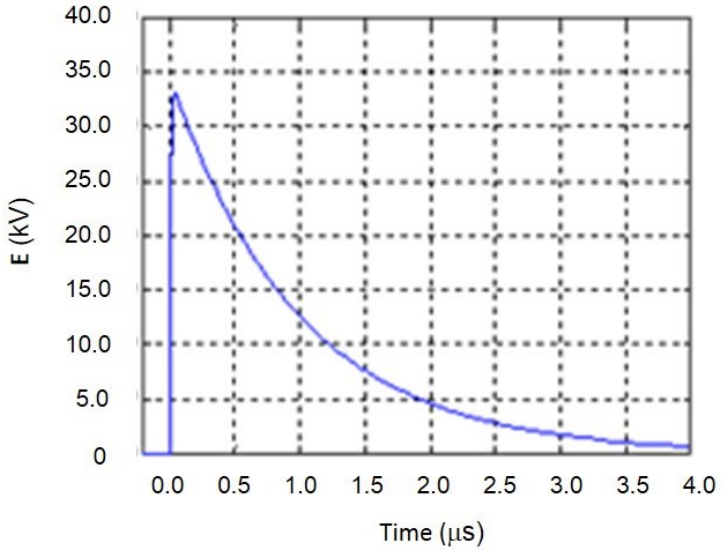

Figure 41. NOTES FDTD Calculated Waveform (in the target area)

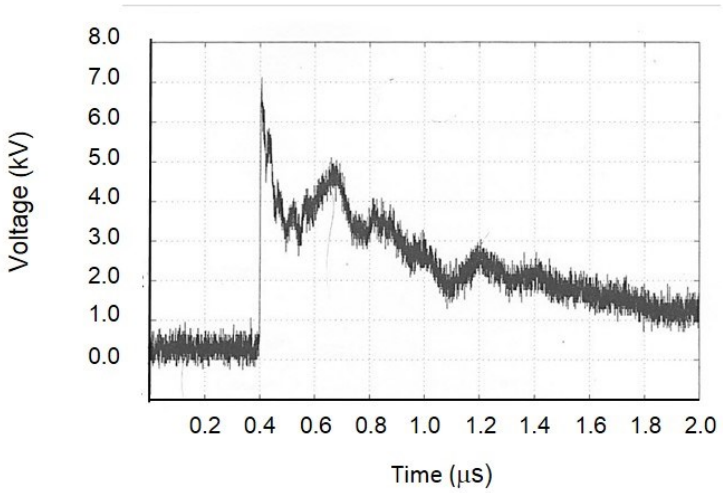

Figure 42. NOTES Measured Output Waveform (in target area)

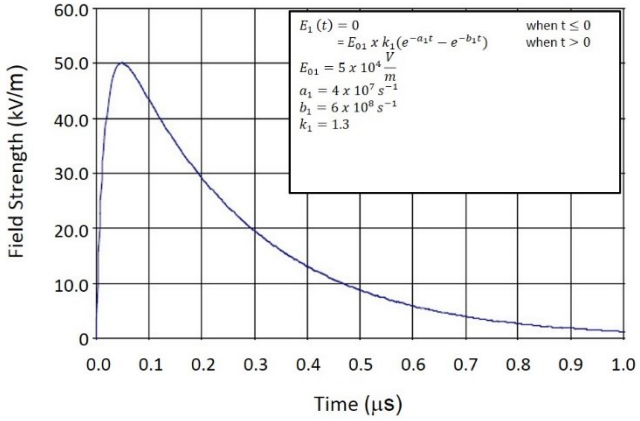

Figure 43. NEMP Standardized Threat [(IEC 61000-2-9)]

Figure 41 shows the TDFD output electric field calculated in the working volume of the BWS. Figure 42 shows the measured output waveform in the working volume. Figure 43 is the standardized unclassified NEMP threat waveform. [International Electrotechnical Commission, IEC 61000-2-9)] A standard Kriging surrogate model was developed for this calculated field. Figures 44 and 45 show the original FDTD calculated waveform and the results of its Kriging surrogate model. Figures 44 through 46 show the true value of the Kriging method. By using sufficient basis points, the plots closely match the FDTD calculations. Figure 44 fails in the framework because only five basis points were used.

Figure 45 shows that by adjusting the surrogate model to 15 basis points significantly reduced the mean square error of the approximate solution as shown in Figure 45 to less than 0.1 V/m. Comparing the use of a Kriging surrogate model's computing time, less than one minute and that of the FDTD model in Table VII, 75 minutes, provides a dramatic example of the difference in runtimes between using a High Fidelity Model and a surrogate model. The surrogate model performed its calculation and outputs over 75 times quicker. These reductions can be realized many times over when optimizing system elements or options during component or system architectural synthesis on any size computer. For example to perform a simple regression analysis of 1000 inputs would take 75,000 minutes but only 75 minutes using the surrogate model. When you compare the 75 minutes to the 9 seconds required to produce the Kriging Model with 15 basis points of the BWS waveform's output in Figure 45, the difference in computation time is even more dramatic.

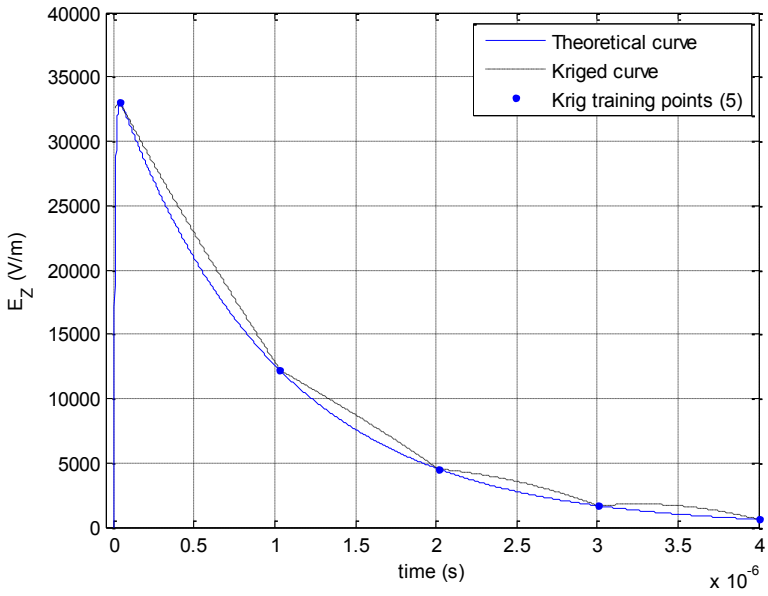

Figure 44. Kriging Model of FDTD Output Field (5 Basis Points)

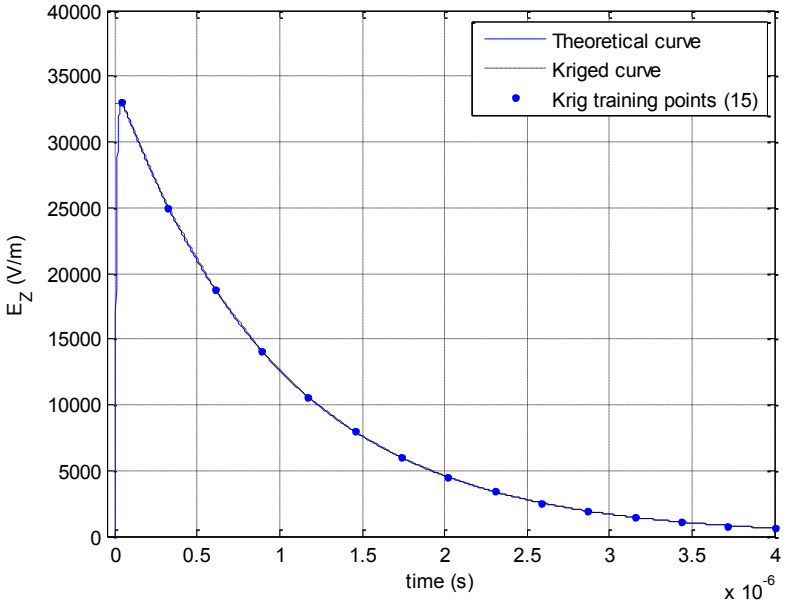

Figure 45. Kriging Model of FDTD Output Field (15 Basis Points)

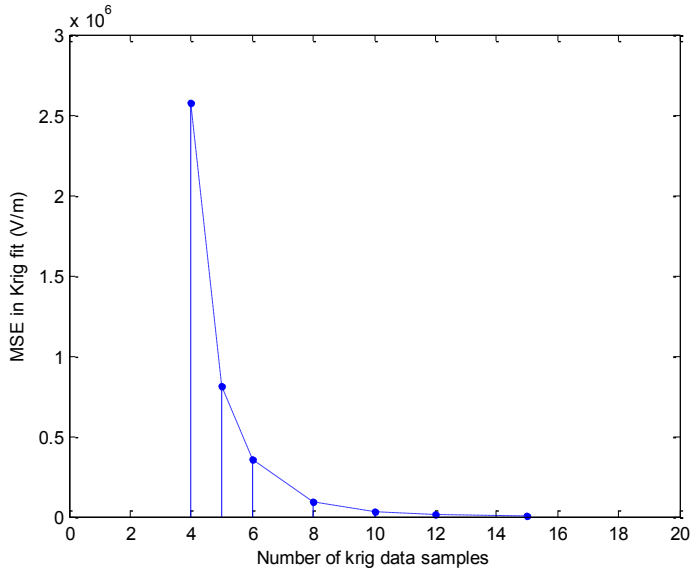

Figure 46. The MSE of the Kriging Plot (# basis points)

4.2.5 Cost

Most program managers justified their M&S investment based on one or more of the following: reducing design cycle time; augmenting or replacing physical tests; helping resolve limitations of funds, assets, or schedules; or providing insight into issues that were impossible or impracticable to examine in other ways." [Brown et al. 2000] An example comparison of the costs of using multi-fidelity and surrogate models with other methods for the NOTES facility modification is shown in Table VIII. The multi-fidelity and surrogate modeling and simulation option is the least expensive option. This option trades M&S cost for the number of prototype systems and number of days to test them in the Build/Test Option and against time and expense of using high-fidelity models only. The return on investment of the physical modeling of complex EM systems comes from the trade-off between the relatively low cost of modeling and the higher cost of building and testing prototype EM systems.

Table VIII. Example Comparison of Cost

Component	Purchase	Modify By Build/Test	Modify by Multi-Fidelity & Surrogate Models	Modify by High Fidelity Models
Marx Sources	$1M	$100K	$40K	$40K
Transition Zone	$12K	$ 0 K	$ 0 K	$ 0 K
Antenna	$20K	$ 0 K	$ 0 K	$ 0 K
Termination	$10k	$0 K	$ 0 K	$ 0 K
Testing $6K/day	$30K/5 days	$120K /20 days	$30K/5 days	$30K/5 days
New Facility	$500K	$ 0 K	$ 0 K	$ 0 K
M&S	$30K	$5K	$20K	$80K
Total	$1602K	$225K	$90K	$150K

4.2.6 Verification and Validation

Aydemir states that "Many simulation methods have been developed for the solution of EM problems. One of the best ways to evaluate the accuracy of these methods is comparing them with actual measurements." [Aydemir 2011] For the NEMP/BWS system-of-systems, the multi-fidelity models were verified and validated to give decision makers the confidence to rely on the framework for the acquisition of this type of complex system. To validate the models, the measured data from the unmodified existing facility was used to verify that the MATLAB^{TM} RLC codes were correctly programmed and provided reasonable results. The results of the PSPICE^{TM} model, a totally separate physical model, were used to verify it produced the same results as the RLC model. Finally, once the modified NOTES system was built and tested, the electric field outputs generated by the three models were compared with the system's measured outputs.

4.2.7 NEMP/BWS Design Summary

A framework that uses increasing fidelity physics-based models together with surrogate models was demonstrated. Lower fidelity and surrogate models were used, in place of higher fidelity models, to investigate variables with significant impact on the system's response. Savings, in addition to the cost reduction in M&S by using the framework, also resulted from being able to make maximum use of existing systems and only modifying the three pulsers. The models also showed that simple adjustments could compensate for most of the uncertainty in values of other components. The three modified pulsers, (Marx Sources), installed in the NOTES facility, are shown in Figure 47.

Figure 47. Installed Marx sources at NOTES

Chapter 5 – Conclusions and Recommendations

The research documented in this dissertation has been driven by the research question "Are there modeling and simulation approaches that make possible the use of systems engineering decision making tools by reducing the time and cost of high fidelity computational models during the design and development of complex physics-based complex systems?" This research stems from the desire to reduce the number of high fidelity models and simulations currently used in the design stage optimization of physics-based systems. The second related but different question: "Can multi-fidelity and surrogate models be used in a methodology that enables the efficient allocation of time and cost for the optimization and performance evaluation/validation of physics-based systems?" suggests that multi-fidelity and surrogate models may reduce the use of time consuming and expensive high fidelity models allowing expanded use of systems engineering tools in the optimization design stage. The research performed to answer these questions has achieved the following objectives:

1. To develop a novel time reducing framework for the design and development of complex physics-based systems by using a mix of variable fidelity physics-based models and surrogate models.
2. To show that this framework for combining increasing fidelity models enables the computationally and cost efficient modeling and simulation of complex systems and their components.
3. To demonstrate the framework with physics-based examples and document the findings in this dissertation.

The methodology and examples documented in this study provide evidence that the objectives have been met. In the next part of this section we discuss the key findings, followed by the major contributions and finally some suggested avenues for future work.

5.1 Key Findings from the Research

There are three key findings from the research documented by this study. They are listed here followed by a discussion.

1. The framework for using the lowest fidelity that answers the question coupled with the choice of further reducing computational time by using surrogate models are key enabling methods that allow the use of classical systems engineering tools during the design stage optimization of physics-based systems.
2. The use of multi-fidelity models and simulations can reduce the number of high fidelity runs necessary to characterize the problem. (e.g. material characteristics of multiple layers of soil in the analysis for Ground Penetrating Radars.)
3. The methodology of using increasing fidelity M&S to analyze, design and develop modifications to the NOTES System was shown to be successful. (e.g. simple RLC circuit to analyze the overall performance of the entire NEMP/BWS system.)
4. The application of multi-fidelity models coupled with the Design of Experiments and Surrogate modeling can greatly reduce the time required by high fidelity models particularly for parameter optimization, reverse engineering and evolutionary design of physics-based systems. (e.g. both system examples.)

Other findings from the literature search include a number of guidelines for choosing and using multi-fidelity and surrogate models. These include:

- It is important to apply modeling in a way that maximizes its impact; otherwise someone will say it is too expensive.

- Introduce modeling early on when it can really make a difference. [Nopper 2012]
- Use the lowest fidelity model that answers the question.
- Use low fidelity models to identify controllable and uncontrollable inputs.
- Most problems are ill-defined at the onset. Use low fidelity models to:
    - Identify constraints on the decision variables.
    - Define measures of system performance and an objective function.
    - Determine a range of potential solutions.
- Use low fidelity models to interrelate the inputs and the measures of performance.
- Use low fidelity models and simulation to define what is important and what is not, and how important various parameters are.
- The low fidelity models provide insight and good test cases for later higher fidelity models.
- Low fidelity models allow investigations of the sensitivities of the models to variations in controlled and uncontrolled inputs.
- Low fidelity models allow statistical systems engineering methods are used to understand and optimize parameters and reduce uncertainty.
- Ranges of allowed variables found in the lower fidelity models is carefully selected may be transferable to models of high fidelity.

5.2 Other Conclusions with Respect to the Framework

With respect to the overall approach we conclude:

- The framework has the potential to allow the use of many Systems Engineering tools that could not be used were all modeling and simulation performed using high fidelity models only.

- The approach allows the generation of far more data that can allow decision makers to consider and evaluate more alternative designs and approaches to meet stakeholder needs.

The framework has several desirable attributes:

- the methodology is extensible and can be used to design and develop any physics-based systems;
- The methodology allows the use of models at any level of fidelity as long as the output answers the question that motivated its use;
- The systems engineer should choose the most efficient lowest fidelity model and simulation that answers the design problem or question, satisfies the stakeholder's needs and provides the results that the stakeholder can trust;
- The methodology is enabled by Systems Engineering that itself is enabled by the methodology;
- The methodology provides multiple steps for the validation of the models.

For the NEMP example, in the first step, simulation results were compared to the analytical formulation. The output of the MATLAB™ RLC program was checked against basic circuit equations involving Kirchhoff's voltage and current laws. The second method involved comparison of results between codes of increasing fidelity. In this case, the results of the PSPICE™ simulation of the output electric field in the target area closely matched that predicted by FDTD. The final validation step involved the comparison of the M&S with actual measurements of the fielded system and the published standardized threat waveform.

5.3 Conclusions with Respect to Systems Engineering

Acceptable confidence in M&S requires the ability to statistically characterize physics-based phenomena in complex systems where the system parameters or geometries are uncertain. The importance of uncertainty in accurate computational electromagnetic codes like FDTD has been investigated. [Ajavi, Sewell et. al. 2008; Shen 2010; Chauviere 2006] To be useful for the application of Systems Engineering tools, a design and development modeling and simulation methodology must be: computationally efficient, account for possible uncertainties in systems parameters and geometries; produce data to allow statistical analysis and estimation of the probability density function of field variables and other quantities of interest. [Shen 2010] Using only time consuming high fidelity models can preclude the use of many useful systems engineering tools. To solve this problem one can either include the variation analysis into the high fidelity code or use the methodology developed in this study. Smith and Furse presented an example of the first approach with "a new stochastic finite difference time domain (S-FDTD) method for calculating the variance in the electromagnetic fields caused by variability or uncertainty in the electrical properties of the materials in the model." [Smith and Furse 2012] They found by including statistical variations of the electrical properties directly into the traditional FDTD method provides a more efficient method of evaluating the statistical variation in the model. [Smith and Furse 2012] The second approach that uses the novel time reducing framework resulting from this study for the design and development of complex physics-based systems by using by using a mix of variable fidelity models and surrogate models has been demonstrated using two examples.

This framework for combining increasing fidelity models enables the computationally and cost efficient modeling and simulation of complex physics-based systems and their components.

5.4 Further Research Needed

Future research is still needed to determine the extensibility of the framework. Although this framework was successful in the design and development of a complex EM system, the NEMP BWS, more research is needed to determine if the technique is extensible to other physics-based design and development domains that require expensive computational physics-based models like computational fluid dynamics, computational physics, or other computational electrodynamics.

References

Ahlfeld D P, Mulvey J M and Pinder, G. F. "Contaminated groundwater remediation design using simulation, optimization, and sensitivity theory 2. Analysis of a field site; *Water Resour. Res.* **24** 443–452. 1988.

Andres, E., Iuliano, E. "Surrogate-Based Global Optimization Methods in Preliminary Aerodynamic Design", 6th. European Conference on Computational Fluid Dynamics (ECFD VI) *July 20 - 25, 2014, Barcelona, Spain*.

Aydemir, M. "Comparison of NEC simulation and measurement methods for the solution of coupling between airborne antennas" *Proceedings of 2011 IEEE International Symposium of Electromagnetic Compatibility*.Long Beach, CA, August 13-18, 2011, pp. 547-552.

Azamathulla, H.,Wu F.C., Ghani, A. A., Narulkar, S. M, Zakaria, N. A. and Chang, C. K. "Comparison between genetic algorithm and linear programming approach for real time Operation." *J. Hydrol. Environ. Res.* **2** 172–181, 2008.

Bahill, A. T. and F. F. Dean, "What is System's Engineering?" *A Consensus of Senior Systems Engineers*, (2009), accessed May10, 2013 <http://www.sie.arizona.edu/sysengr/whatis/whatis.html>.

Baker, G. S., Jordon, T. E., Pardy, J. "An Introduction to ground penetrating radar (GPR)." *The Geological Society of America*: (Special Paper 432, 2007): 2.

Banks, C. "What is Modeling and Simulation." *Principles of Modeling and Simulation: A Multidisciplinary Approach.* Ed. J. Sokolowski and C. Banks. Hoboken, NJ: Wiley and Sons, 2009.

Bilicz, S. "Application of Design-of-Experiment Methods and Surrogate Models in Electromagnetic Nondestructive Evaluation" Ph.D. Thesis. Université Paris Sud-Paris, Paris, France, 2011.

Belli, K., Rappaport, C., Udall, C., Hines, M., Wadia-Fascetti, S. "Use of 2D FDTD Simulation and the Determination of the GPR Travel Path Angle for Oblique B Scans of 2D Geometries." *Geoscience and Remote Sensing Symposium 2010 IEEE International*. 2010.

Blanning, R. W. "The construction and implementation of metamodels." *Simulation* **24** 177–184. 1975.

Bobrow, L. *Elementary Linear Circuit Analysis*, Oxford, UK: Oxford University Press, 1987.

Bourgeois, J. M. and Smith, G. S. "A fully three-dimensional simulation of a ground-penetrating radar: FDTD theory compared with experiment." *IEEE Trans. Geosci. Remote Sensing,* vol. 34, pp. 36–44, Jan. 1996.

Box, G. and Draper, N. *Empirical Model-Building and Response Surfaces*. Hoboken, NJ: Wiley, 1987.

Braack, M. and Ern, A. "Adaptive Computation of Reactive Flows with Local Mesh Refinement and Model Adaptation", Numerical Mathematics and Advanced Applications ENUMATH 2003*,* p. 139.

Brown, C., Grant, G., Kotchman, D. Reyenga, R. and Szanto, T. "Building a Business Case for Modeling and Simulation." *Acquisition Review Quarterly*, Fall 2000. pp. 311-315.

Calhoun, J. "A finite difference time domain (FDTD) simulation of electromagnetic wave propagation and scattering in a partially conducting layered earth." *Proc. 1997 IGARSS—Int. Geosci. Remote Sensing Symp.,* pp. 922–924.

Collins, A. Shefrey, S., Sokolowski, J. Turnitsa, C., and Weisel, E. "Modeling and Simulation Standards Study" Healthcare Workshop Reports, Virginia Modeling Analysis and Simulation Report, Suffolk VA. January 2011.

Crevecoeur, G. Sergeant, P., Dupre, L. and Walle, R. "A Two-Level Genetic Algorithm for Electromagnetic Optimization." *IEEE Transaction Magnetics*. 46:7, July 2010, pp. 2585 – 2595.

Delaunay, Boris: *Sur la sphère vide. A la mémoire de Georges Voronoï, Bulletin de l'Académie des Sciences de l'URSS, Classe des sciences mathématiques et naturelles, No. 6: 793–800, 1934.*

Demarest, K., Plumb, R. and Huang, Z. "The performance of FDTD absorbing boundary conditions for buried scatterers," in *Proc. URSI Radio Sci. Mtg.,* 1994, p. 169.

DOT, Department of Transportation, Federal Highway Administration, "Ground Penetrating Radar for Measuring Pavement Layer Thickness." Pamphlet. assessed 5 Feb 2015 <http://www.fhwa.dot.gov/infrastructure/asstmgmt/gprbroc.pdf>

Duncan, J. "Fidelity versus Cost and its Effect on Modeling and Simulation*." Command and Control Research and Technology Symposium*, 2006.

Eason, J. and Cremaschi, S. "Efficient Surrogate Model Generation" *AP Monitor Symposium on Modeling and Optimization* November 13, 2012.

eField™ Application Note: Anonymous "Simulation of an Implanted PIFA for a Cardiac Pacemaker with Efield® FDTD and hybrid FDTD-FEM" accessed 4 Feb 2015 <http://www.efieldsolutions.com/example_implanted.php>.

Fang, K. T., Lin, D., Winker, P., Zhang, Y., "Uniform design: Theory and application," *Technometrics*, Vol. 42, No. 3, 2000, pp. 237-248.

Forrester, A., Sobester, A. and Keane, A. *Engineering Design via Surrogate Modeling: A Practical Guide*. Hoboken, NJ: Wiley, 2008.

Franks, T. Congressional Testimony to Subcommittee on Cybersecurity, Infrastructure Protection, and Security Technologies, September 12, 2012, accessed `May 2013 <http://homeland.house.gov/sites/homeland.house.gov/files/CIPST%20EMP%20Written%20Testimony.pdf>.

Fritzsche, M. "Detection of buried landmines using ground penetrating radar." *Proceedings of the SPIE:* 2496 (1995): 100-109.

Giunta, A. A., Wojtkiewicz Jr, S. F., and Eldred, M. S. "Overview of Modern Design of Experiments Methods for Computational Simulations," AIAA paper 2003-649, 2001.

Global Scan Technologies. *An Introduction to GPR.* Global Scan Technologies. April 2012. <http://www.gstdubai.com/Download/GPR.pdf>.

Gu, L."A comparison of polynomial based regression models in vehicle safety analysis." In Diaz, A., ed.: 2001 ASME *Design Engineering Technical Conferences – Design Automation Conference*, ASME, Pittsburgh, PA. 2001.

Guan, J. and Aral, M. "Optimal remediation with well locations and pumping rates selected as continuous decision variables." *J. Hydrol.* **221** 20–42 1999.

Gürel, L. "Simulations of Ground-Penetrating Radars Over Lossy and Heterogeneous Grounds" *IEEE Transactions on Geoscience and Remote Sensing*. 39.6. (2001): 1190-1197.

Hakim, A. "The dual Yee-cell FDTD scheme." April 2012. <http://ammar-hakim.org/sj/je/je7/je7-dual-yee.html#>.

Han, Z-H. and Zhang, K-S. "Surrogate-Based Optimization." *Real-World Applications of Genetic Algorithms* Dr. Olympia Roeva (Ed.), ISBN: 978-953-51-0146-8, InTech, DOI: 10.5772/36125.

Hebert, J.L., Eveleigh, T., Holzer, T., Sarkani, S. Ball, J., "Computer Modeling and Simulation of Ground Penetrating Radar using Finite Difference Time Domain Code Computer Modeling and Simulation of Ground Penetrating Radar using Finite Difference Time Domain Code," Proceedings of The 2012 International Conference on Modeling, Simulation and Visualization Methods, Las Vegas, July 16-19, 2012.

Hebert, J. L and Sanchez-Castro, C. *Implementation of a Three-Dimensional Finite Difference Electromagnetic Code for Analysis of Lightning Interaction with a FAA CV-580 Aircraft.* Air Force Wright Aeronautical Laboratory Technical Report, AFWAL-TR-86-3008. Wright-Patterson AFB, PH, May 1987.

Hook, B. J. "FDTD modeling of ground-penetrating radar antennas." *Proc. 11th Annu. Rev. Prog. Appl. Comp. Electromag.,* Monterey, CA, 1995, pp. 740–747.

Hughes, T. and Rolek, E. "Fidelity and Validity: Issues of Human Behavior Representation Requirements Development." *2003 Winter Simulation Conference*.

IMHC,Concept Map created with IHMC Cmap Tools, "Maxwell Equations." accessed 5 Feb 2015 <http://electra.ihmc.us/rid=1257880919306_814355520_7477/a033%20Maxwell's%20Equations.cmap?rid=1257880919306_814355520_7477&partName=htmljpeg>.

INCOSE Systems Engineering Handbook v.3.2.2., San Diego, CA, INCOSE-TP-2003-002-03.2.2, October 2011.

lNCOSE. "Systems Engineering Handbook", V3.1, 2007.

International Electrotechnical Commission Standard IEC 61000-2-9.

Intmath, Interactive Mathematics "8. Damping and the Natural Response in RLC Circuits." assessed Feb 5, 2015 <http://www.intmath.com/differential-equations/8-2nd-order-de-damping-rlc.php>.

Jahangir, E. "IEOR E4571 Systems Engineering Tools and Methods" A course description at the Graduate Engineering Distance Learning from Columbia University, accessed Feb 5, 2015 <http://www.cvn.columbia.edu/review.php?course=IEOR%20E4571&sem=S13>.

Jin, R., Chen, W., Sudjianto, A. "On Sequential Sampling for Global Metamodeling in Engineering Design" *2002 ASME International Design Engineering Technical Conference*. Montreal, Quebec, Canada, 2002, pp. 1-10.

Kawada, N., Yoda, T., Tagawa, N., Tsuchiya, T., Okubo, K., "Evaluation of Acoustic Simulation Using Wave Equation Finite Difference Time Domain Method with Compact Finite Differences" *Japanese Journal of Applied Physics* 51 (July 2012).

Kourakos, G. and Mantoglou, A. "Development of a multiobjective optimization algorithm using surrogate models for coastal aquifer management." *J. Hydrol.* **479** 13–23. 2013.

Koziel, S. and Bandler, J. "Space-mapping modeling of microwave devices using multi-fidelity electromagnetic simulations." *IET Microwave Antenna and Propagation*. 5:3, 2011, pp. 324-333.

Lim, D., Jin, Y., Ong, Y. and Sendhoff, B. "Generalizing Surrogate-Assisted Evolutionary Computation." *IEEE Transactions on Evolutionary Computation.* 14:3, June 2010, pp. 329-356.

Liu, W. H., Medina, M. A. Jr, Thomann, W, Piver, W. T. and Jacobs T. L. Optimization of intermittent pumping schedules for aquifer remediation using a genetic algorithm." *J. Am. Leather Chem. As.* **36** 1335–1348. 2000.

Lophaven, S., Nielsen, H. and Sondergaard, J. "DACE: A MATLAB Kriging Toolbox V.2" *Technical Report IMM-TR-2002-12*, Technical University of Denmark, 2002, p. 1026.

Lu, F., Shi, Y., Zhao, M., and Zhou, B. H. "Numerical Analysis of the Bounded-Wave EMP Simulator" *Antennas, Propagation and Electromagnetic Theory*, 8th International Symposium on Antennas, Propagation and EM Theory, 2008, pp. 1089-1092.

Luo, J. and Lu, W. "Comparison of surrogate models with different methods in groundwater remediation process" *J. Earth Syst. Sci.* **123**, No. 7, October 2014, pp. 1579–1589 Indian Academy of Sciences.

Macdonald, I. "Comparison of Sampling Techniques on the Performance of Monte-Carlo Based Sensitivity Analysis."*Eleventh International IBPSA Conference.* Glasgow, Scotland, July 27-30, 2009, pp. 992-999.

Montgomery, D. C. *Design and Analysis of Experiments*, *7th edition.* Hoboken, NJ: John Wiley and Sons, 2009.

Nagaoka, T. and Watanabe, S. "A GPU-Based Calculation Using the Three-Dimensional FDTD Method for Electromagnetic Field Analysis." *32nd Annual International Conference of the IEEE EMBS*. Buenos Aires, Argentina, August 31 – September 4, 2012.

National Research Council, "Modeling and Simulation in Manufacturing and Defense Acquisition; Pathways to Success", Committee on Modeling and Simulation Enhancements for 21st Century Manufacturing and Acquisition, National Academy Press, 2002

Nopper, R (Guest Editor) "Mathematical Modeling: An Industrial perspective", COMSOL News 2012.

NVIDIA Webpage, "What is GPU Accelerated Computing," accessed 5 Feb 2015 <http://www.nvidia.com/object/what-is-gpu-computing.html>.

Oberguggenberger, M., King, J., Schmelzer, B. "Classical and imprecise probability methods for sensitivity analysis in engineering: A case study." *International Journal of Approximate Reasoning*. Volume 50, Issue 4, April 2009, Pages 680-693.

Oguz, U., and Gürel, L. "Subsurface-scattering calculations via the 3D FDTD method Employing PML ABC for layered media," in *IEEE Antennas Propagation Soc. Int. Symp. URSI Radio Science Meeting*, Montréal, QC, Canada, July 1997.

Olvander, J. "Optimization Techniques for Engineering Design Problems." Department of Management and Engineering, Linkoping University Dec 2009 accessed 5 Feb 2015 <https://www.iei.liu.se/machine/area/otedp?l=en>.

Ong, Y., Nair, P., Keane, A. and Wong, K. W. "Surrogate-Assisted Evolutionary Optimization frameworks for High- Fidelity Engineering Design Problems." *Knowledge Incorporation in Evolutionary Computation Studies in Fuzziness and Soft Computing* Volume 167, 2005, pp. 307-331.

Parnell, G. S., Driscoll, P. J., and Henderson D. L., Editors, *Decision Making for Systems Engineering and Management*, Wiley Series in Systems Engineering, Andrew P. Sage, Editor, Wiley & Sons Inc., 2008.

Pinton, G., Aubry, J., Tanter, M., "Direct Phase Projection and Transcranial Focusing of Ultrasound for Brain Therapy." *IEEE Transactions on Ultrasonics, Ferroelectrics, and Frequency Control.* vol. 59, no. 6, June 2012

Qin, X. S., Huang G. H., Chakma A., Chen, B. and Zeng, G. M. Simulation-based process optimization for surfactant-enhanced aquifer remediation at heterogeneous DNAPL-contaminated sites; *Sci. Total Environ.* **381** 17–37. 2007.

Razavi S., Tolson, B. A. and Burn, D. H. Review of surrogate modeling in water resources; *Water Resour. Res.* **48**, 2012 doi: 10.1029/2011WR011527.

Rymes, M.D. T3DFD User's Manual *Final Technical Report, August 1979--June 1981.*

Schaerlaekens J, Mertens J, Van Linden J, Vermeiren G, Carmeliet J and Feyen J A multi-objective optimization framework for surfactant-enhanced remediation of DNAPLcontaminations; *J. Contam. Hydrol.* **86** 176–194, 2006.

Simpson, T. W., Toropov, V., Balabanov, V. and Viana, F. A. C. "Design and analysis of computer experiments in multidisciplinary design optimization: a review of how far we have come or not". *Proceedings of the 12th AIAA/ISSMO Multidisciplinary Analysis and Optimization Conference, 2008* MAO, Victoria, Canada, 2008.

Simpson, T.,Peplinski, J.,Koch,P., and Allen, J. "Metamodels for Computer-Based Engineering: Survey and Recommendations" *Eng. Comput.*, vol. 17, pp. 129–150, 2001.accessed on 16 May 2013 <http://aircraftdesign.nuaa.edu.cn/MDO/ref/Disciplinary%20Optimization/Data%20Sampling%20and%20Surrogate%20Models/engr-w-computers.metamodels.pdf>

Smith, S. M. and Furse, C. "Stochastic FDTD for Analysis of Statistical Variation in Electromagnetic Fields." *IEEE Transactions on Antennas and Propagation.* 60, no 7, 2012, 3343-3350.

Sokolowski, J.A., Banks, C.M., "Handbook of Real-World Applications in Modeling and Simulation", John Wiley & Sons, Apr 24, 2012

Sreekanth, J. and Datta, B. "Multi-objective management of saltwater intrusion in coastal aquifers using genetic programming and modular neural network based surrogate models" *J. Hydrol.* **393** 245–256. 2010.

Taflove, A, "Application of the finite-difference time-domain method to sinusoidal steady-state electromagnetic penetration problems," *IEEE Trans. Electromagnetic Compatibility.* vol. 22, pp. 191–202, Aug. 1980

Taflove, A. and Hagness, S. *Computational Electromagnetics: The Finite-Difference Time-Domain Method, 3rd ed*., Norwood, MA: Artech House, 2005.

Torgerson, M., Durazo,P., Langley,T., and Ragavassamy,V. "Using systems engineering Techniques to accelerate your next project" *Embedded Newsletter*. October 20, 2013. accessed 4 Feb 2015 < http://www.embedded.com/design/prototyping-and-development/4422991/2/Using-system-engineering-techniques-to-accelerate-your-next-project>.

Trang, A.H. "Simulation of mine detection over dry soil, snow, ice, and water." *Proceedings ofthe SPIE*: 2765 (1996): 430-440.

Turner, C. "Invited Seminar: Surrogate Modeling and Optimization in Design." *Model-Based Systems Engineering Center*, Georgia Tech, Sept 9, 2014.

Ushakov, V. and Ishakov, V. *Insulation of High-Voltage Equipment*, New York: Springer, 2004.

Wang, T., Oristaglio, M. L. and Chew, W. C. "Finite-difference simulation of ground penetrating radar in dispersive soils," Schlumberger–Doll Research, Ridgefield, CT, SDR-EMG Res. Note, Dec. 1995

Wang, G. and Shan, S. "Review of Metamodeling Techniques in Support of Engineering Design Optimization." *ASME Transactions Journal of Mechanical Design* May 4, 2006.

Wei, W., Zhao, J. and Zhou, B. "Simulation of Shielding Effectiveness Test with Bounded-Wave EMP Simulator." *2011 IEEE 4th International Symposium on Microwave Antenna Propagation and EMC Technologies for Wireless*. November 1-3, 2011, Beijing, China, pp. 777-780.

Williford, C.F. "Comparison of Absorption and Radiation Boundary Conditions Using a Time-Domain Three-Dimensional Finite Difference Electromagnetic Computer Code." Thesis. Air Force Institute of Technology, 1985, Wright-Patterson AFB, OH

Williford C., Jost, R.J., Hebert, J.L. "Comparison of Absorption and Radiation Boundary Conditions in 3DFD Code." *Proceedings of 1986 International Aerospace and Ground Conference on Lightning and Static Electricity*. (1986): 44-1--44-10.

Xiong, F., Xiong, Y., and Chen, W. "Quasi-LHD Sequential Sampling Method for Computer Experiments." *12th AIAA/ISSMO Multidisciplinary Analysis and Optimization Conference.* September 10-12 2008, British Columbia, Canada.

Yee, K.S. "Numerical Solution of Initial Boundary Value Problems Involving Maxwell's Equation in Isotropic Media" *IEEE Transactions on Antennas and Propagation*: AP-14 (May 1966): 302-307

You, H., Yang, M., Wang, D., Xinzhang, J. "Kriging Modeling combined with Latin Hypercube sampling for surrogate modeling of analog integrated circuit performance." *10th International Symposium on Quality of Electronic Design (ISQED)* March 16-18, 2009, San Jose, CA, pp. 554-558.

Zhu,Z., "Computer Vision Research Progress", Nova Publishers, 2008 available as a Google e-Book.

Appendix A – Low and Medium Scale Models

Maxwell's Equations and Lower Fidelity Circuit Analysis from EM Models

This appendix provides an example of how lower fidelity models can be derived from computationally complex ones by applying suitable conditions and constraints. Since electromagnetic computational codes are presented in this study, the derivations are presented here. There are similar methods for deriving simpler models for most physics-based computational codes.

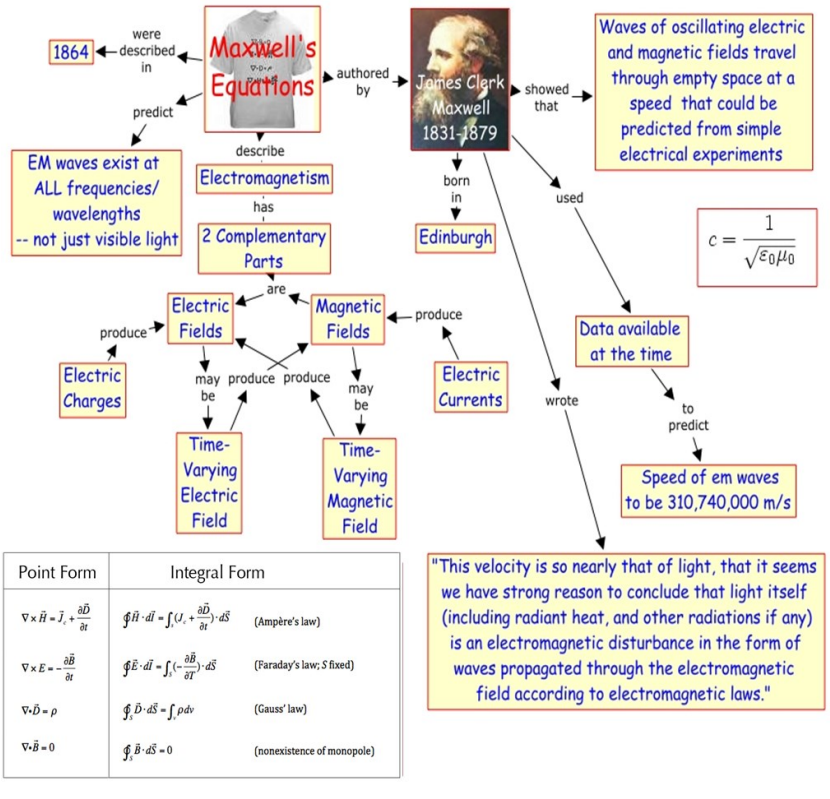

Figure A-1. Maxwell's Equations [IHMC 2015]

The physics-based equations that are generally accepted as accurate representations of electromagnetic phenomena are known as Maxwell's equations. Figure

A-1 provides an overview of the history and interrelationships between the Maxwell equations

The highest fidelity electromagnetic computational codes model Maxwell's equations in their entirety in either the time domain (i.e. the finite difference time domain code (FDTD) that is based on the point or derivative form of the equations) or in the frequency domain (finite element models) that is based upon the integral form of the equations. The Finite Difference Time Domain code is presented in Appendix B.

Deriving simpler lower fidelity models

By applying the following three constraints, known as the Lumped Matter Discipline (LMD), Maxwell's equations may be transformed into simpler ones that can be solved by simple algebra. The LMD provides the basis for the lumped circuit abstraction. The three constraints imposed by LMD are:

1. "The rate of change of magnetic flux, $\frac{\partial \varphi_B}{\partial t} = 0$, linked with any portion of the circuit must be zero at all times (allowed unique voltage across the terminals of an element)

2. The rate of change of the charge, $\frac{\partial q}{\partial t} = 0$, at any node in the circuit must be zero for all time. A node is any point in the circuit at which two or more element terminals are connected using wires (allowed unique current across the terminals of an element)

3. The signal timescales must be much larger than the propagation delay of electromagnetic waves through the circuit.

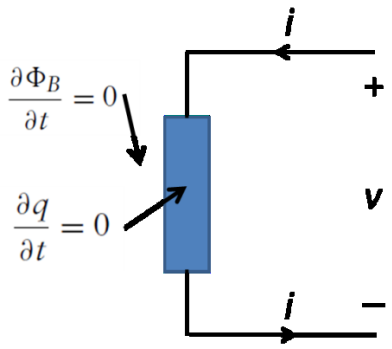

Figure A-2. LMD constraints with an arbitrary two terminal circuit element

Applying the LMD constraints results in a lumped circuit element that is an abstract representation of a component with a complicated internal behavior. Circuit models made up of these lumped circuit elements present an abstract representation of interrelated physical phenomena. Using these elements, we can move from the complicated calculus form of Maxwell's equations into two simple laws that allow the use of simpler algebraic equations. This allows Maxwell's equations for voltages and currents across a variety of lumped circuits to be modeled by two simple algebraic relationships such as Kirchoff's Voltage Law (KVL) and Kirchoff's Current Law (KCL):

Kirchhoff's Current Law (point rule or junction rule) is based upon the conservation of electrical charges. The sum of all currents into and out of any node must be zero: what comes in the node must go out.

$$\sum_{k=1}^{n} I_k = 0$$

Kirchhoff's Voltage Law (loop rule) is based upon the conservation of energy. The sum of all voltage sources and drops around a loop must be zero.

$$\sum_{k=1}^{n} V_k = 0$$

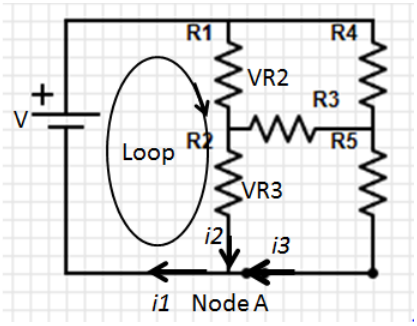

Figure A-3. Example Lumped Parameter Circuit

The voltages around the loop according to KVL add up to be zero:

$$V + VR1 + VR3 = 0;$$

and the currents into and out of Node A according to KCL add up to be zero:

$$i1 + i2 + i3 = 0$$

Devices such as resistors are passive such that the currents and voltages are instantaneous (no delay) and are not a function of time. Devices that store energy either as charges like capacitors or in magnetic fields like inductors have memory and are a function of time. The next higher level of fidelity includes these storage elements.

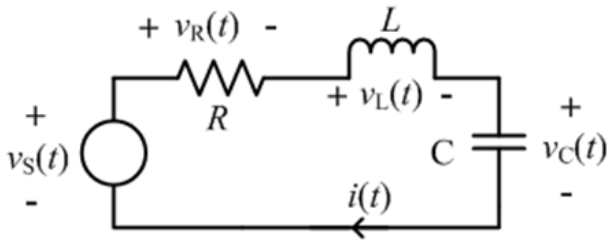

Figure A-4. Simple RLC Circuit

If we consider a circuit with a source, a resistor, an inductor and a capacitor (an RLC circuit) where V is the source voltage, R is the resistance, L is the inductance of the

inductor, C is the capacitance of the capacitor and I is the current through all the components, KVL tells us that:

$$V_R + V_L + V_C = V_S$$

The voltages and currents through and across the elements are given by:

$$i = C \cdot \frac{dV_C}{dt}$$

$$V_R = R\ X\ i = RC \cdot \frac{dV_C}{dt}$$

and

$$V_L = L \cdot \frac{di}{dt} = LC \cdot \frac{d^2V_C}{dt^2}$$

Substituting the expressions for the current from these relationships into the KVL expression, we get the characteristic equation in this form

$$L\frac{d^2q}{dt^2} + R\frac{dq}{dt} + \frac{1}{C}q = 0$$

$$Ls^2 + Rs + \frac{1}{C} = 0$$

has a solution with the two roots. They are:

$$s_1 = -\frac{R}{2L} + \sqrt{\left(\frac{R}{2L}\right)^2 - \frac{1}{LC}}$$

and

$$s_2 = -\frac{R}{2L} - \sqrt{\left(\frac{R}{2L}\right)^2 - \frac{1}{LC}}$$

The current through elements is given by

$$i_c(t) = C\frac{dV_C(t)}{dt} = Cs_1V_i\left(\frac{e^{s_1t}}{1-\frac{s_1}{s_2}}\right) + Cs_2V_i\left(\frac{e^{s_2t}}{1-\frac{s_2}{s_1}}\right)$$

where S_1 and S_2 are the roots of the equation, In S_1 and S_2 expressions under the square root sign determines the type of waveform that the circuit produces. Depending on the values of R, L, and C, Inmath.com identifies three possible solutions that are presented below. [Intmath 2015]

The Over-damped Case (no oscillations):

Here $R^2 > 4L/C$, the expression is real and positive and the waveform is given by:

$$I(t) = Ae^{s1t} + Be^{s2t}$$

An over-damped series RLC waveform is shown in Figure A-5.

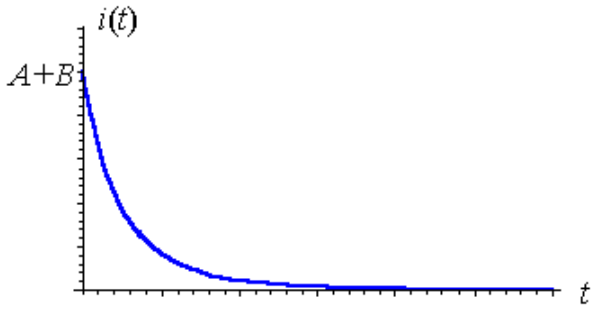

Figure A-5. An Over-damped RLC Waveform [Intmath 2015]

The Critically Damped Case:

Here $R^2 = 4L/C$, the roots are real and equal and the waveform is given by:

$$i(t) = (A + Bt)e^{-Rt/2L}$$

A critically damped RLC waveform is shown in Figure A-6.

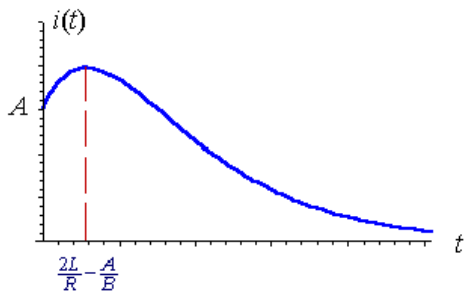

Figure A-6. A Critically damped RLC Waveform [Intmath 2015]

The Under Damped Case:

The under-damped case is oscillatory. Here $R^2 < 4L/C$, the roots are imaginary and the waveform is given by

$$i(t) = e^{\alpha t}(A\cos\omega t + B\sin\omega t)$$

where $\alpha = \frac{R}{2L}$ is known as the damping coefficient and ω is given by $\omega = \sqrt{\frac{1}{LC} - \frac{R^2}{4L^2}}$.An over-damped oscillatory RLC waveform is shown in Figure A-7.

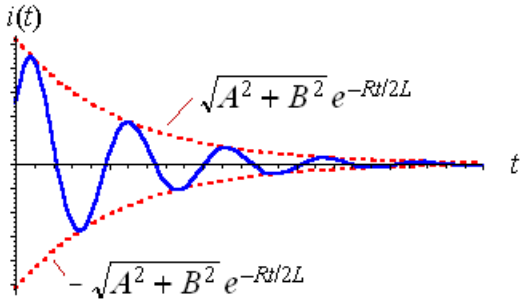

Figure A-7. An Under-damped RLC Waveform [Intmath 2015]

Appendix B

The Finite Difference Time Domain (FDTD) Code

The FDTD method is one of the most widely used high fidelity computational electromagnetic codes. They were used in the GPR system example and again the NEMP/BWS example presented in this study. It was first proposed by K.S. Yee. [Yee 1966] This appendix presents the basic concepts of the FDTD. Further details about the FDTD method can be found in works by Taflove and Hagness. [Taflove 1980; Taflove and Hagness 2005]

The FDTD code uses the central difference approximation to generate two of Maxwell's equations in their curl form: Faraday's and Ampere's laws. The central difference approximation allows derivatives in a partial differential equation to be approximated by linear combinations of function values at grid points. Using this approximation allows the equations for the electric and magnetic fields to time step through a gridded volume in a leap frog manner. The cells in the gridded volume, for the two examples presented in this study, are designated by the Cartesian Coordinates of the corner of the cell closest to the origin; for example the cell is located at (1,1,1) has three electric field values associated with it: $E_x(1,1,1)$, $E_y(1,1,1)$, $E_z(1,1,1)$ and three magnetic fields $H_x(1,1,1)$, $H_y(1,1,1)$, $H_z(1,1,1)$. First, all of the electric field values are calculated at points in the grid followed by the calculation of all the magnetic fields at similar points. For the models and simulations in this study, the computational domain was discretized using a rectangular grid resulting in electric and magnetic fields that are calculated in their rectangular coordinate system: *x* direction, *y* direction and *z* direction as shown in Figure B-1.

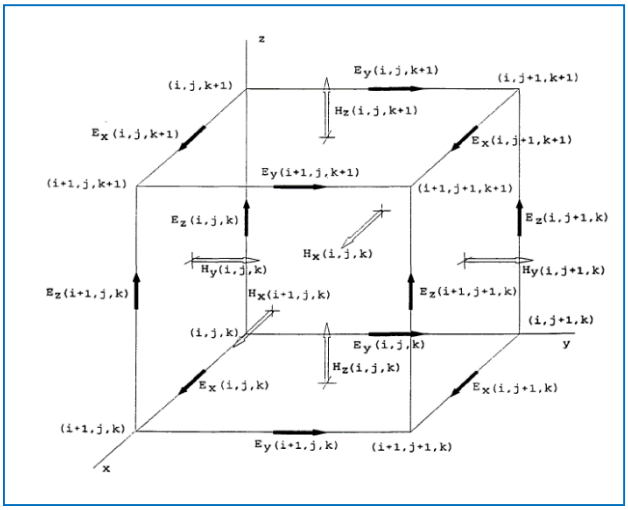

Figure B-1. Locations of Electric and Magnetic fields in the Yee formulation [Yee 1966]

Note that the field quantities are calculated at special points that are on the cell's axis lines or faces of the cube. Electric field points are located on the axis lines and magnetic fields are calculated at the centers of the grid surface with an angle of 90 degrees from that surface. As stated before, during each time step, the electric fields that depend on the values of the orthogonal magnetic fields are calculated followed by the calculation of the magnetic field that depends on the values of the electric fields. This becomes clearer as we look at the equations that make up the FDTD codes.

FDTD produces the solutions of two of Maxwell's equations, Faraday's law and Ampere's law.

$$\nabla \times \vec{E} = -\mu \frac{\partial \vec{H}}{\partial t} = -\sigma_M \vec{H} \qquad \text{(Faraday's law)}$$

$$\nabla \times \vec{H} = \varepsilon \frac{\partial \vec{E}}{\partial t} + \sigma \vec{E} \qquad \text{(Ampere's law)}$$

Expanding the vectors for $\vec{E}$ and $\vec{H}$ in the Cartesian coordinate system, these equations produce six coupled partial differential equations:

$$\frac{\partial H_x}{\partial t} = \frac{1}{\mu_x}\left(\frac{\partial E_y}{\partial z} - \frac{\partial E_z}{\partial y} - \sigma_{Mx} H_x\right)$$

$$\frac{\partial H_y}{\partial t} = \frac{1}{\mu_y}\left(\frac{\partial E_z}{\partial x} - \frac{\partial E_x}{\partial z} - \sigma_{My} H_y\right)$$

$$\frac{\partial H_z}{\partial t} = \frac{1}{\mu_z}\left(\frac{\partial E_x}{\partial y} - \frac{\partial E_y}{\partial x} - \sigma_{Mz} H_z\right)$$

$$\frac{\partial E_x}{\partial t} = \frac{1}{\varepsilon_x}\left(\frac{\partial H_z}{\partial y} - \frac{\partial H_y}{\partial z} - \sigma_x E_x\right)$$

$$\frac{\partial E_y}{\partial t} = \frac{1}{\varepsilon_y}\left(\frac{\partial H_x}{\partial z} - \frac{\partial H_z}{\partial x} - \sigma_y E_y\right)$$

$$\frac{\partial E_z}{\partial t} = \frac{1}{\varepsilon_z}\left(\frac{\partial H_y}{\partial x} - \frac{\partial H_x}{\partial y} - \sigma_z E_z\right)$$

where ε, σ, and μ are the constituent electrical and magnetic properties of the material that occupy the space the cell defines.

The fields propagate through the gridded problem space at least twice as fast as the electromagnetic wave. This is assured by setting the time step to be less than that specified by the Courant condition.

$$\Delta t \leq \frac{1}{c\sqrt{\frac{1}{\Delta x^2} + \frac{1}{\Delta y^2} + \frac{1}{\Delta z^2}}}$$

Using conventional mathematic notations, the discretized fields may then be written as:

$$E_x^n\left(i + \frac{1}{2}, j, k\right) = E_x\left(\left(i + \frac{1}{2}\right)\Delta x, j\Delta y, k\Delta z, n\Delta t\right)$$

$$E_y^n\left(i, j + \frac{1}{2}, k\right) = E_y\left(i\Delta x, \left(j + \frac{1}{2}\right)\Delta y, k\Delta z, n\Delta t\right)$$

$$E_z^n\left(i, j, k + \frac{1}{2}\right) = E_z\left(i\Delta x, j\Delta y, \left(k + \frac{1}{2}\right)\Delta z, n\Delta t\right)$$

$$H_x^{n+\frac{1}{2}}\left(i, j + \frac{1}{2}, k + \frac{1}{2}\right) = H_x\left((i\Delta x, \left(j + \frac{1}{2}\right)\Delta y, (k + \frac{1}{2})\Delta z, (n + \frac{1}{2})\Delta t\right)$$

$$H_y^{n+\frac{1}{2}}\left(i + \frac{1}{2}, j, k + \frac{1}{2}\right) = H_y\left((i + \frac{1}{2})\Delta x, j\Delta y, (k + \frac{1}{2})\Delta z, (n + \frac{1}{2})\Delta t\right)$$

$$H_z^{n+\frac{1}{2}}\left(i+\frac{1}{2},j+\frac{1}{2},k\right)=\ H_z\left((i+\frac{1}{2})\Delta x,(j+\frac{1}{2})\Delta y,k\Delta z,(n+\frac{1}{2})\Delta t\right)$$

with i, j, k being the cell indices

The fields and their locations are associated with actual Cartesian coordinates (x, y, and z) but they are not actually located at these points. The constituent properties of the materials are also associated with the coordinate point for each equation. Using the standard mathematical finite-difference approximation of a derivative:

$$\frac{\partial}{\partial k}F(k=n\Delta k)=\ \frac{F\left(\left[n+\frac{1}{2}\right]\Delta k\right)-F(\left[n-\frac{1}{2}\right]\Delta k)}{\Delta k}$$

Maxwell's Equations can be rewritten to find the FDTD update equations. This form of the equations were programmed into MATLAB™:

$$H_x^{n+\frac{1}{2}}\left(i,j+\tfrac{1}{2},k+\tfrac{1}{2}\right)=\ H_x^{n-\frac{1}{2}}\left(i,j+\tfrac{1}{2},k+\tfrac{1}{2}\right)$$
$$+\left[\frac{\Delta t}{\mu\Delta z}\right]\left(E_y^n(i,j+\frac{1}{2},k+1)-\ E_z^n(i,j+1,k+\frac{1}{2})\right)$$
$$-\left[\frac{\Delta t}{\mu\Delta y}\right]\left(E_z^n(i,j+1,k+\frac{1}{2})-\ E_z^n(i,j,k+\frac{1}{2})\right)$$

$$H_y^{n+\frac{1}{2}}\left(i+\tfrac{1}{2},j,k+\tfrac{1}{2}\right)=\ H_y^{n-\frac{1}{2}}\left(i+\tfrac{1}{2},j,k+\tfrac{1}{2}\right)$$
$$+\left[\frac{\Delta t}{\mu\Delta x}\right]\left(E_z^n(i+1,j,k+\frac{1}{2})-E_z^n(i,j+1,k+\frac{1}{2})\right)$$
$$-\left[\frac{\Delta t}{\mu\Delta z}\right]\left(E_x^n(i+\frac{1}{2},j,k+1)-\ E_x^n(i+\frac{1}{2},j,k)\right)$$

$$H_z^{n+\frac{1}{2}}\left(i+\tfrac{1}{2},j+\tfrac{1}{2},k\right)=\ H_z^{n-\frac{1}{2}}\left(i+\tfrac{1}{2},j+\tfrac{1}{2},k\right)$$
$$+\left[\frac{\Delta t}{\mu\Delta y}\right]\left(E_x^n(i+\frac{1}{2},j+1,k)-\ E_z^n(i+\frac{1}{2},j,k)\right)$$
$$-\left[\frac{\Delta t}{\mu\Delta z}\right]\left(E_y^n(i+1,j+\frac{1}{2},k)-\ E_y^n(i,j+\frac{1}{2},k)\right)$$

$$E_x^{n+1}\left(i+\tfrac{1}{2},j,k\right) = E_x^n\left(i+\tfrac{1}{2},j,k\right)$$
$$+\left[\frac{\Delta t}{\varepsilon\Delta y}\right]\left(H_z^{n+\frac{1}{2}}(i+\frac{1}{2},j+\frac{1}{2},k) - H_z^{n+\frac{1}{2}}(i+\frac{1}{2},j-\frac{1}{2},k)\right)$$
$$-\left[\frac{\Delta t}{\varepsilon\Delta z}\right]\left(H_y^{n+\frac{1}{2}}(i+\frac{1}{2},j,k+\frac{1}{2}) - H_y^{n}(i+\frac{1}{2},j,k-\frac{1}{2})\right)$$

$$E_y^{n+1}\left(i,j+\tfrac{1}{2},k\right) = E_y^n\left(i,j+\tfrac{1}{2},k\right)$$
$$+\left[\frac{\Delta t}{\varepsilon\Delta z}\right]\left(H_x^{n+\frac{1}{2}}(i,j+\frac{1}{2},k+\frac{1}{2}) - H_x^{n+\frac{1}{2}}(i,j+\frac{1}{2},k-\frac{1}{2})\right)$$
$$-\left[\frac{\Delta t}{\varepsilon\Delta x}\right]\left(H_z^{n+\frac{1}{2}}(i+\frac{1}{2},j+\frac{1}{2},k) - H_y^{n+\frac{1}{2}}(i-\frac{1}{2},j+\frac{1}{2},k)\right)$$

$$E_z^{n+1}\left(i,j,k+\tfrac{1}{2}\right) = E_z^n\left(i,j,k+\tfrac{1}{2}\right)$$
$$+\left[\frac{\Delta t}{\varepsilon\Delta x}\right]\left(H_y^{n+\frac{1}{2}}(i+\frac{1}{2},j,k+\frac{1}{2}) - H_y^{n+\frac{1}{2}}(i-\frac{1}{2},j,k+\frac{1}{2})\right)$$
$$-\left[\frac{\Delta t}{\varepsilon\Delta y}\right]\left(H_x^{n+\frac{1}{2}}(i,j+\frac{1}{2},k+\frac{1}{2}) - H_x^{n+\frac{1}{2}}(i,j-\frac{1}{2},k+\frac{1}{2})\right)$$

These equations do not include the fields that occur at the boundaries of the problem space. Additional equations are used at the boundaries. Some of the more common are known as the PEC or tin can boundary condition, the Absorbing Boundary Condition (ABC) and the Perfectly Matching Layer (PML). The PEC boundary condition produces reflections back into the problem space. The ABC and PML boundary conditions eliminate or reduce the reflections at the outer boundary of the problem space. For the examples in this study PML boundary conditions were used.